Metabolic activity assessment of polar microorganisms and metabolic characterization of the cold-adapted *Rhodotorula* yeast JG1b

David Touchette

Natural Resource Sciences

McGill University, Montréal

April 2020

A thesis submitted to McGill University in partial fulfillment of the requirements of the degree of Master of Science

Table of Contents

List of Tables

List of Figures

Acknowledgments

I would like to thank my supervisor Dr. Lyle Whyte for his support, his confidence in my research directions, and for all the opportunities that he offered me throughout my degree. I would also like to thank the members of my committee, Dr. Jennifer Ronholm and Dr. Sébastien Faucher, for their precious advices with my research project. Thanks to Dr. Jacqueline Goordial, Dr. Nina Gunde-Cimerman and Dr. Cene Gostinčar for their input on the *Rhodotorula* project, and to Dr. Antonio Ricco and Michael Padgen for their help with the *µMAMA* project and their generosity during my visit at the NASA Ames Research Center. Thanks to Dr. Barry Bochner for his kindness.

I would like to express my sincere gratitude to Dr. Ianina Altshuler and Dr. Isabelle Raymond-Bouchard for their continuous guidance, advices, support, and supervision toward my projects, but especially for their friendship, love, patience and kindness. I would like to acknowledge the important contribution of Louis-Jacques Bourdages in the *µMAMA* development and for his patience with the not-at-all engineer that I am. A huge thanks to all the other amazing members of the Whyte Lab that made me want to come on campus every day, Brady O'Connor, Olivia Blenner-Hassett, Madison Ellis, Catherine Maggiori, Esteban Gongora, Elisse Magnuson, Evan Marcolefas, Jonathan Sangiovanni, Dr. Miguel Fernandez Martinez, and Dr. Mira Okshevsky. Thanks to the Arctic 2018 and 2019 crews that made my field seasons unforgettable.

Pour terminer, j'aimerais remercier mes proches, particulièrement mes parents, Claire Achim et Gabriel Touchette, mes sœurs Sarah et Justine, ainsi que mes ami(e)s sincères, particulièrement Aymeric Rolland, Alizée Girard et Philippe Touchette, pour leurs encouragements, leur amour, leur support moral et leur compréhension. Un merci particulier à Pierre Masse et Dr. David Morse qui ont motivé mon parcours académique et qui m'ont fait découvrir la beauté de la biologie.

Abstract

Earth's cryosphere contains some of the most extreme habitats on our planet, with the polar regions having some of the driest, coldest, and hypersaline conditions for microbial life, such as permafrost, ice, hypersaline springs and subglacial lakes. Despite this, many cold-adapted microorganisms are capable of metabolic activity and even *in situ* growth in these environments at ambient temperatures. The presence of microorganisms in cryoenvironments opens to the possibility that other cold planetary bodies, such as Mars, Europa and Enceladus, could harbor and support similar extant microbial life forms. Contrarily, no direct extant life detection instrumentation has been included in a space mission since the NASA Viking landers on Mars in the 1970s, and current scientific instruments related to astrobiology are focused on the detection of biosignatures of past microbial life. Moreover, the microbial adaptation strategies to low temperatures are not fully understood, and the study of microbial cold adaptation is challenging. This thesis aims to present a novel and simple way to identify and characterize microbial metabolic activity in an astrobiological context, and to expand on the current knowledge of cold growth metabolisms in a psychrophilic Antarctic yeast.

Firstly, I describe the development and testing of a novel instrument for metabolic activity detection, the microfluidic Microbial Activity MicroAssay (µMAMA). The µMAMA platform will potentially be one of the first automatized extant life-detection instruments. This technology is based on the microbial metabolism-indicator redox dyes. Using the µMAMA, I successfully detected microbial activity with as low as 10_2 cells/ml inoculum, and characterized the microbial communities of environmental samples from Cornwallis Island in the Canadian high Arctic, a relevant Mars analog site. I also assessed the robustness and sensitivity of the six redox dyes and

buffer combinations across different abiotic parameters to determine the robustness of the μMAMA at specifically and unambiguously detecting microbial metabolic activity in analog sites.

In my 2nd project, I characterized the cold-adaptive strategies of a novel Antarctic permafrost yeast, *Rhodotorula* JG1b, through mRNA and small RNA transcriptomic analyses, phenotypic profiling, and ethanol production assessment at 0°C and 23°C. The results suggest that *Rhodotorula* JG1b switches its metabolism from a primarily respiratory metabolism in its optimal growth conditions at 23°C, to a fermentative metabolism while grown in conditions more similar to its natural environment. This was correlated with ethanol production in cultures grown at 0°C. This is the coldest temperature for biological ethanol production documented to date without the aid of added biocatalysts. I also detected an upregulation of many genes involved in well-known adaptations to cold. Most importantly, the results strongly imply that post-transcriptional regulation of gene expression and mRNA silencing by miRNAs in *Rhodotorula* may be a novel key evolutionary adaptation of yeasts in the cryosphere.

Résumé

La cryosphère de la Terre contient des habitats parmi les plus extrêmes de notre planète, avec les régions polaires offrant des conditions parmi les plus sèches, froides et salées pour la vie microbienne. Ceci incluant le pergélisol, la glace, les sources d'eau hypersalines et les lacs sous-glaciaires. Malgré cela, plusieurs microorganismes adaptés au froid sont capables d'activité métabolique et même de croissance *in situ* dans ces environnements. La présence de microorganismes dans les cryoenvironnements démontre la possibilité que d'autres astres planétaires, tels que Mars, Europe et Encelade, pourraient abriter et supporter des formes de vie microbiennes existantes. Toutefois, aucun instrument de détection de vie microbienne n'a été inclus dans une mission spatiale depuis les missions *Vikings* de la NASA dans les années 1970. Ainsi, les instruments scientifiques actuellement utilisés ne focalisent que sur la détection de biosignatures. De plus, les stratégies d'adaptation microbienne aux basses températures ne sont toujours pas bien comprises et l'étude de ces adaptations est soumise à plusieurs défis. La présente thèse vise à présenter une façon simple et nouvelle d'identifier et de caractériser l'activité métabolique microbienne dans un contexte astrobiologique, ainsi qu'à contribuer aux connaissances actuelles sur les métabolismes microbiens de croissance adaptés au froid.

Premièrement, j'ai décrit le développement et l'essai d'un instrument de détection d'activité métabolique novateur, le *microfluidics Microbial Activity MicroAssay* (µMAMA). La plateforme µMAMA est un des premiers instruments automatisés de détection de la vie. Avec cette technologie basée sur les indicateurs de métabolisme colorants redox, j'ai détecté avec succès de l'activité microbienne avec aussi peu de 10_2 cellules/ml et avons caractérisé les communautés microbiennes de plusieurs échantillons environnementaux de l'île Cornwallis, dans l'Arctique Extrême canadien, un site astrobiologique analogue pertinent. J'ai aussi identifié les limites du

contexte chimique dans lequel le µMAMA permet d'obtenir un signal d'activité métabolique microbienne clair et robuste.

De plus, j'ai caractérisé les stratégies d'adaptation au froid de la nouvelle souche de levure *Rhodotorula* JG1b, isolée d'un pergélisol cimenté dans de la glace vielle d'environ 150 000 ans. Pour ce faire, j'ai combiné une analyse transcriptomique d'ARNm et de miARN, un profilage phénotypique et une évaluation de la production d'éthanol à 0°C et 23°C. Les résultats suggèrent que *Rhodotorula* JG1b change d'un métabolisme principalement respiratoire en conditions optimales à 23°C vers un métabolisme de fermentation en conditions similaires à son environnement naturel, confirmé par la détection de production d'éthanol dans les cultures à 0°C seulement. Ceci représente la température la plus froide de production d'éthanol documentée à ce jour, sans l'aide de biocatalyseurs. J'ai aussi détecté une régulation positive de plusieurs adaptations au froid bien connues chez *Rhodotorula* JG1b. Plus important encore, les résultats impliquent que la régulation de l'expression génique post-transcriptionnel et l'extinction d'ARNm par miRNA chez *Rhodotorula* est potentiellement une nouvelle adaptation clé chez les levures de la cryosphère.

Abbreviations

AB-H_2O: AlamarBlue® buffered in H_2O
AB-IF0a: AlamarBlue® buffered in IF-0a
AB-$Na_4P_2O_7$: AlamarBlue® buffered in $Na_4P_2O_7$
AWCD: Average well-color development
CFU: Colony-forming unit
CH_4: Methane
CO_2: Carbon dioxide
DGTS: Diacylglyceryltrimethylhomoserine
EPS: Exopolysaccharide
ETC: Electron transport chain
GS: Gravel soil - rocky active layer of permafrost
H: Shannon-Weaver diversity index
HPLC: High performance liquid chromatography
IF: Inoculating Fluid
Iron.: Iron-oxidizer media
ISS: International Space Station
LS: Lake sediment
MALDI: Matrix-assisted laser desorption ionization
MAPs: Mitogen activated protein kinase
Min Media: Minimal media
miRNA: microRNA
No amend: no substrate amended
N_2O: Nitrous oxide
PCSP: Polar Continental Shelf Program
PDB: Potatoes dextrose broth
PPP: Pentose-phosphate pathway
R: Substrate richness
RNAi: RNA interference
RT-qPCR: Reverse transcription polymerase chain reaction
RSL: Recurring Slope Lineae
R2A: Reasoner's 2A
SIP: Stable isotope probing
sRNA: small non-coding RNA
STW: Fresh stream water
SW: Brackish sea water
Thio.: Thiosulfate media
TSB: Tryptic soy broth
µMAMA: microfluidics Microbial Activity MicroAssay

Chapter 1. Introduction and Literature Review

1.1 Introduction to the microbial habitats of the cryosphere

Earth is considered a cold planet, with around 85% of its biosphere constantly below 5°C (Margesin and Miteva 2011) and a significant portion where water stays in a permanently solid state. This portion is called the cryosphere (Miteva 2008). The majority of the cryosphere is found in polar and alpine regions representing an important part of our planet surface, with the Antarctica covering 14 million km^2, the Arctic covering 7 million km^2 of terrestrial habitats and up to 15 million km^2 in sea ice coverage (Kirby *et al.* 2012). These cryosphere environments (cryoenvironments) have some of the harshest climatic conditions on Earth and are characterized by low water and nutrient availability, high solar irradiation, and multiple freeze-thaw cycles (Buzzini and Margesin 2014b). Since the availability of liquid water, the solvent of biochemistry that allows life, is considered as one limit to life (Bakermans 2017), cryoenvironments were considered as absent of life for a long time, however, multiple recent studies suggest that these cryoenvironments possess diverse microbial communities. Many of these were characterized and identified by cultivation (Margesin and Miteva 2011), and in some cases shown to contain active microbial communities at ambient subzero temperatures (Bakermans *et al.* 2014; Lamarche-Gagnon *et al.* 2015; Mykytczuk *et al.* 2013).

Cryoenvironments include permafrost, sea and freshwater ice, ice sheets and glaciers, and subzero saline lakes. Permafrost soils are found in polar and high altitudes environments and cover 27% of all terrestrial ecosystems (Williams and Smith 1989). They are defined as soils permanently exposed to subzero conditions for at least two consecutive years and are often covered by an active layer that will undergoes multiple freeze-thaw cycles (Goordial *et al.* 2013).

Interestingly, variable amount of microbial biomass is observed between different permafrost sample, ranging from 10^3 to 10^6 cells/g in the McMurdo Dry Valleys permafrost of Antarctica (Gilichinsky *et al.* 2007; Goordial *et al.* 2016a) to 10^5 to 10^9 cells/g in the Arctic permafrost (Hansen *et al.* 2007; Steven *et al.* 2007; Vishnivetskaya *et al.* 2006), and sometimes very high amounts, from 10^8 to 10^{10}, in alpine permafrost (Altshuler *et al.* 2017). Microbial communities were also found to vary in diverse ice habitats, such as sea ice with 10^4 to 10^6 cells/ml (Brakstad *et al.* 2008; Garneau *et al.* 2016; Junge *et al.* 2002), glacial ice with 10^2 to 10^7 cells/ml (Hodson *et al.* 2008; Hotaling *et al.* 2017), and ice from caves with 10^4 to 10^5 cell/ml (Itcus *et al.* 2018; Iţcuş *et al.* 2016).

While these microbial habitats are limited by the amount of liquid water, other cold environments were found to harbor microbial communities in water samples. Between 10^3 to 10^5 cells/ml were reported in the 4°C Icelandic subglacial lakes (Hodson *et al* 2008; Marteinsson *et al.* 2013), 10^3 to 10^5 cell/ml were reported in the hypersaline and subzero springs of the Canadian high Arctic (Lay *et al.* 2012; Niederberger *et al.* 2010; Perreault *et al.* 2008), and microorganisms were identified in multiple hypersaline lakes of Antarctica such as Lake Vida (Murray *et al.* 2012), including some characterized by subzero temperatures (Bowman *et al.* 2000; Naganuma *et al.* 2005).

While the majority of these studies were focusing on the identification and the cultivation of aerobic heterotrophic life forms, anaerobic microbial members, such as *Spirochaetales*, *Thermoanaerobiales*, *Haloanarobiales*, *Acetobacterium*, and *Geobacter* are also found in these cryoenvironments (Bowman *et al* 2000; Marteinsson *et al* 2013). In addition, these cryoenvironments offer suitable habitats for many chemolithoautotrophs, including

Sulfurospirillum, *Sulfuricurvum*, *Thiomicrospira*, and *Halothiobacillus* (Marteinsson *et al* 2013; Perreault *et al* 2008).

1.2 Significance of cryobiology for astrobiology

The search for life on other planetary bodies will be a major focus of astrobiology missions in the coming decades (Hays 2015). Due to technological limitations, this search for life will be oriented toward the solar system, with Mars, Jupiter's moon Europa, and Saturn's moon Enceladus currently the main targets (Goordial *et al* 2013; Hays 2015). With average surface temperatures of -60°C on Mars, -180°C on Europa, and -190°C on Enceladus, these planetary bodies are characterized be extremely low temperature conditions limiting the liquid water availability for potential life forms (Garcia-Lopez and Cid 2017; Goordial *et al* 2013). Earth's cryosphere thus offers amongst the best analog sites to study and understand the cold temperature limits of microbial life on Earth and consequently the possibility of past or extant microbial life present on these frozen worlds (Goordial *et al.* 2017; Hoover and Gilichinsky 2001).

1.2.1 Possible habitability of astrobiology targets

Despite their apparent inhabitability, evidence of past and current habitats that could potentially support active microbial ecosystems have been extensively described in these astrobiological targets (Arvidson *et al.* 2014; Garcia-Lopez and Cid 2017; Grotzinger *et al.* 2014). Europa is one of the icy worlds with the highest potential for microbial life. With its ~3km deep, cold (potentially -3°C), and salty ocean residing under a ~30km ice surface (Garcia-Lopez and Cid 2017; Schmidt *et al.* 2011), Europa has similar environments to Antarctica's Lake Vostok where microbial biomass was found (Bulat *et al.* 2009) and to the recently discovered but yet unexplored high Arctic Devon subglacial lakes in Nunavut, Canada (Rutishauser *et al.* 2018). In addition, phyllosilicates were detected on Europa's surface. These minerals are can be associated with

organic matter, potentially due to organic matter exchange via collision with asteroids and comets (Chyba and Phillips 2001; Marion *et al.* 2003), and could harbor sulphate brines that percolate to the surface providing a liquid media (McCord *et al.* 2001). This organic matter could also indicate the possible presence of microbial communities that are resistant to extreme conditions on Europa including low nutrient availability, multiple freeze-thaw cycles, high oxidative stress and solar irradiation (Buzzini and Margesin 2014b). We know that Earth psychrophilic microorganisms are found to maintain viability for thousands of years under the ice (Hassan *et al.* 2016), perhaps similar ones are found on Europa.

Similar to Europa, Enceladus is characterized by a salty ocean underlying an ice crust (Kite and Rubin 2016). The Cassini spacecraft detected plumes arising from Enceladus constituting of 98% of water mixed with carbon dioxide, methane and ammonia and organic molecules (Garcia-Lopez and Cid 2017; Waite *et al.* 2017). Moreover, the existence of potential serpentinization on Enceladus could provide chemical energy for chemolithoautotroph's metabolism (Sekine *et al.* 2015). In addition, the discovery of silica nanoparticles on Enceladus by the Cassini spacecraft suggests the presence of hydrothermal activity in its interior, since high temperatures (>50°C) are required to form these nanoparticles (Sekine *et al* 2015). This support the possibility of extant microorganism on icy moons.

Closer to our planet, Mars was considerably warmer and wetter from ~ 4.5 to ~3.5 billion years ago, offering habitable conditions for potential microorganisms (Arvidson *et al* 2014; Chevrier *et al.* 2007; Grotzinger *et al* 2014; Westall *et al.* 2013). The Mars Science Laboratory (MSL) mission has identified the Gale Crater as being a fluvial-lacustrine environment in the past, with conditions that could have supported a broad range of prokaryotic microorganisms (Grotzinger *et al* 2014), and could have preserved many biosignatures of a past microbial life.

More interestingly, potential signs of brine water at recurring slope lineae (RSL) on the modern day Mars surface (Ojha *et al.* 2015) and of a polar saline subsurface lake at Mars' south pole (Orosei *et al.* 2018) opens the possibility that Mars could currently support extant microbial life forms still surviving in the Martian subsurface. Chemolithoautotrophic microbial life is thought to be the most likely candidate for microbial life forms on Mars' subsurface environment (Michalski *et al.* 2018). The presence of many chemolithoautotrophs in cryoenvironments and of microorganisms in an RSL analog site in Antarctica (Chan-Yam *et al.* 2019), and in the brine waters of the ice-sealed lake Vida in Antarctica (Murray *et al* 2012), further support the possibility of such microbial ecosystems in Mars RSLs. Furthermore, the NASA Phoenix lander also detected perchlorate, a freezing point depressant, in Martian permafrost (Hecht *et al.* 2009), that could potentially create salty liquid habitats inside the permafrost (Goordial *et al* 2013) and be used as an electron acceptor, instead of oxygen, in anaerobic conditions (Coates and Achenbach 2004). The presence of perchlorate and a viable microbial community in Antarctic permafrost (Goordial *et al* 2016a; Hecht *et al* 2009; Tamppari *et al.* 2012), further support the importance of studying the cryosphere to better understand astrobiology.

1.2.2 Looking for biosignatures on Mars

Despite the importance of life detection in current planetary missions to Mars, no direct extant life detection instrumentation has been included in a space mission since the Viking landers in the 1970s (Davila *et al.* 2010; Levin 1997). Currently, scientific instruments related to astrobiology-targeted space missions are focused on the detection of biosignatures from past life and the identification of new habitable environments and are mainly large, heavy and require high levels of energy. The need for more specific astrobiological instruments is also highlighted by the current difficulties in defining biomarkers. For example, the Mars Organics Detector/Mars Organics

Analyser (Bada 2001; Skelley *et al.* 2005) is limited to the unambigous detection of amino acids and related organics, which are not necessarily considered as biomarkers. Also, the Matrix-assisted laser desorption ionization (MALDI) can detect complex organics, but MALDI requires extensive sample processing (Meng *et al.* 2004), and is therefore not suitable for complex environments. The development of smaller, simple and portable instruments based on advances in microfluidics and nanotechnology that can be easily incorporated into future rovers and that are focused towards life-detection, is required.

1.3 Measuring and characterizing metabolic activity from cryoenvironments

Despite the evident harsh and extreme conditions in Earth's cryoenvironments, there are multiple reports of present diverse microbial communities within these cryoenvironments (Margesin and Miteva 2011). While many of the communities were characterized through laboratory cultivation techniques and 16S sequencing, it is harder to assess whether these microbial communities are active *in situ*. To determine *in situ* microbial activity, various strategies have then been developed.

1.3.1 Gas flux measurements, radio-respiration assays, and stable isotope probing (SIP)

One common way to assess metabolic activity is by studying the flux of gases, such as CO_2, N_2O or CH_4, from an environment. By analysing their gas fluxes, many cryoenvironments were found to harbor active microbial communities, *in situ* or in laboratory experiments at cold and subzero temperature. For example, an active microbial community was suggested to inhabit the wintertime frozen tundra soils (Elberling and Brandt 2003; Fahnestock *et al.* 1999), where a net carbon lost was observed *in situ*. Many subzero laboratory-based studies identified gas exchange due to active microbes using permafrost soil (Larsen *et al.* 2002; Michaelson and Ping 2003), Antarctic soils (Bakermans *et al* 2014), snow (Schmidt *et al.* 2009; Williams *et al.* 2009), and cryoconite holes (Telling *et al.* 2011). In addition, heterotrophic metabolic activity was also identified in numerous

cryoenvironments under subzero conditions using a highly sensitive radiolabelling microbial activity assay; this technique assesses the respiration of radiolabelled carbon sources metabolized by extant microorganisms. For example, subzero metabolic activity was detected in Arctic permafrost (Mykytczuk *et al* 2013; Wilhelm *et al.* 2012), hypersaline spring sediments (Lamarche-Gagnon *et al* 2015; Lay *et al* 2012), frozen soil (Bore *et al.* 2017), Siberian permafrost (Gilichinsky *et al.* 2003), and Antarctic Vostok lake ice core (Miteva *et al.* 2007).

Stable isotope probing (SIP) is a technique used to label the DNA of active microorganism by the incorporation of a heavy 13-carbon into the newly synthetized DNA strand. Contrarily to the respiration assay, SIP allows to differentiate the active members of the microbial community, that were able to replicate their DNA, from the non-active ones (Altshuler *et al* 2017). While only few studies have used this technique to characterize cryoenvironments, microorganisms from the *Acidobacteria*, *Actinobacteria*, *Armatimonadaceae, Chloroflexi*, *Candidatus* Saccharibacteria, *Gemmatimonadetes, Planctomycetaceae, Proteobacteria*, and *Verrucomicrobiaceae* phyla and from the *Acetobacteraceae, Burkholderiaceae,* and *Melioribacteraceae* family been found to perform DNA replication in subzero temperature (Gadkari *et al.* 2020; Tuorto *et al.* 2014).

1.3.2 Metatranscriptomic and transcriptomics of psychrophilic microorganisms

While gas fluxes, radio-respiration, and SIP are important tools to determine if an environment is active *in situ*, they do not provide information and insights on the specific functions of the microbial community and on the cold-adaptation strategies used by these active microbes. Through metatranscriptomics, it is possible to assess if an environment is active while further characterizing the *in situ* preferred metabolic pathways, by analysing a snapshot of the transcriptional profiles within the microbial communities (Carvalhais *et al.* 2012). Numerous cryoenvironment have been surveyed with metatranscriptomics, including glacial, sea and Vostok lake ice (Bertrand *et al.*

2015; Cameron *et al.* 2016; Hamilton *et al.* 2013; Pearson *et al.* 2015; Rogers *et al.* 2013), permafrost and permafrost-affected soil (Altshuler *et al.* 2019; Buelow *et al.* 2016; Hultman *et al.* 2015), and subzero saline springs (Lamarche-Gagnon *et al* 2015; Lay *et al.* 2013; Magnuson *et al.* 2020). Though these metatranscriptomic surveys are important to identify active members of the community, they cannot inform us of the specific cold adaptation strategies used by microorganism. Therefore, controlled transcriptomic laboratory studies under different temperatures are required to understand the molecular mechanisms in cold acclimation. Studies have used transcriptomics to gain knowledge on important metabolisms and adaptations for cold growth (Raymond-Bouchard and Whyte 2017), however, few transcriptomic studies have been performed at subzero temperatures (Bergholz *et al.* 2009; Koh *et al.* 2017; Mock and Hoch 2005; Mykytczuk *et al* 2013; Raymond-Bouchard *et al.* 2018b; Rodrigues *et al.* 2008).

1.3.3 Metabolism-indicator redox dyes

Since the metabolism assessment techniques described above are time consuming, labor intensive, and require specialized equipment, they are not suitable for a rapid and simple characterization of the metabolic capabilities of an environment. Metabolism-indicator redox dyes, such as AlamarBlue® (Rampersad 2012) and tetrazolium dyes (Bochner *et al.* 2001; Bochner 2008), are able to detect changes in cellular metabolic activity through the chemical reduction of the dye via cellular respiration (Hamid *et al.* 2004). For example, Biolog Inc. designed products based on the tetrazolium dye chemistry that are ideal for the characterization of heterotrophic microbial communities in various environments (Garland and Mills 1991) or for the assessment of microbial functional diversity based on the colony-level physiological profile (CLPP) (Insam and Goberna 2004), a “phenotypic fingerprint”. This phenotype characterization is performed in a 96-well plate (EcoPlate) and assesses the metabolic activity of the cells via a colorimetric test. These EcoPlates

are extensively used with environmental samples and have shown to successfully characterized microbial communities from various cryoenvironments, including ice from the Scărişoara Ice Cave (Iţcuş *et al* 2016), the Hans and Werenskiold Glaciers ice and cryoconites (Grzesiak *et al.* 2015a), permafrost soils from Alaska and Canadian high Arctic (Ernakovich and Wallenstein 2015; Goordial *et al* 2017), cold lakes freshwater of Patagonia (Mackenzie *et al.* 2011), and ice from the Ecology Glacier ablation zone of Antarctica (Grzesiak *et al.* 2015b).

1.4 Microbial adaptation strategies in cryoenvironments

Numerous molecular mechanisms, transcriptional changes, and translational regulation differences have been identified in enabling microbial survival in cryoenvironments. Here I describe the most accepted and studied adaptations to microbial life at cold and subzero temperatures:

1.4.1 Increase in membrane fluidity

Modifications in membrane fluidity are one of the most well-known cold-adaption strategies in microorganisms (Gunde-Cimerman *et al.* 2014; Raymond-Bouchard and Whyte 2017). As cold temperatures induce cell membrane rigidification and increased permeability (Cao-Hoang *et al.* 2010; Chu-Ky *et al.* 2005), keeping membrane fluidity is essential for microorganisms living in cold environments. As such, many microorganisms restructure their membrane lipid composition to keep membrane lipids in a fluid phase at cold temperature (Gunde-Cimerman *et al* 2014). While individual microorganisms have different mechanisms for increasing their membrane fluidity, overall strategies include the production of unsaturated fatty acid (Barria *et al.* 2013; Contreras *et al.* 2015; Gunde-Cimerman *et al* 2014), the desaturation of membrane phospholipids via the membrane-associated kinase DesK, in *Bacillus subtilis* (Aguilar *et al.* 2001; Albanesi *et al.* 2004), increases in glycerophospholipids (Loffeld and Keweloh 1996), and an overall increase in biosynthesis of fatty-acid (Bhuiyan *et al.* 2014; Rossi *et al.* 2009). Coupled to this readjustment of

membrane fluidity, some microorganisms may also increase the production of carotenoids at cold temperatures (Fong *et al.* 2001; Raymond-Bouchard *et al.* 2018a). As they induce a decrease in membrane fluidity, carotenoids help maintain membrane rigidity in cold-adapted microorganisms, to balance out the higher percentage of unsaturated fatty acid in the membrane (Raymond-Bouchard *et al.* 2017; Rodrigues and Tiedje 2008). This leads to an equilibrium in the membrane composition that allows an adequate state in membrane fluidity.

1.4.2 Increase in compatible solutes for cryoprotection

To overcome osmotic pressure and prevent water loss caused by ice formation and increased salinity in cryoenvironments, cold-adapted microorganisms promote the production of compatible solutes (Doyle *et al.* 2012; Mykytczuk *et al.* 2016; Raymond-Bouchard and Whyte 2017). These small water-soluble organic molecules balance osmotic pressure and have an important cryoprotection role by increasing the stability of macromolecules, membranes, and proteins (Hassan *et al* 2016; Kawahara 2017) and acting as freezing point depressants ((Mohamad *et al.* 2015). Compatible solutes are found overexpressed under cold temperatures in several psychrophiles (Raymond-Bouchard and Whyte 2017). In addition to their osmoprotection and cryoprotection roles, these compounds can be used as additional carbon, nitrogen and energy sources (Tribelli and López 2018). Amongst them, trehalose acts in the stabilization of proteins and membranes, and provides freezing resistance (Aguilera *et al.* 2007), L-proline is known to enhance freeze tolerance, and act as an antioxidant under stress condition (Chen and Dickman 2005; Terao *et al.* 2003), and the sugar alcohol xylitol reduces the freezing point in cells (Mohamad *et al* 2015). Furthermore, glycoproteins contain compatible solutes as part of their structure, and are found to have a cryoprotection role. For example, mannose-based glycoproteins have a cryoprotective role in preserving enzymes against cold conditions (Kawahara *et al.* 2008), and

some glycoproteins were found to prevent the growth of ice crystals through their ice-binding capacity (Davies *et al.* 2002; Lee *et al.* 2010). Glycoproteins are also able to lower the freezing point of cells (Kawahara 2017).

1.4.3 Translation and cold shock proteins

Under cold temperatures, microorganisms tend to decrease their translation machinery activity, with the exception of cold-inducible and cold shock proteins (Tribelli and López 2018). The protein PY is known to block protein syntheses by binding to the 30S ribosome subunits in the early stage of cold induction (Barria *et al* 2013). In addition, cold induces formation of secondary structures in RNA molecules and the inactivation of many ribosomes (Jones and Inouye 1996), as well as an increase in protein misfolding (Barria *et al* 2013). This considerably reduces mRNA translation in cells. To overcome these challenges, microorganisms have developed multiple features to modulate protein expression at the translation level in response to temperature decreases (Kawamoto *et al.* 2017). When exposed to cold, microorganisms overexpress cold shock proteins. These proteins regulate translation and protein folding by binding to nucleic acids (De Maayer *et al.* 2014). In addition they overexpress chaperones, such as heat shock proteins, DEAD-box and associated RNA helicases (Raymond-Bouchard and Whyte 2017), which can facilitate the degradation of secondary structures (Barria *et al* 2013). One of the main examples of the translation adaptation to cold is the CspA protein, an RNA chaperone of *E. coli.* Under cold temperature, the *cspA* mRNA is more stable than at warmer temperature. This increase in stability will allow the *cspA* mRNA to bind many ribosomes and inhibits general protein synthesis (Phadtare 2012), and leads to an important increase in CspA protein compared to the other proteins. With its chaperone activity, CspA prevents the formation of undesirable RNA secondary structures (Breaker 2010; Jiang *et al.* 1997), and stabilize the synthesis of desired proteins. The protein is also present in

several microorganism from permafrost and ice (Raymond-Bouchard *et al* 2018a). Similarly, the protein ScoF, in the CspA family, and several cold shock proteins were found in *Plannococcus halocryophilus*, growing at as low as -15°C (Mykytczuk *et al* 2013).

1.4.4 Energy metabolism changes

Recent studies have shown that many metabolic pathways modifications are induced in cold-adapted microorganisms growing at low temperatures. Overall, microorganisms generally downregulate their primary respiration metabolism since increase of oxygen solubility in cold conditions leads to an increase in oxidative stress (Tribelli and López 2018). Therefore, a decrease in gene expression related to glycolysis, the tricarboxylic acid cycle, and the electron transport chain is linked to cold-adaptation in many psychrophiles (Raymond-Bouchard *et al* 2018b; Raymond-Bouchard *et al* 2017; Sabra *et al.* 2017; Tribelli and López 2018). To compensate for this decrease in energy metabolism, microorganisms use different strategies and alternative metabolisms. Amongst them are an increases in glyconeogenesis (Ayala-del-Río *et al.* 2010), glyoxylate cycle (Aliyu *et al.* 2016), and maintenance of ATP levels through the increased activity of several enzymes, such as the alcohol dehydrogenase and several oxidoreductases (Mykytczuk *et al* 2013) were observed. Furthermore, increases in expression of genes related to pentose phosphate pathways (PPP) cause a reduction of the citrate cycle activity (Sarkar *et al.* 2009), and allow energy conservation since the PPP consume less energy than the citrate cycle. In addition, the PPP has been linked to the production of xylitol through xylulose fermentation (Bura *et al.* 2012). As xylitol also acts as a cryoprotectant (Mohamad *et al* 2015), this metabolism switch offers multiple benefits that help microorganisms adapt to cold temperatures.

1.5 Yeasts in the cryosphere

1.5.1 Yeast in the cryosphere

While numerous studies have investigated bacteria, archaea and algae form Arctic and Antarctica environments, few have focused on yeasts (Hassan *et al* 2016). This is despite the fact that many fungal species have been isolated and characterized from a diversity of extreme environments such as brine (Gunde-Cimerman *et al.* 2000), Arctic glaciers and Antarctic rocks and deserts (Hassan *et al* 2016; Perini *et al.* 2019; Tojo and Newsham 2012). Fungi play key roles in the cryosphere environments as they are important facilitator of primary biomass production through endophytic and lichenic relationships (Gianoli *et al.* 2004; Rosa *et al.* 2009) and are involved in the nutrients recycling (Duncan *et al.* 2006). Despite many yeasts being well adapted to low temperatures and thriving in a broad range of cold ecosystems (Shivaji and Prasad 2009; Starmer and Lachance 2011), their adaptation strategies to low temperatures are not fully understood. The limited information regarding their molecular mechanisms and transcriptional regulation enabling their survival include the cold adaptation is described in *Section 1.4*. They use the production of antifreeze and cold-active proteins, compatible solutes (glycerol, trehalose, sugar alcohols), and an increase in membrane fluidity (Gunde-Cimerman *et al* 2014; Hassan *et al* 2016) as their main strategies to overcome cold temperatures.

1.5.2 The cold-adapted yeast phylum, Basidiomycota

Even if the basidiomycetous yeasts are ubiquitous, many of them are found in extreme environments. They represent the majority of the yeast identified or isolated from cryoenvironments, such as glacial habitats (Turchetti *et al.* 2011). Overall, they represent 85% of the yeasts found in the worldwide cryosphere, with around one third represented by the *Cryptococcus* genus (Buzzini *et al.* 2012). Even though the predominance of the *Cryptococcus*

yeast, there is also prevalence of the *Rhodotorula* genus in many cold habitats (Buzzini *et al* 2012; Buzzini *et al.* 2017). Recently, the *Rhodotorula* genus undergone a fragmentation, but was historically characterized by numerous extremophiles, especially psychrophilic and psychrotolerant species, such as *R. aurantiaca*, *R. psychrophila*, *R. psychrophenolica*, *R. glacialis*, *and R. himalayensis* (Margesin *et al.* 2007; Sabri *et al.* 2000).

1.5.3 *Rhodotorula* JG1b, a polyextremophile yeast

More recently, the putative novel psychrotolerant *Rhodotorula* JG1b strain was isolated from ~150,000-year-old ice-cemented permafrost soil from University Valley, in the upper-elevation McMurdo Dry Valleys of Antarctica (Goordial *et al.* 2016b), one of the coldest and driest places on Earth (Marchant and Head III 2007). *Rhodotorula* JG1b was one of the only six microorganisms isolated form this ice-cemented permafrost, and showed signs of growth as low as -10°C (Goordial *et al* 2016a). In addition, *Rhodotorula* JG1b was found to tolerate up to 15% NaCl and 12% perchlorate (Goordial *et al* 2016b). These polyextremophiles characteristics of *Rhodotorula* JG1b, makes it an ideal microorganism for the study of cold adaptation in polar yeasts and to better understand how microorganisms could survive beyond Earth.

1.6 Research questions and objectives

Polar desert cryoenvironments provide natural laboratories to study and explore the field of cryobiology. The Canadian high Arctic is characterized by multiple high fidelity analog sites to astrobiology targets (Pollard *et al.* 2009) such as the polar desert on Cornwallis Island (Douglas and Smol 2000). The Antarctic Dry Valley is one of the coldest and driest locations on Earth (Marchant and Head III 2007). Novel microorganisms isolated from these environments such as *Rhodotorula* JG1b, are important for the comprehension of microbial cold adaptations in an

astrobiology context (Goordial *et al* 2016b). My M.Sc. thesis research program consisted of two separate projects as follows.

a. Project 1. I developed and tested a novel biosignature detection platform based on redox dye chemistry with the specific goal to detect metabolic activity form polar microorganisms and Astrobiology related analogue cryoenvironments, and consequently determine its utility to detect extant life on Mars and the icy moons. The main question that my research aimed to address was to determine if *metabolism-indicator redox dyes are suitable for detecting microbial activity from cryoenvironment Mars and icy moon analog sites?*

b. Project 2. My second project was focused on determining cold-adaptation strategies in the cryophilic Antarctic yeast strain Rhodotorula JG1B, isolated from University Valley permafrost. The main question of this project was to determine *what are the metabolic strategies of an Antarctic cold-adapted yeast to growth at cold temperatures?*

To answer these questions, the specific objectives of this thesis were:

1) To develop and field-test the microfluidics Microbial Activity MicroAssay (µMAMA), a novel life-detection platform based on metabolism-indicator redox dyes. My goal was to assess the potential of redox dyes to metabolically characterize and detect microbial life of cryoenvironments, by testing their robustness, sensitivity and automation (Chapter 2).

2) To identify and characterize the metabolic activity pathways and the regulatory mechanisms of *Rhodotorula* JG1b in response to cold. My goal was to physiologically characterize, assess the ethanol production capabilities, and to identify transcriptional changes using mRNA and miRNA transcriptomics in *Rhodotorula* JG1b grown under cold temperature (Chapter 3).

Connecting text

To answer the first research question, in chapter 2, I investigated the potential of redox dyes to metabolically characterize and detect microbial life of cryoenvironments. My overall objective was to develop and field-test the robustness and sensitivity of several redox dye and buffer combinations. In addition, I was in charge of designing a novel extant life-detection instrument, the microfluidics Microbial Activity MicroAssay (µMAMA), that would be suitable for detecting microbial metabolic activity with the selected redox dyes/buffer combinations on other planetary bodies. This chapter corresponds to the manuscript titled "*µMAMA: development of an automated in situ microbial metabolic detection platform*", which will be submitted to the *Astrobiology* journal.

Contribution of Authors: The manuscript was made in collaboration with Louis-Jacques Bourdages, Dr. Isabelle Raymond-Bouchard, Dr. Ianina Altshuler, and Dr. Lyle G. Whyte from McGill University. I wrote the manuscript, performed all laboratory experiments and data analysis. LJB helped with the engineering design. IRB helped with experimental design and manuscript editing. IA helped with the data analysis and manuscript editing. LGW provided guidance with the overall experiment design and manuscript preparation.

Chapter 2. µMAMA: development of an automated *in situ* microbial metabolic detection platform

D. Touchette[1], I. Raymond-Bouchard[1], L-J. Bourdages[1,2], I. Altshuler[1], and L.G. Whyte[1*]

[1]McGill University, Department of Natural Resource Sciences, Sainte-Anne-de-Bellevue, Québec, Canada.

[2]McGill University, Faculty of Engineering, Montréal, Québec, Canada.

2.1 Abstract

The search for extant life on other solar system bodies will be a major focus of astrobiology missions in the coming decades, especially on Mars, Europa, and Enceladus. In order to successfully detect potential life in these places, it is crucial to better study and understand life in astrobiology analog sites on Earth. With no direct extant life detection instrumentation included in a space mission since the Viking landers in the 1970s, it is imperative that we develop new life-detection technologies that can be included in future astrobiology-themed space missions and that can detect extant active microbial life forms. Here, we describe the development and testing of the microfluidics Microbial Activity MicroAssay (µMAMA), a prototype semi-automated life-detection instrument. The µMAMA platform is able to characterize metabolic activity and detect microbial life in a simple, low cost, and low energy method. We identified the AlamarBlue® buffered in IF-0a, and the Biolog IF-C dye/buffer combinations as the most sensitive to microbial metabolic activity, as low as 10^2 cells/ml, while offering a broad physiochemical range of usage.

We characterized the *in situ* and *ex situ* microbial communities of four astrobiology analog environmental samples from the Canadian high Arctic and evaluated the potential of metabolic redox dyes to detect activity from chemolithoautotrophic life forms. The µMAMA was capable of direct detection of extant and active cold-adapted microbial life, including from sulfate-oxidizing and Fe(II)-oxidizing metabolisms. These microorganisms and metabolisms are relevant as they are similar to the potential life forms that could be found beyond Earth. Given µMAMA's small size, simple design, and low energy requirements, we believe that it should be considered as a strong candidate for further automation and incorporation into larger platforms for future life detection missions on Mars, Europa, and Enceladus.

2.2 Introduction

The search for life on other planetary bodies will be a major focus of astrobiology missions in the coming decades, with Mars, Enceladus and Europa as the main targets (Hays 2015). These targets are characterized by extremely low temperatures and extreme environmental conditions that are much harsher for microbial life than those on Earth. Despite their apparent inhabitability, evidence of past and current habitats that could support extant microbial ecosystems on these planetary bodies have been described (Arvidson *et al* 2014; Garcia-Lopez and Cid 2017; Grotzinger *et al* 2014), largely based on our knowledge of the limits of microbial life in similar cryoenvironments on Earth.

Mars was considerably warmer and wetter ~ 4.5 to ~3.5 billion years ago, offering habitable conditions for many microorganisms (Arvidson *et al* 2014; Chevrier *et al* 2007; Grotzinger *et al* 2014; Westall *et al* 2013). The Mars Science Laboratory (MSL) mission has identified the Gale Crater as a past fluvial-lacustrine environment, with conditions that could

support a broad range of prokaryotic microorganisms (Grotzinger *et al* 2014), and could have preserved many biosignatures of a past microbial life. More interestingly, potential signs of brine water at Recurring Slope Lineae (RSL) on the modern day Mars surface (Ojha *et al* 2015) and of a polar saline subsurface lake at Mars' south pole (Orosei *et al* 2018) opens the possibility that Mars could currently support extant microbial ecosystems. The presence of microorganisms in an RSL analog site in Antarctica (Chan-Yam *et al* 2019), in the brine of the ice-sealed lake Vida in Antarctica (Murray *et al* 2012), and hypersaline subzero high Arctic springs in Canada (Lamarche-Gagnon *et al* 2015) further confirms the possibility of such microbial ecosystems in Mars RSLs. In addition, the discovery of cold and salty oceans under the ice surface of Europa and Enceladus, and the presence of organics in Enceladus' water vapor plumes (Carr *et al.* 1998; Waite *et al.* 2006) also suggests that there is potential for extant microbial life on these icy moons (Garcia-Lopez and Cid 2017).

Despite the importance of life detection in current planetary missions to Mars, no direct extant life detection instrumentation has been included in a space mission since the Viking landers in the 1970s (Davila *et al* 2010; Levin 1997). In addition, current scientific instruments related to astrobiology-targeted space missions are focused on the detection of biosignatures from past life and the identification of new habitable environments and are mainly large, heavy and require high levels of energy. The development of smaller, simple and portable instruments based on advances in microfluidics and nanotechnology that can be easily incorporated into future rovers and that are focused towards life-detection, is required. Recently, advances have been made in the design of extant life-detection instrument of smaller size, mass and energy requirements, such as the instruments SPLIce, which includes a mass spectrometer (Chin *et al.* 2018), and O/OREO, detecting metabolic activity from *Bacillus subtilis* spores in orbit (Nicholson *et al.* 2011). There

has been significant progress in the development of microfluidic systems for life sciences in space, such as O/OREO, BioSentinel, and nanopore sequencing on the International Space Station (ISS) (Castro-Wallace *et al.* 2017; Lewis *et al.* 2014; Matin *et al.* 2017; Nicholson *et al* 2011).

Metabolism-indicator redox dyes, such as AlamarBlue® (Rampersad 2012) and tetrazolium Biolog dyes (Bochner *et al* 2001; Bochner 2008), are able to detect changes in cellular metabolic activity through the chemical reduction of the dye by microbial cellular respiration (Hamid *et al* 2004). Essentially, the redox dyes are reduced by transfer of electrons produced by extant cellular metabolism leading to a change in coloration which is readily detectable. Since this technology is relatively simple, low-cost and highly sensitive, it is amongst the best candidates for the development and automation of an unambiguous microbial activity detection instrument. AlamarBlue® has already been tested in a space exploration context, as part of NASA's BioSentinel Project (Santa Maria *et al.* 2020) and O/OREO (Nicholson *et al* 2011), and the Biolog system using has already been successfully tested in an analog environment (Goordial *et al* 2017).

Here, we describe the development and testing of the microfluidics Microbial Activity MicroAssay (μMAMA), a life-detection platform able to metabolically characterize and detect extant microbial life. It is designed based on the metabolism-indicator redox dyes and tested through a combination of laboratory and field work analyses. The signal robustness of six redox dye/buffer combinations was determined by characterizing the physiochemical range and limits in which these redox dyes can be used. This was done to assess the environmental conditions in which these dye/buffer combinations would detect life without false positive results. Then, we tested the sensitivity of these dye/buffer combinations to identify the lowest initial number of cells (bacteria/yeast) required to obtain a strong metabolic activity signal. This was done to assess the lower limits of detection to help identify potential false negative results. For the sensitivity assays

we used pure cultures of the cryoenvironment model extremophiles, namely *Planococcus halocryophilus* which is capable of growth at the coldest temperature recorded (Mykytczuk *et al* 2013), and *Rhodotorula* JG1b, a psychrotolerant yeast isolated from ~150,000-year-old ice-cemented permafrost soil from University Valley of Antarctica (Goordial *et al* 2016b). The most sensitive and robust dye/buffer combinations were then tested with environmental samples from four analog sites in the Canadian high Arctic. Finally, we incorporated two redox dye/buffer combinations in a unique machined and semi-automated µMAMA card and successfully detected microbial activity using samples from our extreme analog environments. We complemented these tests by determining the microbial functional diversity of these environments with conventional methods in order to compare the results with the µMAMA platform.

2.3 Material and Methods

2.3.1 Laboratory-based metabolic redox dye selection

We tested a set of metabolic redox dyes and buffer combinations to determine their robustness and sensitivity in detecting microbial activity. We characterize robustness as the range of physiochemical parameters at which the dye can still detect activity without providing false positive and sensitivity as the lowest concentration of cells necessary for positive detection of activity. We selected the following dye/buffer combination for testing: the **AlamarBlue®** redox dye (Bio-Rad, Hercules, CA, United States) buffered at 10% in either H_20 (referred to as AB-H_2O in this manuscript), 0.1% $Na_4P_2O_7$ saline solution (AB-$Na_4P_2O_7$), or the Biolog IF-0a buffer (AB-IF0a), and a set of commercially available **Inoculating Fluids** that have the redox dye and buffer premixed, the IF-A, IF-B, and IF-C dye/buffer combination (BIOLOG, Hayward, CA, United States R#72401, 2402, 2403, 72268). In order to determine robustness of the signal, each dye/buffer combination was incubated 14 days in 96-well plates with a gradient of salinities (NaCl

and $NaClO_4$ 0%, 10%, 20%, and 30%), a gradient of pHs (0 to 14), and Mars analog soil simulant (MMS-2, The Martian Garden, Austin, TX, United States). Each of the 24 conditions were performed in duplicate and were performed at multiple temperatures (37°, 23°C, 5°C and -10°C).

To determine minimal initial concentration of cells needed for detection of activity (sensitivity), the dyes were incubated at 23°C for 14 days in 96-well plates with increment concentrations of the extremophile microorganisms *Plannococcus halocryophilus* (bacteria), and *Rhodotorula* JG1b (yeast). *P. halocryophilus* was cultured in TSB media 50ml liquid cultures (BD Biosciences, Franklin Lakes, NJ, United States), and *Rhodotorula* JG1b was cultured in PDB media 50ml liquid cultures (HIMEDIA, Shenzhen, China), before being transfer to 96-well plates for the sensitivity assay. These media were used as substrates to trigger the metabolic activity. The inoculum ranged from 0 to $5.04x10^7$ cells/ml for *P. halocryophilus* and from 0 to $1.99x10^7$ cells/ml for *Rhodotorula* JG1b. The concentrations were initially determined by colony-forming units (CFUs) count.

2.3.2 Study site and sampling

Our study sites are located near the Polar Continental Shelf Program facilities (PCSP), at Resolute Bay, on the Cornwallis Island in the Canadian high Arctic (74°42' N, 94°49). Resolute Bay has a mean annual temperature of -15.7°C, with a minimum average of -32.4°C in February and a maximum average of 4.5°C in July (Environment Canada 2014). Resolute Bay is a polar desert (≤ 250 mm annual precipitation; (Douglas and Smol 2000)), and is located in proximity to relevant astrobiological analog sites. A variety of samples were collected for this study: gravel soil from the rocky active layer above permafrost (GS), lake sediment (LS), fresh stream water (STW) and brackish sea water (SW). All samples were collected either using ethanol-sterilized metal sampling tools and were placed into sterile Whirl-Pak® bags (soil samples) or collected with sterile plastic

serological pipettes and placed into 1L sterile Nalgene™ bottles (liquid samples). Samples were kept at 5°C while conducting *in situ* analysis at the study site and were placed at -20°C for their transportation back to our McGill facilities. Samples were stored at -20°C in between subsequent experiments.

2.3.3 Characterization of microbial communities

Viable microorganism counts were determined for each sample type using the aerobic heterotrophic plate count method on R2A agar (BD Biosciences, Franklin Lakes, NJ, United States). Soil samples (LS, GS) were processed as follows: 5 g of soil was diluted with 15 ml of 0.1% $Na_4P_2O_7$ saline solution (1:4 dilution) and combined with 2.5 g of 3 mm glass beads. Samples were vortexed for 2 min, diluted 10-fold and plated on six replicate R2A agar plates. Water samples (SW, STW) were processed as with the soil samples without the initial dilution with $Na_4P_2O_7$. For each sample, a set of triplicate plates was incubated at 23°C for two weeks, and a set was incubated at 4°C for four weeks, before counting CFUs.

Microbial functional and metabolic diversity of each sample was assessed using the Biolog EcoPlates consisting of 31 different carbon substrates in triplicate. Samples were prepared as for the viable counts experiment and 100 µl of the processed samples were added to each well of the EcoPlates. For each sample, one EcoPlate was incubated at 15°C at the McGill facilities and one EcoPlate was incubated at 23°C in the field, at the PCSP facilities. For the 15°C plates, well colour change was monitored by measuring the absorbance at 590 nm on a SpectraMax M2e microplate reader (Molecular Devices, San Jose, CA, United States). Calculations of the average well-color development (AWCD), substrate richness (R), and Shannon-Weaver diversity index (H) were performed as per (Iţcuş *et al* 2016), with $AWCD = \sum OD_i/31$, R = number of metabolized substrates (positive OD readings), and $H = -\sum p_i(\ln p_i)$, where $p_i = OD_i/\sum OD_i$ (Garland and Mills 1991; Iţcuş

et al 2016). The measurements were normalized by the subtraction of both the T_0 and the negative control. Absorbance values ≥ 0.2 were considered as positive values, as per (Rico and Preston 2008). R and H parameters were calculated after 22 days of incubation, once the AWCD hit a plateau phase (Pessi *et al.* 2009). Due to the absence of a spectrophotometer in the field, well colour change for the 23°C plates were monitored after a 4-days incubation by taking photographs of the plates with a Canon EOS 6D camera with the same settings and in identical light conditions. The plates images were analyzed with the ImageJ 1.52 program (Schneider *et al.* 2012), were a numeric value of the color intensity (histogram) of each well was determined. We modified the values using 1/(mean value of the histogram) to obtain a positive correlation between the color intensity value and the color development of the well. R and H indexes were calculated as described above, with values ≥ 0.002 considered as positive values.

2.3.4 Environmental-based metabolic redox dye sensitivity testing

We determined the detection sensitivity of the two most robust dye/buffer combinations (AB-IF0a and IF-C) with complex environmental samples (LS, GS, SW, and STW). This was done by incrementally diluting and incubating the LS, GS, SW, and STW samples in 96-well plates containing previously dehydrated R2A and IF-0a in each well. One redox dye was added to each sample, so either with 10% AlamarBlue®, to form the AB-IF0a combination, or with 1% Biolog Dye Mix G (Biolog R#74227), to form the IF-C combination. The samples were prepared as described for the viable count (section 2.3). Values for the concentration of cells were based on the CFU counts described above and varied from 0 to $1.1x10^7$, 0 to $3.7x10^6$, 0 to $2.5x10^3$, and 0 to $2.6x10^4$ of viable microorganisms per millilitre for the LS, GS, SW, and STW samples respectively. The viable number of cells required to reduce AB-IF0a and IF-C were adjusted to predicted the total concentration of cells, considering that only 5% of the microbial life in

permafrost soil samples and 0.5% of microbial life in water samples can be cultured (Junge *et al* 2002; Zhang *et al.* 2013a).

2.3.5 Technical design of the µMAMA cards

The µMAMA cards designed in our laboratory and presented here (**Figure 2.1**) aim to combine the ease of use, simple design, affordability, and sensitivity of Biolog plates, while incorporating this concept into a more robust and automated system that could have applications for planetary exploration. The µMAMA well plates and the lids were created with low resource overhead using milled CNC polycarbonate (McMaster-Carr Elmhurst, IL, United States R#1749K529). The card has a length of 50.8 mm, a width of 47.0 mm, and a height of 12.7 mm. The lid of the card is 5.56 mm thick and covers the surface of the card. It is fastened to the card using 4 6-32 stainless steel screws (**Figure 2.1**). Machining the shape of the card and its wells results in more accurate measurements for the dimensions of the wells and smoother surfaces to ensure that the final volume of the wells is precise. Polycarbonate is also resistant to shattering and warping damage. The smooth finish allows the implementation of a sealing method for the wells of the plate by a silicone gasket fabricated by molding a liquid silicone (Smooth-On Dragon Skin™ 30) compound into a shape adapted to the well plate. This gasket, when squeezed between the well plate and its lid, forms a perfect seal for each individual well and stop any exchange of fluid with the environment (**Figure 2.1**). Each set of eight wells is connected internally to allow for the automated filling of the wells. The seal is effective due to the smooth surface of the machined sealing surfaces. Finally, our µMAMA is designed with automation in mind, and provided threaded ports for easy interfacing with tubing. Miniature barbed fittings (McMaster-Carr R#5463K2) and 0.125-inch OD transparent plastic tubing (McMaster-Carr R#5155T12) were used in this study and were connected to a miniature peristaltic pump (Takasago electric, Nagoya, Japan,

RP-QIIIX1.5S-2P2Z-DC3V). Peristaltic pumps can both prevent backflow and distribute precise amounts of fluids, two characteristics that were desired in this application. The peristaltic pump required to distribute liquid into the wells is very small, with low energy requirements, and thus can be powered using small and common source such as standard AA or 9-volt batteries. Even with such low energy requirements, the wells were filled in less than a minute.

2.3.6 µMAMA testing with environmental samples

To assess the metabolic activity detection capabilities of the µMAMA, we prepared the µMAMA cards and incubated them with the same environmental samples as described above. The µMAMA cards were washed, incubated for 20 minutes in 70% ethanol, and autoclaved. 200 µl of IF-0a was dehydrated in each well in a sterile environment. Since microorganisms that inhabit analog extreme environments are likely to be adapted to oligotrophic growth conditions (Song *et al.* 2016; Vartoukian *et al.* 2010), we included a range of substrate amendments targeting a variety of heterotrophic microorganisms, ranging from very poor nutrient (no amendment, Minimal media, 1/10 R2A, 1/3 R2A) to very rich nutrient (PDB, TSB) conditions. Since chemolithoautotrophic life may be the most likely candidate for microbial life forms on Mars' subsurface environment (Michalski *et al* 2018), we also included amendments with no carbon sources. In order to detect metabolic activity from chemolithoautotrophs, we included a thiosulfate media targeting sulfate-oxidizing bacteria (Taylor and Hoare 1971) and a mineral media targeting Fe(II)-Oxidizing bacteria (Hohmann *et al.* 2009). Iron and sulfate-based metabolisms have been suggested to be likely important metabolisms, amongst other, for potential microbes in Mars subsurface given the presence of sulfur and of the iron-rich Basalt mineral, widely spread on Mars (McCollom 2006; McSween *et al.* 2009). Therefore, to be able to detect a variety of metabolisms, two sets of wells were inoculated in each µMAMA card and dried in a sterile environment with a substrate mix as

follows (**Figure 2.1**): wells 2 and 15 were inoculated with minimal media (Min. Media, ATCC Medium 2511), wells 3 and 14 with 1/10 R2A, wells 4 and 13 with 1/3 R2A, wells 5 and 12 with PDB, wells 6 and 11 with TSB, wells 7 and 10 with thiosulfate media (Thio., (Taylor and Hoare 1971)), and wells 8 and 9 with iron-oxidizer media (Iron oxid., (Hohmann *et al* 2009)). No substrate amendment was added to wells 1 and 16. The same pattern was repeated in a 96-well plate as a technical replicate. LS, GS, SW, and STW samples were processed as previously described, and amended with either 10% AlamarBlue® or 1% Biolog Dye Mix G. The four prepared samples, and a sterile 0.1% Na4P2O7 saline solution (control), were inoculated in the µMAMA cards with the RP-QIIIX1.5S-2P2Z-DC3V peristaltic pump, and in the replicate 96-well plates. Following filling of the wells, the µMAMA miniature barbed fittings were sealed with tubing and incubated at 23°C for 14 days.

2.3.7 Plates incubations and OD measurements

For the incubations, all the plates were sealed with a paraffin film and placed in Whirl-Pak® bag containing a wet paper towel to avoid dryness of the wells, and protection from light. OD_{570}, and OD_{590} of the plates was measured to assess the redox dye reduction on a SpectraMax M2e microplate reader (Molecular Devices, San Jose, CA, United States). The measurements were normalized by the subtraction of the negative control (no physiochemical modification, no microorganisms or no environment sample inoculation) and by the subtraction of the T_0. For the AlamarBlue® redox dye, we assigned a cut-off of ΔOD_{570} values ≥ 0.15 with a p-value < 0.05 to be considered as positive reduced values, for the Biolog redox dye, ΔOD_{590} values ≥ 0.20 with a p-value < 0.05 were considered as positive reduced values (Rico and Preston 2008). For IF-A sensitivity testing, the metabolic activity detection was determined by visual inspection of the wells color change only.

2.4 Results

2.4.1 Signal robustness and sensitivity of dye/buffer combinations

The physiochemical incubation parameters where we did not detect artificial chemical reduction of the dye/buffer combination, leading to false positives, are summarized in **Table 2.1**. The dye/buffer combinations tested varied in their tolerance to different pH conditions (**Table 2.1**). The AB-H_2O and AB-IF0a were found not significantly chemically reduced by pH 4 to 13, while the AB-$Na_4P_2O_7$ was not significantly chemically reduced by pH 3 to 13 (**Figure 2.2**). The Biolog IF-B and IF-C incubated in pH 14 was found to be chemically reduced (**Figure 2.3**). Although not significant, we observed a considerable change in the IF-B and IF-C stability at pH 13, and in the IF-A stability in pH 13 and 14. When incubated at different temperatures (-10, 5, 37°C), all dye/buffer combinations remained in their original form, with the exception of the AB-H_2O that showed a significant chemical reduction when incubated at 37°C (**Table 2.1**). All six combinations of redox dye/buffer combinations remained in their original oxidized form after a 14-day incubation with a range of NaCl concentrations (10, 20, 30%), $NaClO_4$- concentrations (10, 20, 30%), and the Mars analog soil MMS-2 (**Table 2.1**).

Table 2.1. Summary of the physiochemical conditions of detection at which no artificial chemical reduction (robustness) was observed, and the lowest initial microbial inoculation required for detection of dye reduction (sensitivity) of each dye/buffer combinations

		AlamarBlue®			Biolog dyes (tetrazolium)		
	Conditions	**H_2O**	**$Na_4P_2O_7$**	**IF-0a**	**IF-A**	**IF-B**	**IF-C**
Robustness tests	Temperature (Tested: -10, 5, 23, 37°C)	-10 to 23	-10 to 37	-10 to 37	-10 to 37	-10 to 37	-10 to 37
	NaCl and $NaClO_4$ (Tested: 0, 10, 20, 30%)	All tested	All tested	All tested	All tested	All tested	All tested
	pH (0 to 14)	4 to 13	3 to 13	4 to 13	All	0 to 13	0 to 13
	MMS-2 simulant test	Yes	Yes	Yes	Yes	Yes	Yes
Sensitivity (min. cells/	*P. halocryophilus*	No detection	2.52 x 10^7	252	252 *	2520	504
	Rhodotorula JG1b	100	199	100	9.95 x 10^7 *	100	199

* The IF-A dye reduction for each cell concentration was based on visual verification only.

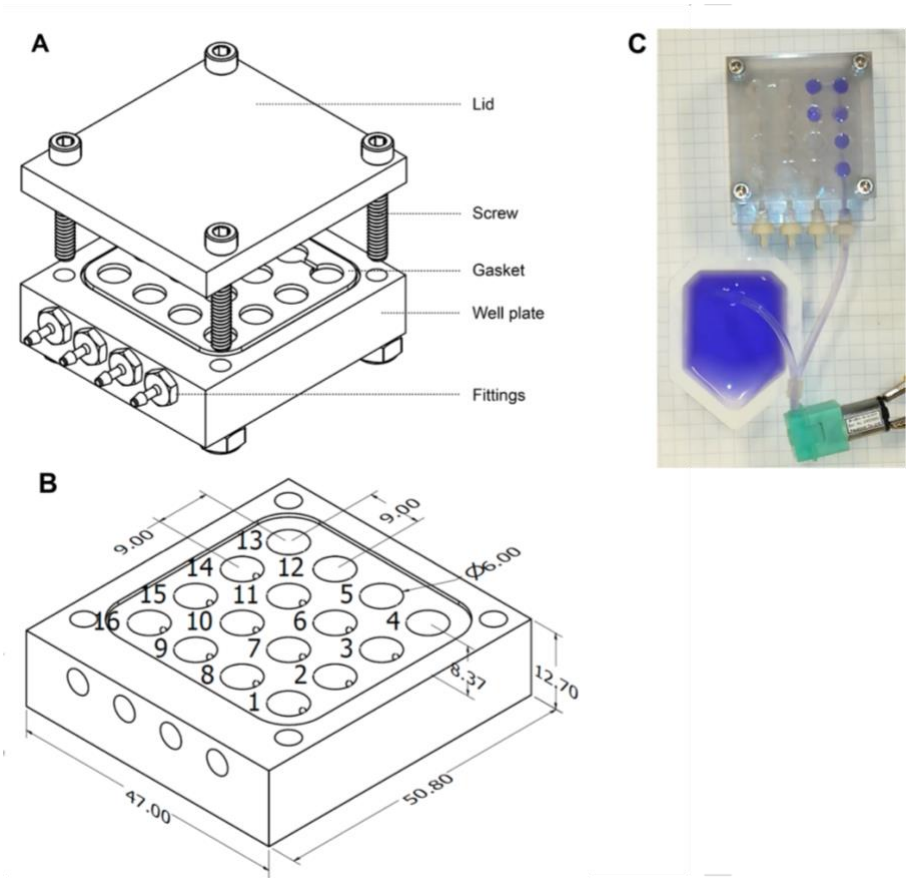

Figure 2.1. Technical design of the µMAMA cards
(**A**) Main components of the µMAMA cards. (**B**) µMAMA well plate identification and dimensions (in millimetres). (**C**) Example of inoculation of the µMAMA with the miniature peristaltic pump.

Microbial detection limit (sensitivity) of the six redox dye/buffer combinations is summarized in **Table 2.1**. The AB-H_2O dye/buffer combination was reduced by as low as 100 cells/ml of *Rhodotorula* but was not reduced by any concentration of *P. halocryophilus* tested. The AB-$Na_4P_2O_7$ and AB-IF0a dye/buffer combinations were significantly reduced by ~200 cells/ml and 100 cells/ml of *Rhodotorula*, respectively, and by $2.52x10^6$ cells/ml and 252 cells/ml of *P. halocryophilus* respectively. The Biolog IF-B, IF-C, and IF-A redox dye/buffer combinations were significantly reduced by 100 cells/ml, ~200 cells/ml, and $9.95x10^6$ cells/ml of *Rhodotorula*

respectively, and by 252x10$_3$ cells/ml, 504 cells/ml, and 252 cells/ml of *P. halocryophilus* respectively.

Figure 2.2. AlamarBlue® redox dye and buffers combinations stability under a pH gradient

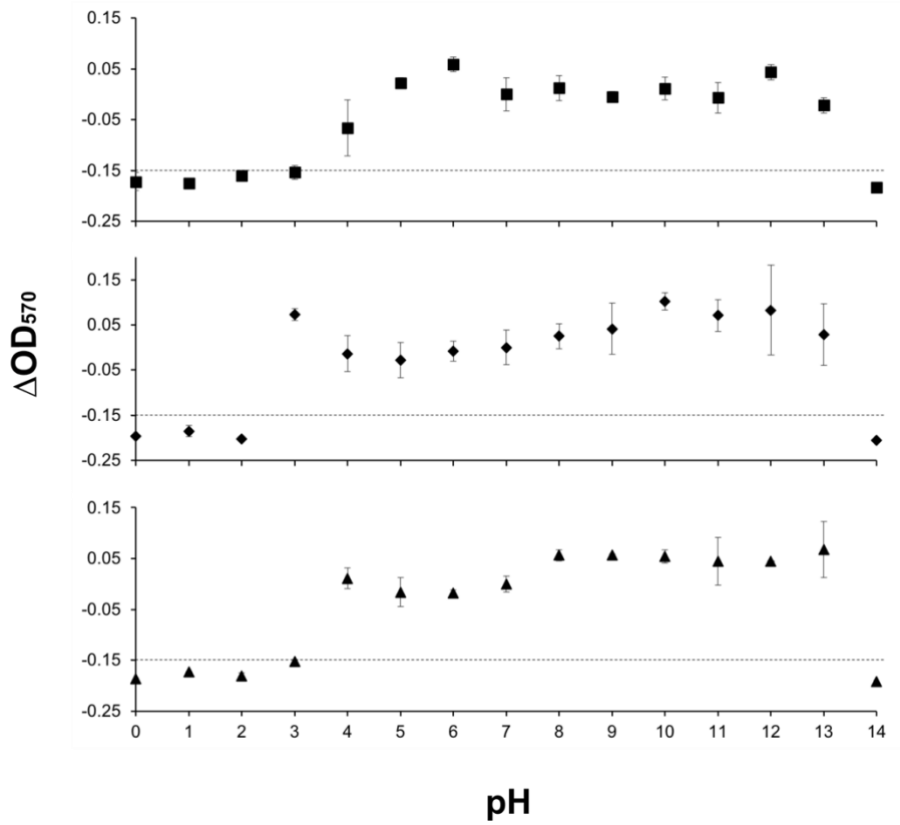

Squares indicate values for the AB-H_2O combination, diamonds indicate values for the AB-$Na_4P_2O_7$ combination, triangles indicate values for the AB-IF0a combination. Dashed lines indicate the ≥ -0.15 threshold cut-off of chemical reduction of the dye; values below the threshold indicate a false positive reaction due to pH, values above the threshold indicate pHs under which the AlamarBlue® does not give a false positive. The error bars are based on the standard deviation.

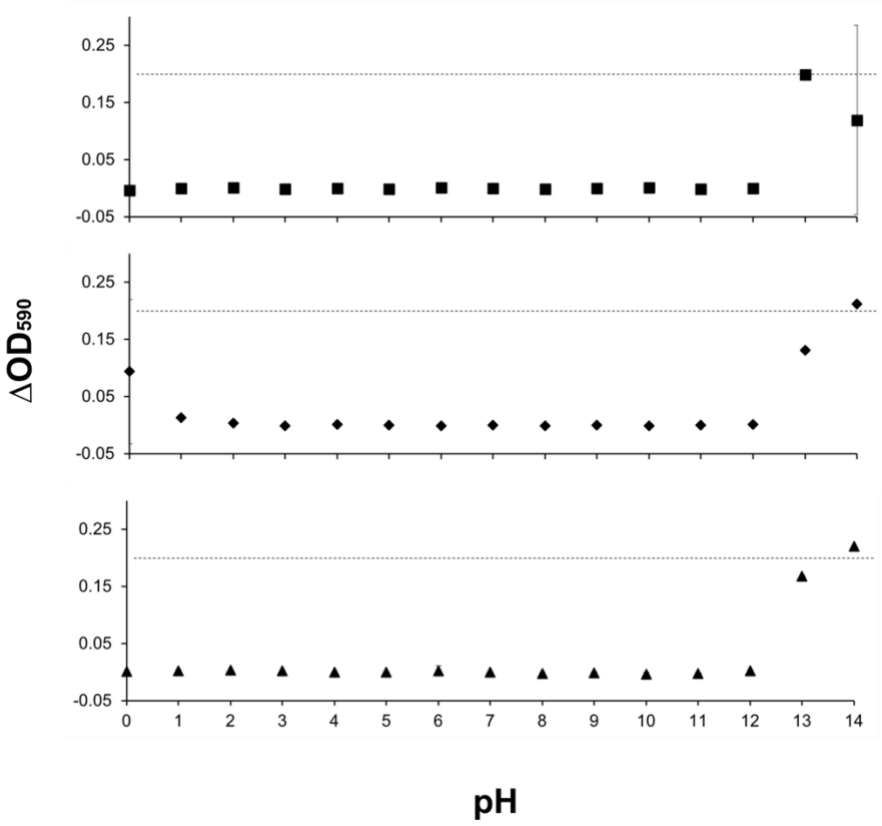

Figure 2.3. Biolog redox dye and buffers combinations stability under a pH gradient
Squares indicate values for the IF-A combination, diamonds indicate values for the IF-B combination, triangles indicate values for the IF-C combination. Dashed lines indicate the ≥ 0.20 threshold cut-off of a chemical reduction of the dyes; values above the threshold indicate a false positive reaction due to pH, values under the threshold indicate pHs under which the Biolog dyes do not give a false positive. Even if really small, the error bars present are based on the standard deviation.

2.4.2 Characterization of microbial communities from analog sites

To characterize the microbial communities, viable microorganism counts were performed for each sample. Both soil samples (lake sediment, gravel soil) had a higher number of viable cells/ml than the water samples (sea and stream water) (**Table 2.2**). In addition, the soil samples had a higher number of cells at 23°C than 5°C. The opposite phenomenon was observed with water samples, where the viable biomass was lower at 23°C compared to 5°C (**Table 2.2**).

Table 2.2. Environmental characterization of analog environmental samples

Sample	GPS coordinates	*In situ* temperature (°C)	Viable biomass (CFUs/ml)		Viable sensitivity (min. CFUs/ml)		Predicted sensitivity (min. CFUs/ml)	
			5°C	23°C	AB-IF0a	IF-C	AB-IF0a	IF-C
Lake sediment (LS)	N74°42.980 W095°00.697	3.61	9.1×10^6	1.1×10^7	9.6×10^4	1.1×10^5	1.9×10^6	2.2×10^6
Gravel soil (GS)	N74°42.976 W095°00.402	2.60	3.7×10^7	1.7×10^6	3.3×10^3	3.7×10^3	6.6×10^4	7.4×10^4
Sea water (SW)	N74°44.553 W095°03.578	0.27	2.5×10^3	4.3×10^3	6	3	1.2×10^3	6.0×10^2
Stream water (STW)	N74°42.981 W094°59.905	3.19	2.6×10^4	3.9×10^4	15	16	3.0×10^3	3.2×10^3

To further characterize the microbial communities, the metabolic diversity was assessed using the Biolog EcoPlates. There was no specific pattern of carbon utilization detected, with the exception of D-xylose that was not used as a sole carbon source by any microbial communities. Tween 80 was the only substrate used by all microbial communities, with the exception of the sea water 15°C sample. Substrate Richness (R) and Shannon-Weaver diversity index (H) for each sample type using EcoPlates incubated at 23°C and 15°C are summarized in **Figure 2.4**. An overall increase in microbial functional diversity (R and H) was noted for sea water, lake sediment, and stream water samples with increase in temperature (**Figure 2.4**). Contrarily, we observed a significant decrease in microbial functional diversity (R and H) with increase in temperature in the gravel soil sample (**Figure 2.4**).

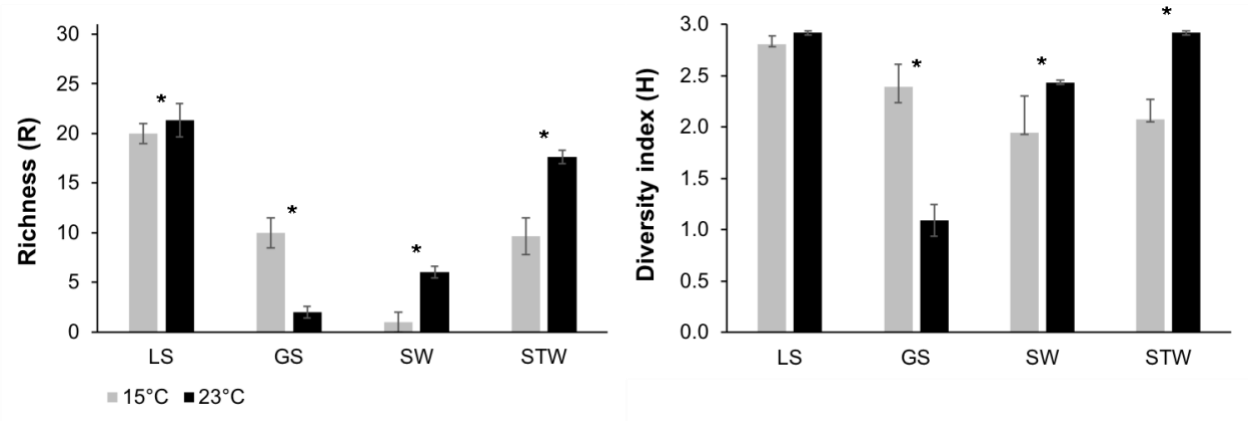

Figure 2.4. Microbial functional diversity of high Arctic analog samples assessed with the Biolog EcoPlates

Biolog EcoPlates were incubated with Lake Sediment, Gravel Soil, Sea and Stream Water samples at 15°C (light gray) and 23°C (black). Substrate richness (R) and the Shannon-Weaver diversity index (H) were calculated as described in *Materials and Methods.* Significant difference ($p \leq 0.05$) between the temperatures of each sample is denoted with a star. Error bars are based on SEM.

2.4.3 Signal sensitivity of dye/buffer combinations with analog samples

Two of the six dye/buffers combinations, AB-IF0a and IF-C, were determined to be both robust and sensitive in detecting activity using pure cultures, based on section 2.4.1 results. These two dye/buffers combinations were then tested for their sensitivity using the four environmental samples and the results are summarized in **Table 2.2**. The minimum number of cells needed to reduce AB-IF0a dye/buffer combination was 1.9×10^6 cells/ml for lake sediment, 6.6×10^4 cells/ml for gravel soil, 1.2×10^3 cells/ml for sea water, and 1.2×10^3 cells/ml for stream water (**Table 2.2**). To reduce the IF-C dye/buffer combination, the minimum number of cells needed was 2.2×10^6 cells/ml for lake sediment, 7.4×10^4 cells/ml for gravel soil, 600 cells/ml for sea water, and 3.2×10^3 cells/ml for stream water (**Table 2.2**).

2.4.4 µMAMA testing with environmental samples

We compared the ability of µMAMA to detect metabolic activity in environmental samples with OD measurements of a mock 96-well plate under the same incubation conditions, using the AB-IF0a and IF-C dye/buffer combinations. After a 14-day incubation at 23°C, we observed reduction with a variety of substrate combinations (**Table 2.3**). For the AB-IF0a dye/buffer combination, we detected significant reduction of the dye under all incubation conditions (including no substrate amendment) for the gravel soil sample, while for lake sediment and stream water we detected reduction with 100% TSB, 100% PDB, 1/3 R2A, 1/10 R2A, Min. Media, and no substrate amendment. The sea water sample only showed reduction of 100% TSB and 100% PDB with the AB-IF0a dye/buffer combination. For the IF-C dye/buffer combination, we detected significant reduction of the dye with 100% TSB, 100% PDB, 1/3 R2A, and Min. Media substrates for the gravel soil, lake sediment and sea water samples, while the stream water sample showed reduction with 100% TSB, 100% PDB, 1/3 R2A, 1/10 R2A and Min. Media conditions.

Table 2.3. µMAMA card tested with environmental analog samples and different substrates
The results are organised based on the substrate amendment of the µMAMA card. Grey squares indicate a metabolic activity detection, white squares indicate that no activity was detected.

Sample	Redox dye/buffer comb.	Substrate amendment							
		No amend.	Min. Media	1/10 R2A	1/3 R2A	PBD	TSB	Thio.	Iron oxid.
Lake sediment (LS)	AB-IF0a	■	■	■	■	■	■		
	IF-C		■		■	■	■		
Gravel soil (GS)	AB-IF0a	■	■	■	■	■	■	■	■
	IF-C		■		■	■	■		
Sea water (SW)	AB-IF0a					■	■		
	IF-C		■		■	■	■		
Stream water (STW)	AB-IF0a	■	■	■	■	■	■		
	IF-C		■	■	■	■	■		

No amend.: no substrate amended, Min. Media: minimal media, 1/10 R2A: 10% strength of regular R2A media, 1/3 R2A: 33.3% strength of regular R2A media, Thio: thiosulfate media, Iron: iron-oxidizer media.

2.5 Discussion

2.5.1 AB-IF0a and IF-C dye/buffer combinations, best candidates for use in analog sites

We evaluated different combinations of redox dyes and buffers for their application in astrobiology analog sites. We tested the robustness, that is the ability to detect activity over the greatest range of physiochemical parameters without providing a false-positive dye reduction, and the sensitivity, that is the lowest amount of initial cell concentration required to detect a signal of metabolic activity, for six combinations of redox dye and buffer.

According to our results, the AB-H_2O was the only dye/buffer combination that gave a false positive reduction due to an exposure at 37°C, therefore, it was not selected for tests with the µMAMA. None of the sodium chloride and sodium perchlorate concentrations, nor the incubation with the Martian analog soil, gave a false positive chemical reduction of any dye-buffer combination tested. This is promising as perchlorate is abundant on Mars surface (Catling *et al.* 2010), and multiple astrobiologically relevant extraterrestrial sites are characterized by salty environments (Garcia-Lopez and Cid 2017). False positive dye reduction was observed in some of the more extreme pH treatments tested (**Table 2.1**). While our results demonstrate that AlamarBlue® in combination with all three buffers tested could be used in pH conditions ranging from 4 to 13. The only exception was the AB-$Na_4P_2O_7$ combination, which also worked down to pH 3, but not below (**Table 2.1, Figure 2.2**). Contrastingly, all Biolog dye/buffer combinations worked across a much broader range of pH environments, especially in the more acidic conditions (pH < 4) (**Table 2.1, Figure 2.2**). Given that Mars analog environments on Earth have a broad range of conditions, including the extremely acidic environments of the Rio Tinto river with a pH of 2.3 (Gómez *et al.* 2011; Sánchez-García *et al.* 2020), the Biolog dyes would seem to be the most versatile candidates for detection of metabolic activity in acidic analog environments.

We identified AB-IF0a and the IF-C dye/buffer combinations as the most sensitive, requiring fewer cells to provide a significant reduction of the dyes (**Table 2.1**). AlamarBlue® buffered with H_2O and IF-0a was more sensitive to the *Rhodotorula* yeast than when buffered with $Na_4P_2O_7$ (**Table 2.1**). In addition, the AB-IF0a was the only AlamarBlue® based combination able to detect low concentrations of the *P. halocryophilus* bacteria, with as low as 252 cells/ml (**Table 2.1**). Therefore, AB-IF0a is the most sensitive dye/buffer combination, for the AlamarBlue® dye, making it viable for use with µMAMA in analog sites. For Biolog dyes, although the IF-A combination was reduced with the lowest number of bacteria, this dye was not found to be sensitive with yeast cells (**Table 2.1**) disqualifying it for future use. The IF-C combination overall required the least number of cells (bacterial and yeast) to detect metabolic activity, thus identifying it as the best Biolog dye/buffer combination to be used with µMAMA and analog sites.

Overall, the AB-IF0a was more sensitive that IF-C, but had a narrower usable pH range, this suggests that IF-C dye/buffer combination is more ideal for acidic analog environments, while AB-IF0a dye/buffer combination is more ideal for lower biomass analog environments. Fortunately, both dye/buffer combination did detect metabolic activity with fewer than 1000 cells/ml. This cell concentration is closely representative of the most extreme and low biomass environments on our planet, including the Antarctic RSL-like water track, Antarctic permafrost, and deep subsurface ground water of the Savannah River, all of whom have 10_3 cells/g (Chan-Yam *et al* 2019; Goordial *et al* 2016a; Hazen *et al.* 1991). Since IF-C and AB-IF0a were able to detect activity at these low concentrations, we believe these metabolism-indicator redox dyes have great potential to be used for unambiguous microbial activity detection in very low biomass analog environments. Because of this, IF-C and AB-IF0a were selected as the most *robust* and *sensitive* dyes and used in the subsequent µMAMA field-testing experiments.

Our results are in accordance with previous studies on redox dye sensitivity. AlamarBlue® is commonly used to assess cell viability and enumeration (Rampersad 2012) and is able to accurately enumerate the cell concentration with as low as 10^2 cells/ml (Shiloh *et al.* 1997). It has previously been shown to be more sensitive than tetrazolium dye (ie. Biolog dyes) (Hamid *et al* 2004). Here we demonstrated that unlike with pure cultures, environmental samples require more cells to detect metabolic activity with both AlamarBlue® and Biolog dyes (**Table 2.1** and **Table 2.2**). Moreover, AlamarBlue® has shown to be gradually reduced in absence of cells over time (Munshi *et al.* 2014), indicating the importance of the control conditions for background measurement. The optimal conditions for AlamarBlue® were previously determined to be in a pH range of 7.0 and 7.4, at 37°C for a 4 hours incubation period (Rampersad 2012), but no studies have previously analysed the physiochemical range and the possible false positives of this redox dye. Contrary to previously studies, we showed that AlamarBlue® in combination with IF-0a buffer can also be utilized in a broader range of condition than these ideal conditions, such as high salinity and perchlorate concentration, low temperature and pH 4 to 13.

A cell density of 10^8 cells/ml (Konopka *et al.* 1998) is recommended for the Biolog products, but a minimum of 10^4 cells/ml inoculum has previously been identified in being able to reduce Biolog dyes (Insam *et al.* 1996; Van Heerden *et al.* 2002). Contrary to this, we have determined that as few as 100 cells is required to reduce Biolog dye. While the Biolog products are designed for environmental samples, they can still be reduced abiotically, according to the manufacturer, mainly by substrate amendments. In addition, high temperature and high pH are found to change the dyes stability, especially the easily reduced ones such as the IF-C.

2.5.2 Environmental characterization of Arctic analog sites

Our investigation identified the presence of viable microorganisms in all our samples, ranging from 3.7 x 10^7 to 2.5 x 10^3 CFUs/ml, similar to other permafrost-associated active layer samples (Altshuler *et al* 2017; Zhang *et al.* 2013b) and to Arctic sea water samples (Gilichinsky *et al.* 2008; Junge *et al* 2002). We observed a decreased in viable counts from the Gravel Soil sample when incubated at the warmer temperature of 23°C, indicating that cold-adapted microorganism in this specific site may be sensitive to higher temperatures (**Table 2.2**) and suggesting a potentially higher proportion of psychrophilic microorganisms in that environment, since the optimum temperature of psychrophile is normally below 15°C (Cavicchioli *et al.* 2002). In contrast, we detected a slight increase in cultured microorganisms at 23°C for the lake sediment, sea and stream water samples (**Table 2.2**), suggesting these sites may harbour more psychrotolerant microorganisms (cold-adapted with an optimum temperature above 15°C) (Cavicchioli *et al* 2002). With our overall low R values (21.33-1.00) and H values (2.92-1.08), our samples have low functional diversity similar to other cryoenvironments, such as ice from the Scărişoara Ice Cave (Iţcuş *et al* 2016), the Hans and Werenskiold Glaciers ice and cryoconites (Grzesiak *et al* 2015a), permafrost soils from Alaska and Canadian high Arctic (Ernakovich and Wallenstein 2015; Goordial *et al* 2017), cold lakes freshwater of Patagonia (Mackenzie *et al* 2011), and ice from the Ecology Glacier ablation zone of Antarctica (Grzesiak *et al* 2015b). Higher R and H values of our samples at the warmer temperature suggests that they also have a higher functional diversity at 23°C (Iţcuş *et al* 2016). Since we observed a temperature-dependent difference in functional diversity and viability with our cryoenvironment samples, we believe that future incubations using astrobiological target samples should include a range of temperatures to capture the greatest metabolic diversity of these potential habitats.

We wanted to test the sensitivity of the two best redox dye/buffer combinations (AB-IF0a and IF-C) with analog environmental samples. Since conventional cultivation methods allows for the growth of only a small subset of microorganisms, we adjusted our viable count to a predicted total concentration of cells, as explained in *Material and Methods*. We did not observe a major difference of sensitivity between the AB-IF0a and IF-C dyes (**Table 2.2**). For both dyes, we noticed a change from 10^2 cells/ml sensitivity using pure cultures to a 10^2 - 10^3 cells/ml using water samples, and 10^4 - 10^6 cells/ml using soil samples (**Table 2.2**). This suggests that redox dyes are more sensitive to, and more suitable for, water samples than soil samples. Furthermore, due to this discrepancy between pure culture and environmental samples, care should be taken when determining dye/buffer sensitivity based on pure cultures.

2.5.3 Metabolic detection using the µMAMA

Using the two most promising dye/buffer combinations (AB-IF0a and IF-C), we assessed the metabolic detection capabilities of the semi-automated µMAMA cards. Metabolic activity was successfully detected from extant microbial life through the µMAMA platform. Based on our results, the rich nutrient amendments (PDB, TSB, and 1/3 R2A) were the ones providing the strongest a fastest metabolic activity detection. This could be due to an enhancement of the metabolism by a higher concentration of substrates. Overall, IF-C showed a similar pattern of metabolic detection for all the samples. In contrast, the AB-IF0a differed in its detection of metabolic activity depending on the environment used, and detected metabolic activity across a more diverse range of conditions (**Table 2.3**). This indicates that the AB-IF0a successfully characterized the microbial communities of the environment tested. Microbial activity was detected in µMAMA wells containing the thiosulfate media and the iron-oxidizer media. This suggests that the chemolitoautotrophs sulfate-oxidizing bacteria and Fe(II)-oxidizing bacteria were

present on our analog environments and that were able to be successfully detected with the µMAMA platform. Future molecular studies would need to be performed to identify which specific microorganisms were responsible for the dye reduction. This is an important consideration for future astrobiology life-detection missions since chemolithoautotrophic life may be the most likely candidate for microbial life forms on Mars' subsurface environment (Michalski *et al* 2018).

As compared to Viking Labeled Release experiment, designed to detect heterotrophic metabolism (Levin and Straat 1976) by the production of radioactive carbon dioxide, metabolic redox dyes are not dependent on any type of metabolism as they are reduced by the electron transport chain (Maldonado *et al.* 2012). This support the usage of metabolic redox dyes, especially the AB-IF0a that detected activity from chemolithoautotrophy, to detect activity form a broader range of metabolisms. In addition, the Viking Labeled Release experiment had been tested with a low limit of 50 CFU using a permafrost sample of the Victoria Valley of Antarctic (Levin and Straat 1976), which could mean a concentration of 1000 cells/ml, if extrapolated as explained above. As we detected metabolic activity with as low as 600 cells/ml using environmental samples (**Table 2.2**), the sensitivity of the metabolic-indicator redox dye AB-IF0a and IF-C is similar, or even better, than the one of the Labeled Release. Furthermore, the AlamarBlue® was successfully used to assed survival of microorganisms in the Cube-format payload O/OREOS (Nicholson *et al* 2011), and will be employed in the soon-to-be launch BioSentinel payload (Santa Maria *et al* 2020), which further prove the robustness and accuracy of metabolic redox dyes in an space exploration context, and strongly indicate the potential of the µMAMA as an unambiguous microbial activity detection system.

2.5.4 µMAMA caveats and future directions

The µMAMA platform can be further developed and improved in several ways. It is important to note that, due to the inherent limitations of the µMAMA design, we observed minimal movement of fluid across some wells in the µMAMA cards. Despite this potential well to well cross-contamination within the same µMAMA card, the observed positive reduction in the µMAMA cards was confirmed and validated with the mock replicate 96-well plate, where there was no movement of fluid. Therefore, we are confident in the results observed with the µMAMA. Nevertheless, this demonstrated the need for a new µMAMA design where each well can independently be inoculated. Fully drying the redox dye in the wells will considerably decrease the labor related to sample preparation and will improve the µMAMA platform by bringing it closer to a full automation. In addition, we acknowledge the need for further testing of the metabolism-indicator redox dyes sensitivity towards chemolithoautotrophic and anaerobic microorganisms, using pure cultures and environmental samples, to confirm the redox dye suitability for astrobiological applications (Michalski *et al* 2018; Westall *et al.* 2015).

While the µMAMA prototype presented here is a great tool to quickly identify the microbial metabolic capabilities of an analog environment, it does need to be modified to provide more complete metabolic detection characterization. Increasing the number of wells will allow for a greater number of substrate amendments and would definitely provide a more complete microbial characterization, similar to the Biolog EcoPlate, but with greater speed, ease of use, and sensitivity.

2.6 Conclusions

Our findings indicate that the semi-automated µMAMA platform successfully detected metabolic activity and metabolically characterized diverse astrobiology analog sites. The metabolism-indicator redox dyes, AlamarBlue® buffered in IF-0a and the Biolog IF-C, were found to be the

most sensitive and robust of the multiple combinations tested. Their incorporation into the µMAMA platform resulted in a small, portable, and low energy requiring instrument capable of rapid and unambiguous extant microbial life-detection. Since AlamarBlue® buffered in IF-0a offers the most sensitive signal but the Biolog IF-C can be used in the broadest range of environments, we recommend the usage of these two metabolic dyes in concert, as well as incubation under a range of temperatures to obtain a more accurate detection and characterization of the microbial life in analog samples. Despite the need of a further development and improvement of the µMAMA, we shown promising results that indicate its potential for life-detection. Given its small size, simple design and low energy requirements, we believe that the µMAMA should be considered as a strong candidate for further automation and incorporation into larger platforms for life detection missions.

2.7 Acknowledgements

We acknowledge the precious input from Dr. Jacqueline Goordial for their critical feedback and for the setting up of the project, Dr. Barry R. Bochner, from Biolog Inc. for his precious advice with the Biolog Dye Mix selection, and Dr. Antonio Ricco and the NASA Ames BioSentinel team form their collaboration and help with the design development.

Connecting text

To answer the second research question, in chapter 3, I investigated the cold adaptation strategies of *Rhodotorula* JG1b to identify novel putative mechanisms of acclimation to low temperatures. My overall objective was to identify and characterize, through a transcriptomic survey, the metabolic activity pathways and the regulatory mechanisms of *Rhodotorula* JG1b at 0°C compared to 23°C. This chapter corresponds to the manuscript titled "*Antarctic yeast response to cold involves increase in miRNA, transcriptional changes, and switch in metabolic strategy*", which will be submitted to *The ISME Journal*.

Contribution of Authors: The manuscript was made in collaboration with Dr. Ianina Altshuler, Dr. Isabelle Raymond-Bouchard, and Dr. Lyle G. Whyte from McGill University, and with Dr. Cene Gostincar, and Dr. Nina Gunde-Cimerman from University of Ljubljana. I wrote the manuscript, performed all laboratory experiments and data analysis. IA helped with the experimental design, laboratory experiments, data analysis, figure creation and manuscript editing. CG performed the bioinformatic pipeline analysis of the raw RNAseq data (mRNA). IRB helped with experimental design and manuscript editing. LGW and NGC provided guidance, advise and helped with the manuscript editing.

Chapter 3. Antarctic yeast response to cold involves increase in miRNA, transcriptional changes, and switch in metabolic strategy.

D. Touchette[1], I. Altshuler[1], C. Gostincar[2], I. Raymond-Bouchard[1], N. Gunde-Cimerman[2], and L.G. Whyte[1]*

[1]McGill University, Department of Natural Resource Sciences, Sainte-Anne-de-Bellevue, Québec, Canada.

[2]University of Ljubljana, Department of Biology, Biotechnical Faculty, Slovenia.

3.1 Abstract

Earth's cryosphere contains some of the most extreme habitats on our planet, with Antarctic permafrost being one of the harshest. Despite this, many cold-adapted microorganisms are capable of metabolic activity and even *in situ* growth in these environments, including fungi. The extremophilic basidiomycetous yeast *Rhodotorula* JG1b strain was isolated from ~150,000-year-old ice-cemented permafrost in Antarctica. To characterize its cold-adaptive strategies, we performed mRNA and small RNA transcriptomic analyses, phenotypic profiling, and assessed ethanol production, at 0°C and 23°C. Our results suggest that *Rhodotorula* JG1b switches its metabolism from a primarily respiratory metabolism in its optimal growth conditions at 23°C, to a fermentative metabolism while grown at 0°C, more similar to its natural environment. We report the production of ethanol by *Rhodotorula* JG1b at 0°C, while no ethanol production was detected in 23°C cultures. This is the coldest temperature for biological ethanol production documented to date without the aid of added biocatalysts. Based on transcriptomic analysis, at 0°C, *Rhodotorula*

JG1b upregulated its expression of genes involved in lipid and membrane fluidity, fermentation, and the pentose phosphate pathway, suggesting that these are important adaptations to the extremely cold Antarctic permafrost environment. We also detected a significant increase in the ratio of small RNAs to total RNAs in cultures grown at 0°C compared to 23°C. Furthermore, the diversity and abundance of miRNAs in the 0°C cultures were significantly higher compared to cultures grown at 23°C. This was consistent with an increase in transcription of Dicer, a key protein for miRNA processing. Our results strongly imply that post-transcriptional regulation of gene expression and mRNA silencing by miRNAs in *Rhodotorula* may be a key evolutionary adaptation in the cryosphere and potentially in other extreme environments.

3.2 Introduction

The majority of the Earth's biosphere exists at permanently cold temperatures, below 5°C, and includes multiple cryoenvironments (always below 0°C), many of which are characterized by some of the most dry, low biomass, cold, and salty conditions on Earth. Despite these harsh conditions, microorganisms capable of metabolic activity and even growth *in situ* have been reported in these habitats and include bacteria, archaea, algae, fungi (Margesin and Miteva 2011). These cold-adapted microorganisms are termed as psychrophiles (optimum temperature below 15°C) or psychrotolerant (optimum temperature above 15°C), as they can growth and thrive at these conditions (Cavicchioli *et al* 2002; Morita 1975), and are able to maintain viability for thousands of years under the ice (Hassan *et al* 2016). Microbial communities in these environments have to overcome numerous biochemical and physiological challenges, including low water and nutrient availability, high oxidative stress, high solar irradiation and multiple freeze-thaw cycles, coupled with a major decrease in membrane fluidity, and enzymatic activity, and protein folding, with the

creation of stable secondary inhibitory DNA/RNA structures (Buzzini and Margesin 2014a; De Maayer *et al* 2014).

While numerous studies have investigated bacteria, archaea and algae form Arctic and Antarctica environments, few have focused on yeasts (Hassan *et al* 2016). This is despite the fact that many fungal species have been isolated and characterized from a diversity of extreme environments, such as brines (Gunde-Cimerman *et al* 2000), Arctic glaciers and Antarctica rocks and deserts (Hassan *et al* 2016; Perini *et al* 2019; Tojo and Newsham 2012). Fungi play key roles in the cryosphere environments as they are important facilitator of primary biomass production through endophytic and lichenic relationships (Gianoli *et al* 2004; Rosa *et al* 2009) and are involved in the nutrients recycling (Duncan *et al* 2006). Although many basidiomycetous yeasts are well adapted to low temperatures and can be found in a broad range of cold ecosystems (Shivaji and Prasad 2009; Starmer and Lachance 2011), their adaptation strategies to low temperatures are not fully understood. Molecular mechanisms enabling yeast survival include the production of antifreeze and cold-active proteins, compatible solutes (glycerol, trehalose, sugar alcohols), and an increase in membrane fluidity (Gunde-Cimerman *et al* 2014; Hassan *et al* 2016).

The basidiomycetous *Rhodotorula* genus is composed of 42 pink-pigmented and unicellular yeast species (Fell *et al.* 2000), many of which are extremophiles and resistant to the harshest conditions (Buzzini and Margesin 2014b). These include numerous psychrophilic and psychrotolerant species, such as *R. aurantiaca*, *R. psychrophila*, *R. psychrophenolica*, *R. glacialis*, and *R. himalayensis* (Margesin *et al* 2007; Sabri *et al* 2000). References to this genus dates back to 1902, where "red *Torula"* yeasts were found to grow at 0°C (Schmidt-Nielsen 1902). More recently, the putative novel psychrotolerant *Rhodotorula* JG1b strain, was isolated from ~150,000-

year-old ice-cemented permafrost soil from University Valley, in the upper-elevation McMurdo Dry Valleys of Antarctica (Goordial *et al* 2016b).

sRNAs are short RNA sequences (>200 nucleotides) that have numerous functions, including ribosomal RNAs and transfer RNAs, and transcript regulation through RNA interference (RNAi) (Dozmorov *et al.* 2013). The role of small non-coding RNA (sRNA) and RNAi is not well understood, but they have been linked with the stress response in some organisms such as plants, flies and worms (Ambros 2003; Sunkar *et al.* 2012). The microRNAs (miRNAs) (~20 to 30 nucleotides) are a major component of gene regulation and gene silencing by RNAi in eukaryotic cells, including yeasts (Jiang *et al.* 2012). At present, their function and pattern of expression in yeast is very poorly understood, and to date, they have not been linked with cold adaptation.

Here, we identify and characterize the metabolic activity pathways and the regulatory mechanisms of *Rhodotorula* JG1b in response to cold. Specifically, we physiologically characterized this strain through the use of metabolic activity and phenotypic profiling assays at 0°C, using the Biolog Phenotypic MicroArray™ (PM) technology, and assessed this strains ethanol production capability at 0°C compared to its optimal growth conditions at room temperature (23°C). To determine transcriptional changes in *Rhodotorula* JG1b at colder temperatures, we performed transcriptomic mRNA-seq analysis in cultures grown at 0°C and 23°C. In addition, we carried out a transcriptomic analyses of small non-coding RNAs to determine their role in post-transcriptional gene regulation to cold adaptation. Thus, we investigated novel adaptations to low temperature and gained a better understanding of cold growth metabolisms in the yeast.

3.3 Materials and Methods

3.3.1 Culturing and growth conditions

Rhodotorula JG1b was cultured on PDB agar (HIMEDIA, Shenzhen, China). Biological triplicates of *Rhodotorula* were grown in 50ml liquid cultures to early exponential phase in PDB at 0°C without shaking, and 23°C at 150 RPM. Growth was monitored using OD_{600} for all subsequent experiments. OD_{600} to number of cells/ml conversion was determined based on CFU counts. Lack of shaking was necessary for the 0°C treatment to enhance growth at this low temperature since growth was not observed under shaking conditions at 0°C. The O_2 limitation in this treatment was likely minimal because of the small culturing volume and the slow growth rate at this temperature.

3.3.2 Phenotypic MicroArray analysis

Assimilation of different carbon and nitrogen sources by *Rhodotorula* JG1b at 0°C was assessed using the Biolog Phenotypic MicroArray (PM) technology (BIOLOG, Hayward, CA, United States). PM1 MicroPlate™ and PM2A MicroPlate™ were used for the carbon metabolism, and PM3B MicroPlate™ was used for nitrogen metabolism. The plates were inoculated following Viti *et al.* (2015) protocol (Viti *et al.* 2015) with the following modifications: the initial inoculum was adjusted to OD_{600} 0.200, and the BIOLOG Dye Mix G was used. The plates were incubated at 0°C, and at room temperature of 23°C as a control, in biological duplicate. The absorbance was measured at 590 nm on a SpectraMax M2e microplate reader (Molecular Devices, San Jose, CA, United States). The absorbance readings were taken at day 0, 1, 2, 6, 9, 14, 21, 28, 42, 56, 70 and 91 of incubation. The measurements were normalized by the subtraction of both the T_0 and the negative control. Absorbance values > 0.2 were considered as positive values, as per (Rico and Preston 2008).

3.3.3 Ethanol production assay

Triplicate *Rhodotorula* JG1b cultures were inoculated in 50 ml PDB broth at 0°C and 23°C. OD_{600} of the cultures was measured at regular time points over the course of 83 days for 0°C and 17 hours for 23°C. Aliquots (1 ml) of the cultures at each time point were analysed for ethanol production according to manufacturer's instructions using the EnzyChrom™ Ethanol Assay Kit (BioAssay System, Hayward, CA, United States). Analysis of the ethanol production was done by comparing the trendline of ethanol concentration over time to the trendline of cell density over time. Ethanol concentrations were normalized to the ethanol evaporation rate that was experimentally calculated using the same culture medial (sterile PDB broth) inoculated with 0.05% of ethanol.

3.3.4 RNA extraction, library preparation, and sequencing

Biological triplicate cultures of each condition were grown as previously described to reach early exponential phase, OD_{600} 0.95 at 0°C and OD_{600} 6.20 at 23°C. RNA extraction was performed using the Direct-zol RNA Miniprep Plus kit (#R2070) from Zymo Research (Irvine, CA, United States) on cultures with an initial resuspended pellet of approximately 10_8 cells. An addition step of bead beating has been added to the manufacturer's instructions: cell suspensions were complemented with 1:3 sterile glass beads (0.1 mm), bead beat for 45 s using the Mini-BeadBeater-24 (Biospec Products, Ba23°Clesville, OK, United States) and centrifuged at 10,000 RCF for 2 min. A DNAse treatment was performed on the eluted RNA using the TURBO DNAse kit according to manufacturer's instructions (Invitrogen, Carlsbad, CA, United States). The RNA concentration was assessed with the Qubit 3.0 Fluorometer (Thermo Fisher Scientific, Waltham, MA, United States). The RNA integrity was analyzed using an RNA Nano 6000 Assay Kit on the 2100 Bioanalyzer system (Agilent Technologies, Santa Clara, CA, United States) according to manufacturer's instructions. mRNA libraries were prepared following the Illumina (San Diego,

CA, United States) TruSeq Stranded mRNA LT Sample Prep Kit according to the manufacturer's instructions with an input material of 1.2µg of total RNA. Libraries band sizes were confirmed on a 4% agarose gel. Small RNA libraries were prepared following the NEBNext Multiplex Small RNA Library Prep Workflow (New England Biolabs, Ipswich, MA, United States). The cDNA constructs were purified with the Monarch PCR and DNA kit from New England Biolabs. Libraries band sizes were assessed with the Agilent High Sensitivity DNA kit on the 2100 Bioanalyzer system. Library bands from 105 to 210 bp were selected using the Pippin Prep 3% Agarose Gel Cassette from Sage Science (Beverly, MA, United States). mRNA sequencing was performed by RNA-Seq on the Illumina MiSeq system using the Reagent Kit v2 50 cycles and a 1 x 55bp single-end configuration. Small RNA sequencing was performed by RNA-Seq on the Illumina MiSeq system using the Reagent Kit v2 300 cycles and a 2 x 151 bp paired-end configuration.

3.3.5 Bioinformatics analysis and genome annotation

The mRNA raw sequencing reads were quasi-mapped and quantified with Salmon software (Patro *et al.* 2017) to the genome of *Rhodotorula* JG1b with the GenBank number GCA_001541205.1, and JGI IMG Genome ID 276120717 (Goordial *et al* 2016b). The analysis of the resulting quantifications was performed in R using the package DESeq2 (Love *et al.* 2014; Team 2013). Low count genes with less than 10 reads were removed before normalisation of the samples. Hierarchical clustering and principal component analyses were used to check if the samples within the treatment (biological replicates) were more similar than between the treatments. The p-value threshold for differential expression was 0.05. Log2 fold-change threshold was not used, but log2 fold-change shrinking was used for data visualisation and gene ranking. Gene with a $\log_2$ fold-change ($\log_2$FC) ratio $\geq |1.5|$, and a p-value < 0.05 were considered as differentially expressed

between the two growth conditions. Predicted protein KEGG assignments for each differentially expressed genes were downloaded from BlastKOALA website (Kanehisa *et al.* 2016), to obtain function and metabolic pathway assignments. Heat maps of the relative abundance of transcripts expression of specific pathways were created. For those heat maps, the relative abundance of each sample was calculated by tacking its abundance (corrected on sequencing depth and length) and subtracting the average abundance across all samples.

Small RNA Illumina raw data were adapter sequences trimmed and quantified using the CLC Genomics Workbench version 12 (https://www.qiagenbioinformatics.com/). The miRNA sequences (15-30 nt) were extracted and counted from the total small RNA sequences using the CLC Genomics Workbench Small RNA Analysis tool. Identical miRNAs were grouped together and low count sequences with less than 10 reads were removed. The miRNAs were normalized based on sequencing coverage, and differential expression was analysed, with a p-value threshold of 0.05. The mRNA target of the ten highest expressed miRNA were predicted using the RNAhybrid computational method using the miRNA sequences and all possible transcribed mRNA sequences as potential targets (Krüger and Rehmsmeier 2006; Rehmsmeier *et al.* 2004). The predicted protein mRNA targets of the miRNAs were identified with KEGG (Kanehisa *et al* 2016).

3.4 Results and discussion

3.4.1 Phenotypic MicroArray response at cold temperatures

The Biolog Phenotypic MicroArray plates are a 96-well assay that evaluate the ability of a microorganism to utilise a variety of nutrients as a sole source of carbon or nitrogen. Positive detection of metabolic activity relies on reduction of tetrazolium redox dye, which can be reduced

by cellular respiration (NADH) into a violet colored formazan molecule (Bochner *et al* 2001; Bochner 2008; Greetham 2014). The violet coloration is indicative of metabolic activity. Out of 190 carbon (PM1 and PM2A plates) sources and 95 nitrogen (PM3B plate) sources tested, *Rhodotorula* was able to utilize 35 substrates as a sole carbon source at 0°C for growth, after 91 days of incubation (**Figure 3.1, Table S3.1**). Only two (L-Proline, L-Pyroglutamate) of the 95 nitrogen sources were utilized as sole nitrogen sources at 0°C after 91 days of incubation (**Table S3.1**). Surprisingly, of the 35 positive carbon substrates, only six (D-Trehalose, D, L-α-Glycerol Phosphate, D-Mannose, Tween 20, Tween 40, and Tween 80) showed reduction of the dye in addition to evidence of microbial growth (**Figure 3.1**). This is puzzling because, in the remaining 29 carbon sources, we observed active growth in the wells (based on OD and visual inspection) without reduction of the dye. The dye was reduced with all 37 substrates at 23°C. As the tetrazolium dye is reduced via the electron transport chain (ETC) (Maldonado *et al* 2012), the observation of growth but no reduction of the dye suggest that at 0°C *Rhodotorula* JG1b potentially produces most of the energy for cellular growth through other metabolic pathways, such as glycolysis or perhaps fermentation. Tetrazolium dye could also be reduced by non-ETC products (Maldonado *et al* 2012). Therefore, the reduction of the dye in the six substrates could have been linked to ascorbic acid, cysteine and glutathione metabolism instead of the ETC. These six substrates have been shown to be linked with cold stress response in yeasts (Buzzini and Margesin 2014b), suggesting that the use of these substrates could promote an increase in metabolism in cold conditions, other than the ECT, due to their cryoprotective role. For example, the accumulation of trehalose acts as a cryoprotectant for the yeast stabilization of protein and membrane, and resistance to freezing (Aguilera *et al* 2007), glycerophospholipids (of which D,L-α-Glycerol Phosphate is the precursor) play an important role in membrane fluidity specific to

cold-adapted yeast (Loffeld and Keweloh 1996; Turk *et al.* 2011), and mannose-based glycoproteins have a cryoprotective activity to preserve enzymes against cold conditions (Kawahara *et al* 2008). Furthermore, thirty-two fungal strains isolated from Antarctica showed an increase in lipase production while exposed to different Tweens (Fenice *et al.* 1997), and the Tween 80 hydrolysis has been shown to be higher at cold temperatures in *Rhodotorula glacialis* and *R. laryngis* (Vaz *et al.* 2011). Therefore, the redox dye reduction that we observed with these substrates could be due to an increase in metabolism in *Rhodotorula* JG1b due to the response to cold. Interestingly, the only substrate used both as a sole carbon and sole nitrogen source by *Rhodotorula* was L-Proline. In fungi, L-proline is known to have a cryoprotective activity that enhance freeze tolerance, and to be an antioxidant responsible for apoptosis reduction under stress conditions (Chen and Dickman 2005; Terao *et al* 2003). By providing cryoprotection, part of the L-proline may then enhance cell survival, while the remaining molecules may be utilized as a nutrient source.

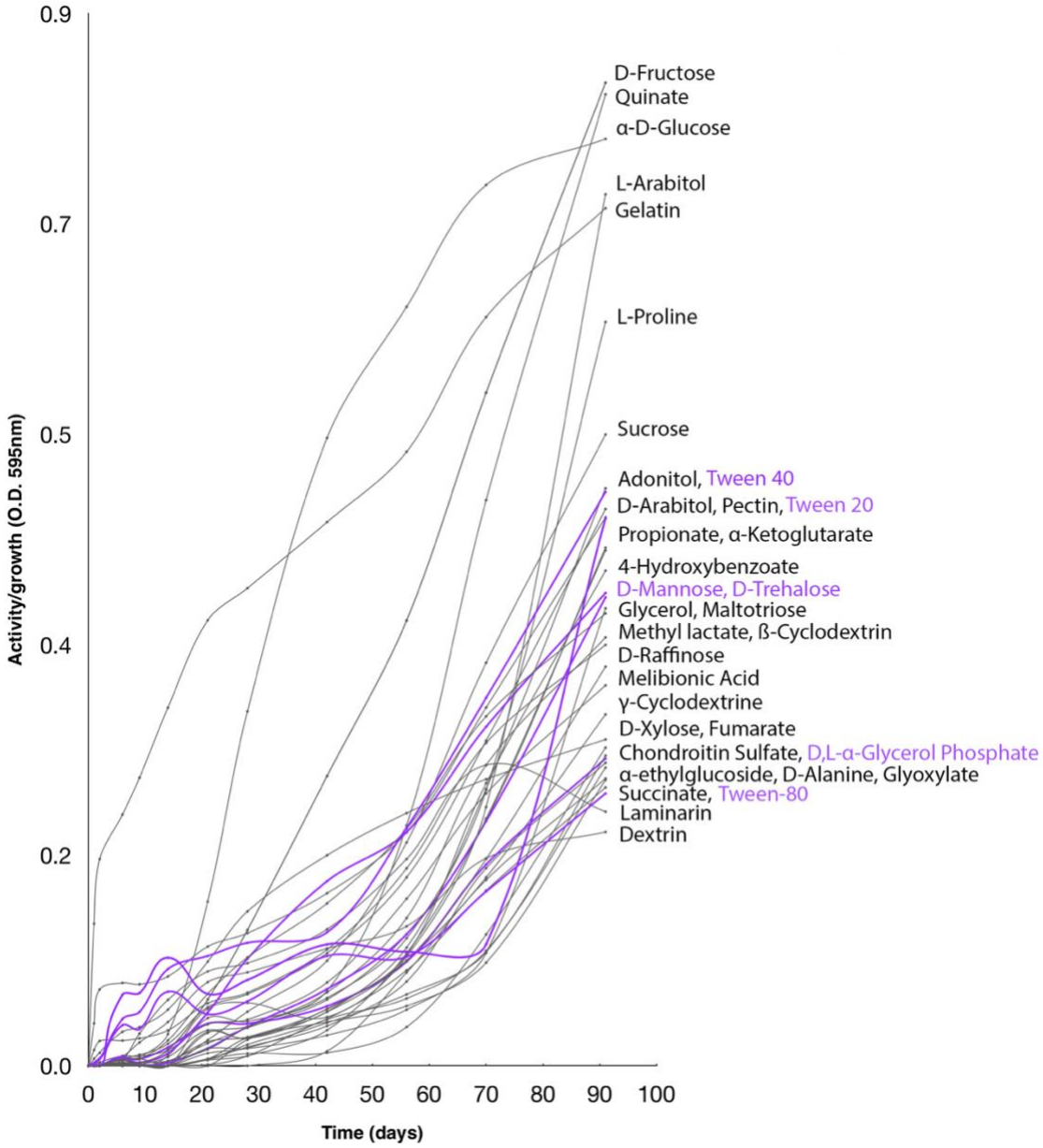

Figure 3.1. Carbon sources metabolized by *Rhodotorula* JG1b at 0°C in MicroPlate™

The black curves represent carbon sources that were utilized for growth by *Rhodotorula* JG1b. The purple curves represent nutrient sources that were utilized for growth by *Rhodotorula* JG1b and were also able to reduce the redox dye in the wells.

3.4.2 *Rhodotorula* JG1b produces ethanol at 0°C

Generation time for the 0°C and the 23°C treatments were 33.78 days and 3.05 hours respectively. Ethanol production was observed at 0°C, at an average rate of 1.51 x 10^{-5} moles of ethanol, per liter, per day. (**Figure 3.2A**). No ethanol production was detected in our 23°C cultures (**Figure 3.2B**). Other *Rhodotorula* species are known to be capable of ethanol fermentation at 28°C, such as *Rhodotorula minuta, R. mucilaginosa,* and *R. pallida* (Rao *et al.* 2008), but ethanol fermentation at 0°C by *Rhodotorula* has not been previously reported. Little is known about yeast ethanol production at extremely cold temperatures apart from very few studies of fermentation with *Saccharomyces cerevisiae* on wine (0 and 2°C) and beer (6°C) production (Bakoyianis *et al.* 1992; Kanellaki and Koutinas 1999; Kourkoutas *et al.* 2003), however, all of these studies included an addition of an immobilized biocatalysts to facilitate fermentation. To our knowledge, *Rhodotorula* JG1b is able to naturally produce ethanol at the lowest recorded temperature for microbial fermentation. Ethanol fermentation has previously been linked with an increase in carotenoid production (Gu *et al.* 1997; Tang *et al.* 2019). Since carotenoids play an important role in UV and sunlight protection in yeast (Moliné *et al.* 2009; Moliné *et al.* 2010; Villarreal *et al.* 2016), ethanol fermentation in *Rhodotorula* JG1b might be linked both to carotenoid production and increased UV protection, as well as to depression of environmental freezing point due to increased ethanol concentration (Koga and Yoshizumi 1979). Ethanol fermentation occurs also in another Antarctic yeast, *Mrakia blollopis*, but only at low temperatures (Tsuji *et al.* 2014). Interestingly, *Mrakia blollopis* ethanol production rate was enhanced with the addition of Tween 80 in the media (Tsuji *et al* 2014). Thus, the redox dye reduction in the wells of the PM assay containing the Tween substrates in our study (**Figure 3.1**), may be linked to a rapid increase of the glycolytic flux

characteristic to a switch from respiratory metabolism to fermentation metabolism, producing NADH reduction power (Van den Brink *et al.* 2008) from Tween as sole carbon source.

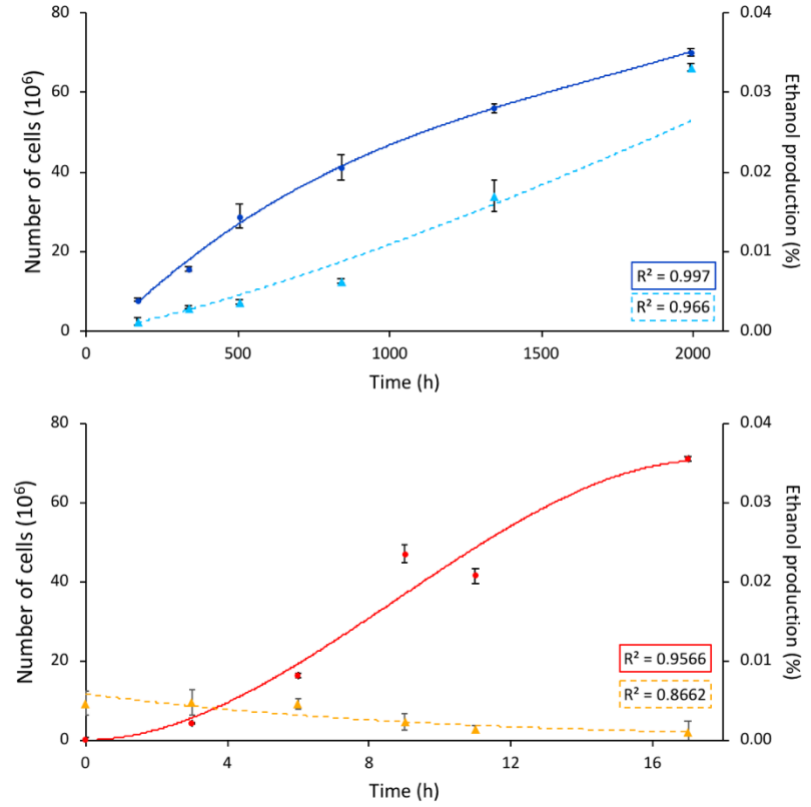

Figure 3.2. Ethanol production and growth by *Rhodotorula* JG1b at 0°C and 23°C, in PDB media

(**A**) Cell growth (circle, full line) and ethanol production (triangle, dashed lines) over time at 0°C (**B**) Cell growth (circle, full line) and ethanol production (triangle, dashed lines) over time at 23°C. R_2 values represent the coefficient of determination of the best fit trendline.

3.4.3 mRNA transcriptional responses to cold temperature

Using RNAseq, we performed an mRNA transcriptomic analysis on triplicate exponential phase cultures of *Rhodotorula* JG1b grown at 0°C and 23°C. Overall, 1,772 genes were differentially expressed between these two conditions, including 994 genes upregulated, and 778 genes downregulated at 0°C compared to 23°C (**Table S3.2**). Of these genes, 52% were able to be

annotated with KEGG. The major differences in transcript abundance between 0°C and 23°C, were found in genes related to carbohydrate metabolism, energy metabolism, amino acid metabolism, lipid metabolism, glycan biosynthesis/metabolism, transcription machinery, translation, protein folding, signal transduction, and cellular community development (**Figure 3.3**)

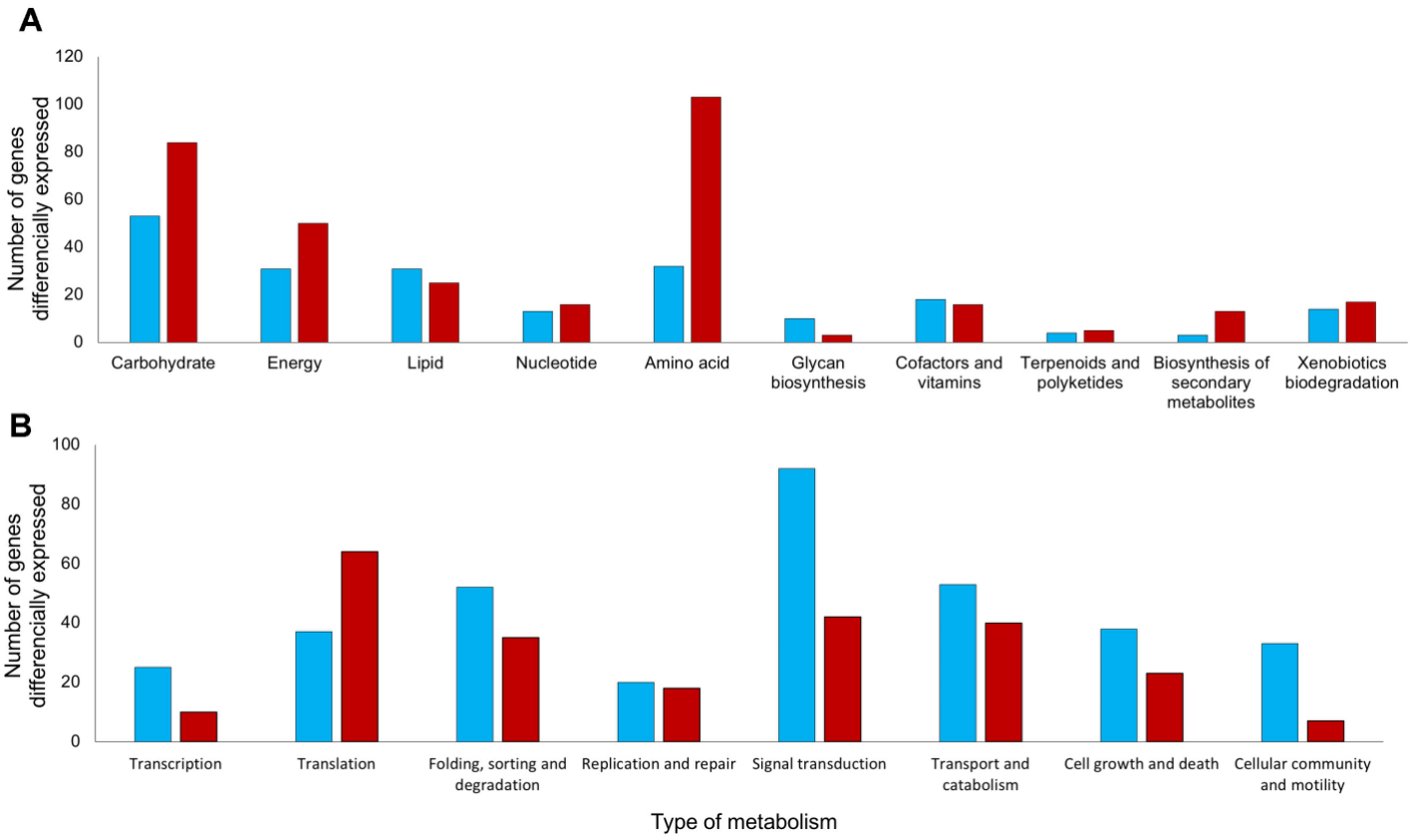

Figure 3.3. Differentially expressed KEGG metabolic pathways in *Rhodotorula* JG1b at 0°C compared to 23°C

(**A**) Genes differentially expressed and their corresponding cell metabolisms. (**B**) Genes differentially expressed that are involved in genetic information processing, in environmental information processing, and in other cellular processes. The genes with a significant ($p < 0.05$) differential expression of ≥ 1.5 FC are indicated in *blue* (overexpressed at 0°C) or *red* (overexpression at 23°C).

3.4.3.1 Switch from citrate cycle to PPP and fermentation at 0°C compared to 23°C

The major gene regulation differences observed in carbohydrate metabolism were in the citrate cycle, pentose phosphate pathways, and alcohol fermentation. At 23°C, *Rhodotorula* JGb1 overexpressed the entire citrate cycle, with the sole exception of the succinyl-CoA synthetase gene, and overexpressed glycolysis genes linked to oxaloacetate and acetyl-CoA syntheses, both important molecules feeding into the citrate cycle (**Figure 3.4**). Contrarily, at 0°C, we observed a significant increase in the expression of the glycolysis genes towards ethanol fermentation, and a significant increase in expression of the pentose phosphates pathway (PPP) genes (**Figure 3.4**).

The increase in PPP promotes the production of erythrose-4-phospate, allowing energy (NADH) conservation due to a reduction of the citrate cycle activity (Sarkar *et al* 2009). The PPP is also involved in the xylulose fermentation in yeast, including some *Rhodotorula* species (Bura *et al* 2012; da Silva *et al.* 2011; Johansson and Hahn-Hägerdal 2002). A decrease in the 6-phosphogluconate dehydrogenase activity is correlated with production of ethanol via xylulose fermentation (Eliasson *et al.* 2000). In addition, xylulose fermentation also produces xylitol, a cryoprotectant and a freezing point reducer in yeast (Mohamad *et al* 2015), via the xylulose reductase (Bura *et al* 2012). Furthermore, the non-oxidative PPP enzymes increase the yield of ethanol fermentation, through the conversion of pentose phosphates into intermediates of the glycolysis pathway which feeds back into fermentation (Johansson and Hahn-Hägerdal 2002). In cold conditions, *Rhodotorula* JG1b cultures overexpressed genes coding for xylulose reductase, three out of four non-oxidative PPP enzymes, and alcohol dehydrogenase, and under-expressed the gene coding for 6-phosphogluconate dehydrogenase (**Figure 3.4**). This suggests that at 0°C, *Rhodotorula* JG1b promotes xylitol production and redirects the pentose phosphates to ethanol fermentation.

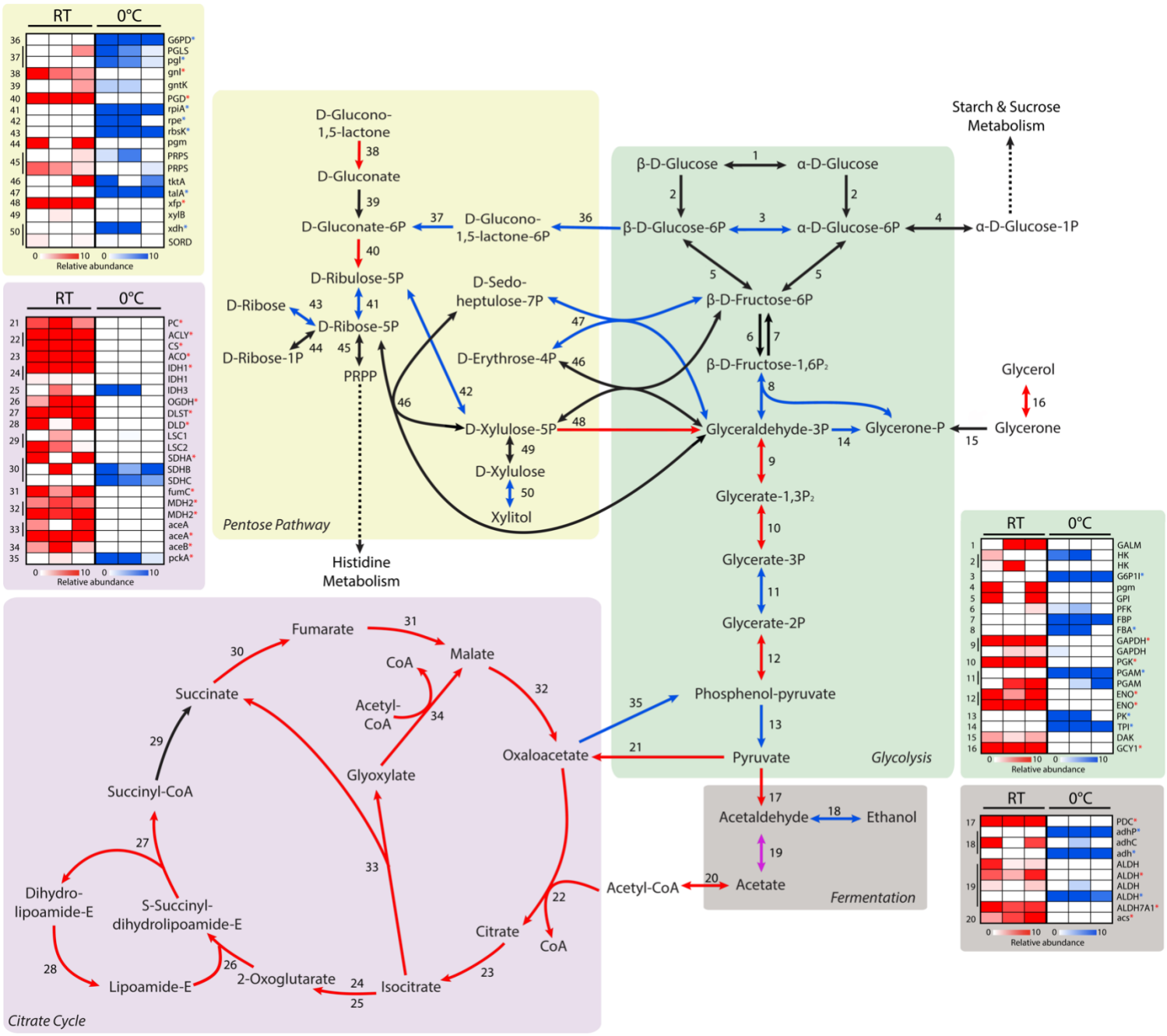

Figure 3.4. Reconstruction of the *Rhodotorula* JG1b major carbohydrate metabolic pathways mapped with transcriptomic data

Reconstructed carbohydrate metabolic pathways of *Rhodotorula* JG1b based on the KEGG gene annotations and their relative differential gene expression profiles of each triplicate culture. The genes with a significant ($p < 0.05$) differential expression of ≥ 1.5 FC are indicated with an arrow (pathway) and a star (heatmap) in *blue* (overexpressed at 0°C), *red* (overexpression at 23°C), or *purple* (different homolog overexpressed at both 0°C and 23°C). The *numbers* in the pathways correspond to the numbers in the heatmaps. For the heatmaps, *blue* indicates an overexpression of the gene at 0°C, *red* indicates and overexpression of the gene at 23°C, and *white* indicates genes that are not differentially expressed between the two temperatures. A list of the abbreviations is included in the supplementals (**Table S3.5**).

In the snow algae *Chlamydomonas nivalis*, an increase in UV exposure stimulated phenolic antioxidant production through the proline-linked PPP, by providing the key precursors of the phenylpropanoid pathway (Duval *et al.* 1999). A similar oxidative stress response has been proposed in yeast (Shetty and Wahlqvist 2004), especially under low temperatures (Sarkar *et al* 2009). We did not observe this difference in gene expression of the phenylpropanoid pathway in *Rhodotorula* JG1b grown at 0°C compared to 23°C, however, *Rhodotorula* does use L-Proline as a sole carbon and a sole nitrogen source (**Figure 3.1**, **Figure S3.1**), without reducing the redox dye. This suggests that L-Proline may be used by *Rhodotorula* in the proline-linked PPP, leading to a decrease in citrate cycle activity, resulting in decrease of the electron transport chain activity and lack of redox dye reduction. This results in redirection of the erythrose-4-phospate to accelerate the fermentation pathways. Therefore, the increase in transcription of the PPP genes could help *Rhodotorula* JG1b to limit energy loss, and to enhance ethanol production.

In addition, our RNAseq data suggests a significant decrease in expression of the citrate cycle genes at 0°C (**Figure 3.4**). A similar decrease of the citrate cycle and increase in PPP fluxes has been observed in *Yarrowia lipolytica* under limited oxygen conditions (Sabra *et al* 2017), but it has not yet been reported under low temperature conditions. Combined together, our results suggest that *Rhodotorula* JG1b switches from a mainly respiratory metabolism when incubated at 23°C to a mainly fermentative metabolism when cultured in conditions similar to its natural environment (0°C). These results are also confirmed by the lack of ethanol detection at 23°C, and positive ethanol production in *Rhodotorula* at 0°C (**Figure 3.2**).

3.4.3.2 Major downregulation of ETC genes at 0°C

Overall, a higher number of genes related to energy metabolism were overexpressed at 23°C compared to 0°C (**Figure 3.3A**). In accordance with our carbohydrate metabolism results, this

significant change was related to an overall overexpression of the genes coding for the electron transport chain (ETC) subunits at 23°C, and a significant decrease in the succinate dehydrogenase, the fumarate reductase, and the cytochrome c reductase complexes expression at 0°C (**Figure 3.5**). The temperature effect on the ETC activity remains unclear, but some studies confirm a general trend in decrease of ETC expression in microorganisms at lower temperatures (Fonseca *et al.* 2011; Raymond-Bouchard *et al* 2018b). For example, the Antarctic permafrost *Rhodococcus* JG3 grown at -5°C compared to 23°C downregulated multiple cytochromes (Raymond-Bouchard *et al* 2018b), and the ubiquitous *Pseudomonas putida* decreased its type-1 proton-translocating NADH dehydrogenase and succinate dehydrogenase when cultured at 10°C, compared to 30°C (Fonseca *et al* 2011). The gene expression patterns in *Rhodotorula* JGb1, complements our hypothesis related to the lack of dye reduction in the PM assay at 0°C as being due to the downregulation of the ETC, and its potential reduction in NADH formation. Since the tetrazolium dye is reduced via the ETC (Maldonado *et al* 2012), the observation of growth and no reduction of the dye (**Figure 3.1**) suggest that at 0°C, *Rhodotorula* is using different metabolic pathways to produce its energy. This is further supported by our observation of a switch in gene expression from the citrate cycle pathway at 23°C to the fermentation pathways (ethanol and xylitol) at 0°C for its primary energy production (**Figure 3.4**). Combined, the downregulation of the ETC subunits and citrate cycle gene expression (**Figure 3.5, Figure 3.4**), the upregulation of fermentation gene expression (**Figure 3.4**), our observation of growth but non-reduction of the redox dye in the PM assay (**Figure 3.1**), and our discovery of ethanol production at 0°C (**Figure 3.2**) confirm that *Rhodotorula* JG1b induce a switch from a respiratory metabolism at 23°C, to an ethanol fermentation metabolism at low temperatures. This is the first time that ethanol fermentation has been shown to be utilized as the major energy pathway in response to cold.

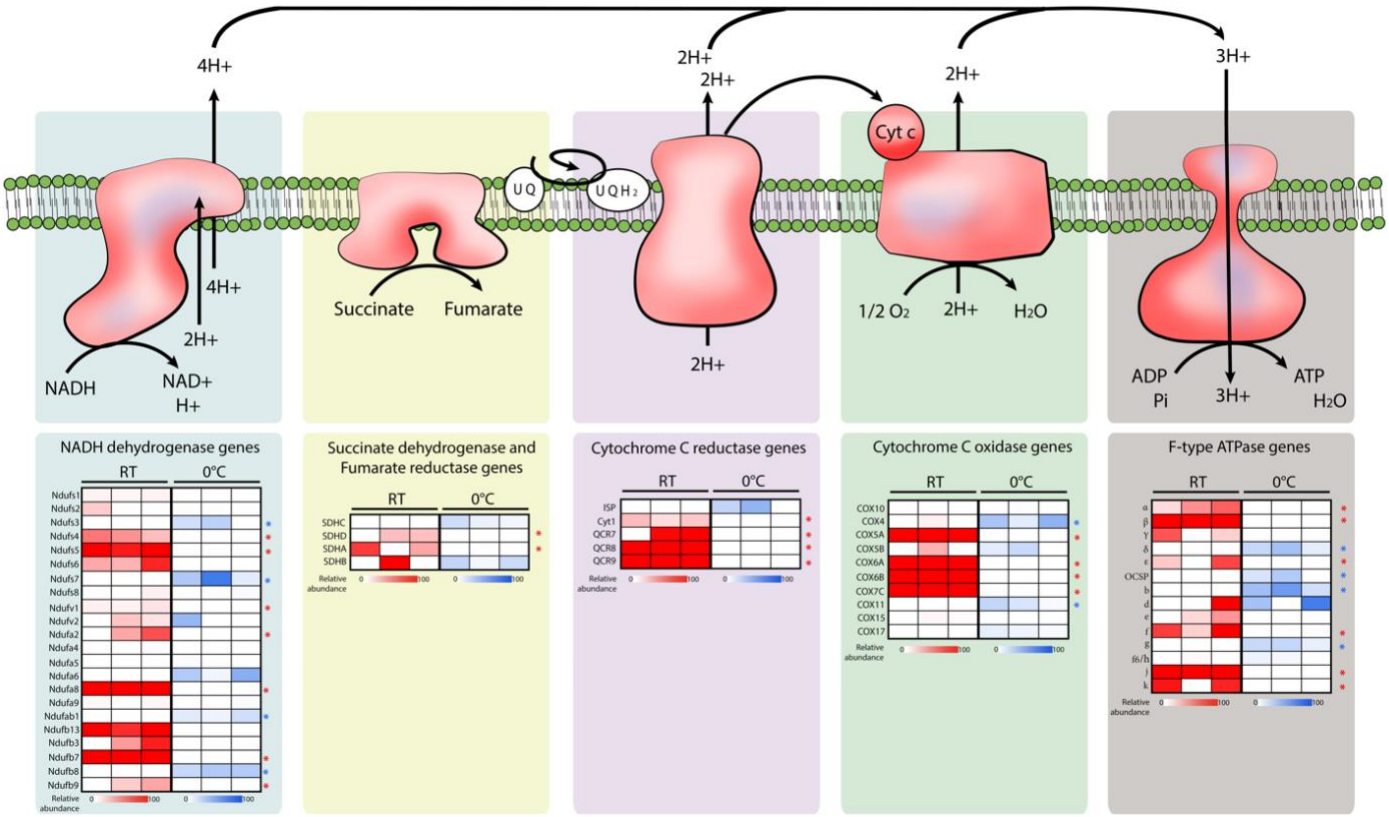

Figure 3.5. Reconstruction of the *Rhodotorula* JG1b electron transport chain

Reconstructed electron transport chain complexes of *Rhodotorula* JG1b based on the KEGG genes annotation (top) and their relative differential gene expression profiles of the electron transport chain subunits (bottom) of each triplicate culture. The genes with a significant ($\alpha < 0.05$) differential expression of ≥ 1.5 FC are indicated with a star in *blue* (overexpressed at 0°C), or *red* (overexpression at 23°C). For the heatmaps, *blue* indicates an overexpression of the gene at 0°C, *red* indicates and overexpression of the gene at 23°C, and *white* indicates genes that are not differentially expressed between the two temperatures.

3.4.3.3 Increase lipid and carotenoid biosynthesis at 0°C

Modification in membrane fluidity is one of the most well-known adaption strategies in microorganisms (Gunde-Cimerman *et al* 2014). Keeping membrane fluidity is essential for microorganisms living in cold environments (Gunde-Cimerman *et al* 2014). Overall, in *Rhodotorula* JG1b genes involved in lipid metabolism were overexpressed at 0°C compared to

23°C (**Figure 3.3A**). In accordance with previous studies on cold-adapted yeasts, the majority of genes overexpressed at 0°C in *Rhodotorula* JG1b were related to biosynthesis of fatty-acids, known to promote membrane fluidity (Bhuiyan *et al* 2014; Rossi *et al* 2009). Contrary to 0°C, the genes overexpressed in 23°C *Rhodotorula* JG1b were overall related to lipid degradation. In eukaryotes, palmitate is the precursor of the fatty acid degradation metabolism (Kawamoto *et al.* 1978). Accordingly, genes involved in palmitate degradation were over expressed at 23°C, likely to generate Acetyl-CoA to feed into the citrate cycle. While at 0°C, palmitate degradation fed into the alcohol metabolism **(Table S3.3)**. Differential expression of palmitate degradation genes at 0°C and 23°C is concurrent with observed increased ethanol production at 0°C (**Figure 3.2**). Moreover, we observed a switch in glycerophospholipid metabolism, from the production of diacylglyceryltrimethylhomoserine (DGTS) at 23°C to lecithin synthesis at 0°C, and a significant increase in the unsaturated fatty acid biosynthesis at 0°C compared to 23°C. Relatively high amounts of unsaturated fatty acids were also reported in psychrophilic basidiomycetous yeasts, including two *Rhodotorula* species, isolated from Antarctic and Patagonian ecosystems, and some were increased at 6°C compared to 15°C (Contreras *et al* 2015; Libkind *et al.* 2008; Thomas-Hall and Watson 2002). The unsaturated fatty acids are linked to cold adaptation as they promote membrane fluidity at low-temperature (Gunde-Cimerman *et al* 2014).

Sphingolipid metabolism genes were highly upregulated at 0°C compared to 23°C in *Rhodotorula* JG-1b (**Figure 3.6**) presumably leading to increased biosynthesis of ceramide and phytoceramide. Other genes involved in the phytoceramide synthesis were previously shown to be consistently up-regulated during low temperatures fermentation (12°C) in *Saccharomyces cerevisiae* (López-Malo *et al.* 2014; Tai *et al.* 2007). Ceramide and other sphingolipid products

can induce cell cycle arrest (Mao *et al.* 1997) indicating growth suppression in *Rhodotorula* as an adaptation to freezing conditions in Antarctic permafrost.

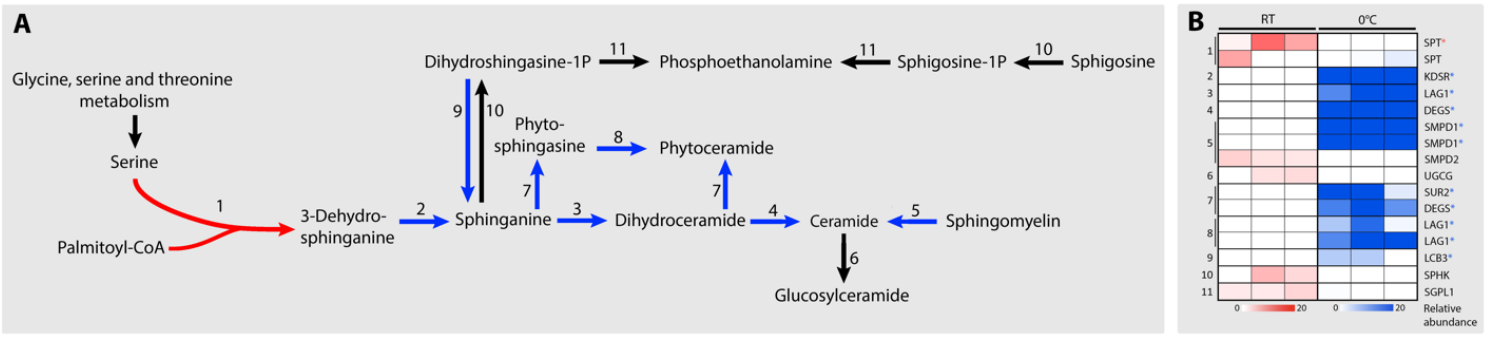

Figure 3.6. Reconstruction of the *Rhodotorula* JG1b sphingolipid metabolic pathways mapped with transcriptomic data

(**A**) Reconstructed sphingolipid metabolic pathways of *Rhodotorula* JG1b based on the KEGG genes annotation. (**B**) Differential gene expression profiles of the sphingolipid metabolic pathway genes of each triplicate culture. The genes with a significant ($\alpha < 0.05$) differential expression of $\geq$ 1.5 FC are indicated with an arrow (**A**) and a star (**B**) in *blue* (overexpressed at 0°C), or *red* (overexpression at 23°C). The *numbers* in the pathways correspond to the numbers in the heatmaps. For the heatmaps, *blue* indicates an overexpression of the gene at 0°C, *red* indicates and overexpression of the gene at 23°C, and *white* indicates genes that are not differentially expressed between the two temperatures. A list of the abbreviations is included in the supplementals (**Table S3.5**).

Multiple *Rhodotorula* species produce lipid antioxidants, and photoprotective carotenoids (Liu and Nizet 2009; Mata-Gómez *et al.* 2014; Moliné *et al* 2010), especially high concentration of β-carotene, torulene, and torularhodin. Carotenoids help maintain membrane rigidity in cold-adapted microorganisms, as they balance out the higher percentage of unsaturated fatty acids in the membrane (Raymond-Bouchard *et al* 2017; Rodrigues and Tiedje 2008). *Rhodotorula* JG1b expressed the phytoene desaturase, gene involved in synthesis of torulene and β-carotene at both 0°C and 23°C; however, we did observe an overexpression at 0°C of the phytoene desaturase gene, an enzyme that catalyses the conversion of phytoene to lycopene, the precursor of both torulene

and β-carotene. Thus, at low-temperature, *Rhodotorula* JG1b may increase carotenoid biosynthesis through an over-expression of their precursor, to adapt to its natural environment.

3.4.3.4 Increased glycan biosynthesis and metabolism at 0°C compared to 23°C

A significant increase in glycan biosynthesis genes was observed in *Rhodotorula* at 0°C compared to 23°C (**Figure 3.3A**). Glycans are carbohydrate-based polymers commonly associated with cellular protection and storage (Varki and Gagneux 2017). They are also important component of glycoproteins, including cell-surface membrane proteins, such as receptors and adhesion proteins (Colley *et al.* 2017; Varki and Gagneux 2017). *Rhodotorula* species produce mannan, a mannose glycan extracellular polysaccharide (EPS) (Cho *et al.* 2001; Frengova *et al.* 1997; Pavlova *et al.* 2005). Microbial EPS are components of microbial biofilms and constitute a protective matrix against the desiccation and environmental fluctuations (Nichols *et al.* 1989), including to damages caused by freeze-thaw cycles (Selbmann *et al.* 2002). At 0°C, *Rhodotorula* JG1b overexpressed genes from the fructose and mannose pathway involved in GDP-D-mannose synthesis, the precursor of the glycan biosynthesis pathway, and overexpressed multiple genes coding for glycosyltransferase and glycosidases, which regulated, assembled and processed glycans (Rini and Esko 2017). In comparison, only one glycotransferase was overexpressed at 23°C (**Table S3.3**). These results indicate that *Rhodotorula* JG1b increases EPS synthesis at cold temperatures, and overexpresses glycan biosynthesis pathway genes to produce mannan and other glycoproteins, facilitating adhesion and aggregation of cells as an adaptation to cold temperatures. *Rhodotorula* growth and reduction of the redox dye in the wells of the PM assay containing D-Mannose (**Figure 3.1**) supports this hypothesis as mannose favorizes EPS formation.

3.4.3.5 Increased transcription and decreased translation and amino acid metabolism at 0°C

Compared to 23°C, *Rhodotorula* JG1b overexpressed multiple genes involved in the transcriptional machinery at 0°C (**Figure 3.3B**). Of the 25 polymerase subunits expressed in *Rhodotorula*, six genes, coding for subunits across all three RNA polymerase complexes, were overexpressed at 0°C (**Table S3.3**). No overexpression of any polymerase genes was observed at 23°C. There was a significant increase at 0°C in the transcription of the RNA Polymerase I, responsible for the ribosomal RNA synthesis, of RNA Polymerase II, responsible for the pre-messenger RNA synthesis, and of Polymerase III, responsible for the small RNA and transfer RNA synthesis (Cramer 2002). Increased expression of the RNA polymerase II transcription factor, responsible for transcription initiation (Barrera and Ren 2006), was also observed at 0°C. A similar increase in the transcriptional machinery at 10°C and 4°C was reported in other yeast (Becerra *et al.* 2003; Homma *et al.* 2003; Sahara *et al.* 2002; Strassburg *et al.* 2010).

Contrarily to transcription related genes, *Rhodotorula* JGb1 decreased expression of genes related to translation at 0°C. Specifically, we observed a downregulation of the majority of the genes involved in ribosomal protein synthesis and of the genes coding for the aminoacyl-tRNAs. At 0°C, we also observed an overexpression of proteasome genes involved in protein degradation. Cold temperature can reduce the translation efficiency by inducing formation of secondary structures in RNA molecules and the inactivation of ribosomes (Jones and Inouye 1996), as shown for the mesophilic *Saccharomyces cerevisiae* exposed to 10°C (Sahara *et al* 2002; Schade *et al.* 2004).

In addition to the translational machinery decrease and the proteasome synthesis increase, the *Rhodotorula* JG1b amino acid metabolism is strongly downregulated at 0°C compared to 23°C (**Figure 3.3A**). Most genes involved in the amino acid biosynthesis were downregulated at 0°C,

with the notable exception of the upregulated histidine pathway. A similar result was reported in the basidiomycetous yeast *Mrakia blollopis,* with an accumulation of aromatic amino acids, such as histidine, at -3°C compared to 10°C (Tsuji 2016), which is part of the membrane's cold sensors histidine kinases (Mikami *et al.* 2002). The bacteria *Polaromonas* sp. also downregulated genes involved in amino acid metabolism and transport (Raymond-Bouchard *et al* 2018b). These observations suggest that at low temperatures *Rhodotorula* decreases amino acid synthesis and transport, to slow down translation and focus energy on cold acclimation, in parallel with increased protein degradation, probably to recycle amino acids to synthesis of specific proteins, important in freezing conditions.

3.4.3.6. Signal transduction, cellular motility and cellular community

We observed an increase in expression of genes involved in cell signal transduction, cellular motility and community at 0°C compared to 23°C. The PI3k-Akt, Hippo, TGFß, VEGF, RAS, MAPK, RAP1, FoxO and Wnt pathways, all transduction signaling pathways related to gene regulation, actin cytoskeleton formation, and cellular adhesion, were overexpressed at 0°C (**Figure 3.3**, **Table S3.3**). Little is known about signal transduction modulation in microorganisms in response to cold stress, but it has been linked to survival at low and freezing temperatures in many plants (Heino and Palva 2003; Huang *et al.* 2012). Since membrane proteins, including transduction signal receptors are more likely to be sensitive to temperature fluctuations, they initiate signal transduction pathways (Heino and Palva 2003). Perception of cold in *Rhodotorula* via membrane receptors could lead to a cascade response.

Protein phosphorylation/dephosphorylation is known to be important in signal transduction in response to low temperature, such as those carried out by the mitogen activated protein kinase (MAPKs) (Heino and Palva 2003). In yeast, MAPK cascades play major roles in

gene transcription and cytoskeletal organization (Storey and Storey 2001); cold-induced membrane rigidification could trigger a restructuration of the actin cytoskeleton in plants (Örvar *et al.* 2000). Actin filaments mediate the transport of phospholipids, sphingolipids and sterols to the membrane (Woodman *et al.* 2018), the major lipids upregulated by *Rhodotorula* JG1b at low temperature (**Figure 3.3**, **Figure 3.6**). This could explain why at 0°C, *Rhodotorula* overexpresses genes coding for the formation of the actin cytoskeleton, such as cdc42 and the actin δ/γ subunits (**Table S3.3**). This would allow for transport of these lipids to the membrane to maintain membrane fluidity.

3.4.3.7. Differential expression of homologous proteins between 0°C and 23°C

We observed 19 differentially expressed homologous protein categories between *Rhodotorula* JG1b cultures grown at 0°C and 23°C (**Table S3.4**). Eight of these differentially expressed homologous protein categories were connected to membrane structure or transport across membranes. For example, YAT, an amino acid transporter, had three homolog genes overexpressed at 0°C, two homologs overexpressed at 23°C, and two homologs that were not differentially expressed between the two temperatures. Homologous proteins arise from gene duplication and sometimes these duplicated genes gain new functions (Li *et al.* 2005). As such, genomes are able to evolve, allowing organisms to adapt to a wider range of environmental conditions. Gene duplication and increase in paralogous (homologs) genes in the genome increases the organism's ability to grow under varied conditions (temperatures, substrates, pH, salinity, etc.) (Wagner 2002). This comes at a price of having a larger genome with an increased requirement for upkeep (DNA repair) and replication (Lynch and Marinov 2015). This trade-off might explain differential expression of homologous genes involved in cold adaptation, such as fermentation, lipid transport, and mannan production (**Table S3.4**).

3.4.4 Stress induces increase in abundance and diversity of sRNA and miRNA

miRNAs are non-coding RNA sequences of approximatively 22 nucleotides that play an important role in gene regulation in eukaryote cells, including fungi (Lau *et al.* 2013; Zhou *et al.* 2012). Through the action of two RNAse III-type proteins, Drosha and Dicer, miRNAs can recognize specific "target" mRNA and silence it in a process called RNA interference. Drosha is responsible for the primary transcript cleavage to create precursor miRNA, while Dicer cleaves the precursor miRNA to form a double strand miRNA. One miRNA strand interacts and is incorporated into the RNA-induced silencing complex (RISC), that will target an mRNA and silence its expression (Zhou *et al* 2012). No link between cold adaptation in prokaryotic and fungal microorganisms and miRNA gene regulation has been reported yet, although this mechanism has been identified as a cold temperature adaptation mechanism in multiple plant species, including *Arabidopsis*, spruce, soybean, wheat, and rice (Miura and Furumoto 2013; Wang *et al.* 2014; Yakovlev *et al.* 2010; Zhang *et al.* 2014). miRNA specific targeted genes are still poorly understood, but seems to be involved in epigenetic regulation mechanism and with the nodule protection in plants (Miura and Furumoto 2013; Yakovlev *et al* 2010; Zhang *et al* 2014). Based on the RNA quantification of the total *Rhodotorula* RNA extracted on the 2100 Bioanalyzer system, we observed a significantly higher ($p = 0.0003$) proportion of small RNAs (200 nucleotides or less) in the 0°C cultures compared to the 23°C cultures (**Table S3.5, Figure S3.1**). On average, 53.40 ± 0.99 % of the total RNA were characterized to be small RNAs at 0°C compared to 27.70 ± 1.84 % at 23°C cultures. Of the total small RNA fraction of *Rhodotorula* JG1b, we observed a significantly ($p = 0.03$) higher proportion of miRNA (15-30 nt) at 0°C compared to 23°C (**Table S3.5, Figure S3.2**); 1.27 ± 0.34 % of the total small RNA were characterized to be miRNAs at 0°C compared to 0.09 ± 0.01% in 23°C cultures. In addition, there was a higher diversity in miRNAs at cold temperature than at

23°C (**Figure 3.7A**, **Figure S3.1**). Based on PCoA analysis (Bray-Curtis distance), the 0°C miRNAs were different from the miRNAs at 23°C (**Figure 3.7B**).

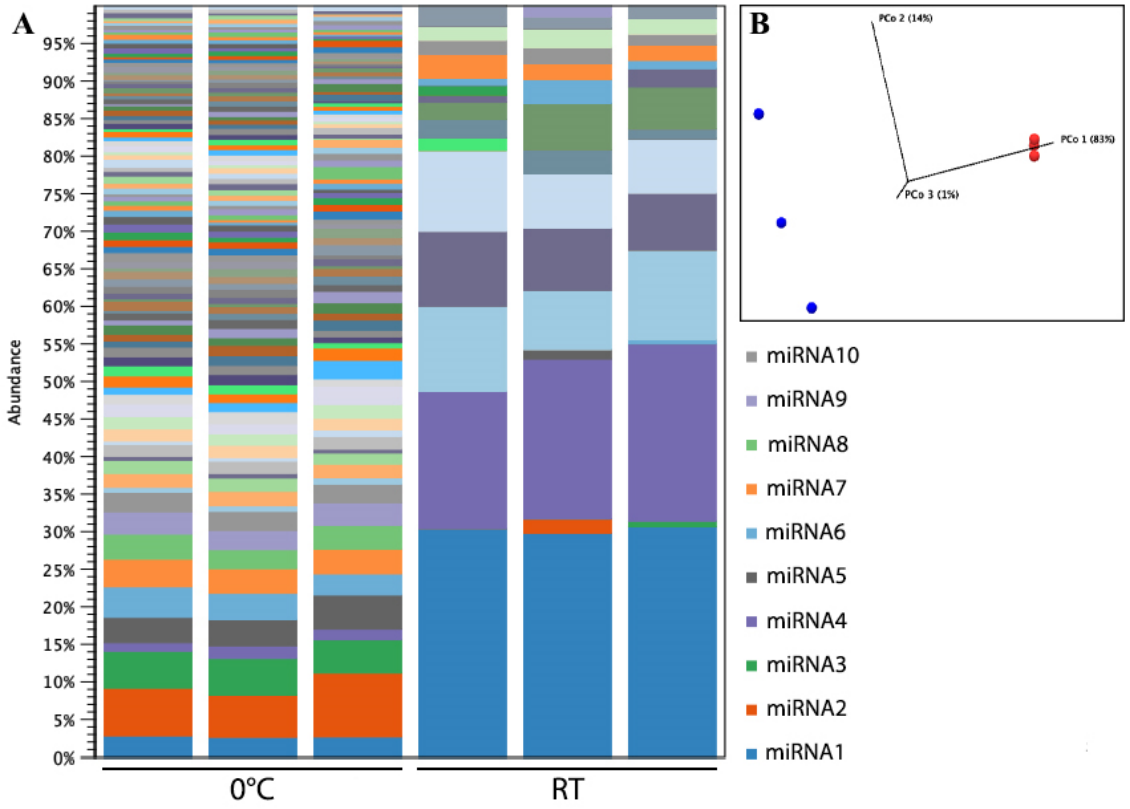

Figure 3.7. Diversity and PCoA analysis (Bray-Curtis) of miRNAs in *Rhodotorula* JG1b at 0°C and 23°C

(**A**) Abundance and diversity of the miRNAs (15-30 nt), with a minimum of 50 reads, of the three 0°C and the three 23°C *Rhodotorula* JG1b cultures. (**B**) PCoA analysis (Bray-Curtis) of the three 0°C (*blue*) and the 23°C (*red*) *Rhodotorula* JG1b miRNAs. The legend on the right lists only the 10 most abundant miRNAs.

Using the RNAhybrid computational method (Rehmsmeier et al 2004), we predicted the top putative mRNA targets for the ten most expressed miRNAs (**Table 3.1**), based on the lowest energy of hybridization required to form a duplex (Zhou *et al* 2012). The highly expressed miRNA1 and miRNA4 in our dataset likely target the mRNA coding for arsenite/tail-anchored protein-transporting ATPase, an enzyme involved in the attachment of tail-anchored protein to the ER membranes (Hemmingsson *et al.* 2009). While miRNA1 was not differentially expressed

between the two conditions, miRNA4 expression increased at 23°C, which corresponded with the decrease in expression of its mRNA target, the arsenite/tail-anchored protein-transporting ATPase. The eight other most abundant miRNAs were overexpressed (from 98.68% to 99.38% increase) or only express in the 0°C *Rhodotorula* JG1b cultures. Unfortunately, we could not correlate the expression of these eight miRNAs and expression of their putative mRNA targets. This could be due to incorrect target predictions, or more likely because RNA interference plays only a partial role in the regulation of these genes, with other cellular factors also involved.

Although the gene coding for Drosha was not differentially expressed at the two temperatures, the Dicer gene was significantly overexpressed (3.83-fold) at 0°C. The significant overexpression of Dicer is consistent with the observation of a significantly higher proportion of miRNAs at 0°C compared to 23°C while mRNA transcriptomic results suggest that *Rhodotorula* JG1b overexpresses numerous RNA polymerase III subunits and decreases its translational machinery at 0°C (**Figure 3.3B**, **Table S3.3**). Taken together, these results suggest that as with plants, *Rhodotorula* JG1may induce a miRNA gene regulatory mechanism in response to cold that triggers translational repression. Further molecular characterizations of the miRNAs, such as stem-loop RT-qPCR and northern blot analysis, are necessary to confirm the involvement of RNA interference in cold adaptation in *Rhodotorula*.

Table 3.1. Characteristic of the ten most abundant miRNA expressed in *Rhodotorula* JG1b

Summary of the transcription origin, and differential expression of Rhodotorula JG1b miRNAs. Putative mRNA gene targets of the miRNAs were predicted using the RNAhybrid computational method (Rehmsmeier *et al* 2004).

miRNA ID	Size (nt)	Location of miRNA in genome	Differential expression of miRNA	Characteristics	Main target	Hybrid of miRNA and target
miRNA1	30	ITS region	Not differentially expressed between 0°C and 23°C	**miRNA's targeted gene**	arsA	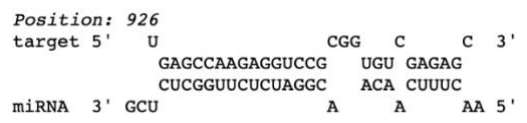
				Target's function	arsenite/tail-anchored protein-transporting ATPase	
				KO number	K01551	
				Differential expression of target	Overexpressed at 0°C	
				Binding energy kcal/mol	-41.6	
miRNA2	18	5.8S region	Overexpressed at 0°C	**miRNA's targeted gene**	GST	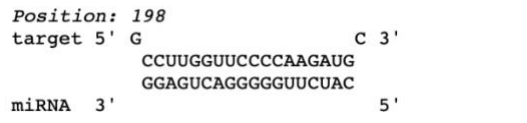
				Target gene function	glutathione S-transferase	
				KO number	K00799	
				Differential expression of target	Overexpressed at 0°C	
				Binding energy	-34.7	
miRNA3	27	Hypothetical protein	Overexpressed at 0°C	**miRNA's targeted gene**	NADK	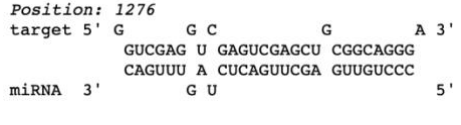
				Target gene function	NAD+ kinase	
				KO number	K00858	
				Differential expression of target	none	
				Binding energy	-43.2	
miRNA4	28	5.8S region	Overexpressed at 23°C	**miRNA's targeted gene**	arsA	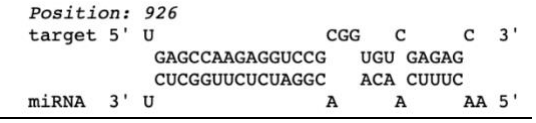
				Target gene function	arsenite/tail-anchored protein-transporting ATPase	
				KO number	K01551	
				Differential expression of target	Overexpressed at 0°C	
				Binding energy	-41.6	
miRNA5	17	5.8S region	Overexpressed at 0°C	**miRNA's targeted gene**	COPS7	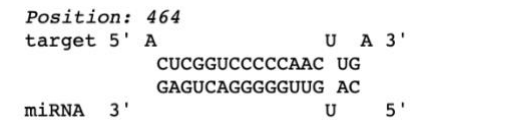
				Target gene function	COP9 signalosome complex subunit 7	
				KO number	K12180	
				Differential expression of target	none	
				Binding energy	-34.9	

miRNA6	20	Hypothetical protein	Overexpressed at 0°C	**Target gene name** **miRNA's targeted gene**	Hypothetical protein	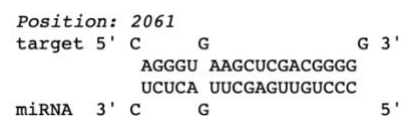
				KO number	none	
				Differential expression of target	none	
				Binding energy	-35.9	
miRNA7	22	Hypothetical protein	Overexpressed at 0°C	**Target gene name**	SND1	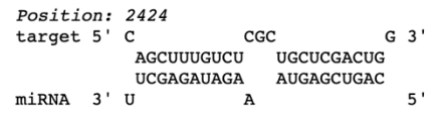
				Target gene function	staphylococcal nuclease domain-containing protein 1	
				KO number	K15979	
				Differential expression of target	none	
				Binding energy	-33.6	
miRNA8	22	5.8S region	Overexpressed at 0°C	**miRNA's targeted gene**	PDCD6IP	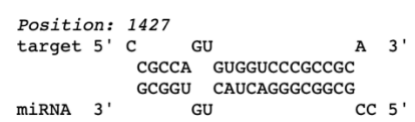
				Target gene function	programmed cell death 6-interacting protein	
				KO number	K12200	
				Differential expression of target	none	
				Binding energy	-47	
miRNA9	29	25S region	Overexpressed at 0°C	**miRNA's targeted gene**	BRF1	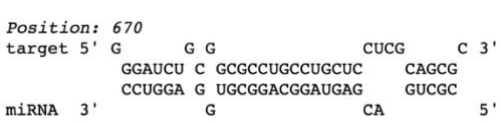
				Target gene function	transcription factor IIIB 90 kDa subunit	
				KO number	K15196	
				Differential expression of target	none	
				Binding energy	-51.8	
miRNA10	17	Genomic scaffold	Overexpressed at 0°C	**miRNA's targeted gene**	LYS1	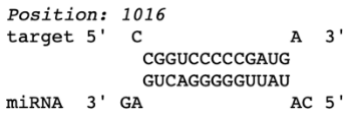
				Target gene function	saccharopine dehydrogenase	
				KO number	K00290	
				Differential expression of target	none	
				Binding energy	-28.6	

3.5 Conclusions

Overall, our results suggest that *Rhodotorula* JG1b at 0°C upregulated many cold-adaptive mechanisms, such as the increase in the pentose phosphate pathway, increase in production of carotenoids, sphingolipids, unsaturated fatty acid, and exopolysaccharides, coupled with a reduction in growth, amino acid metabolism and translation. We identified novel cold adaptation features. At low temperature *Rhodotorula* JG1b decreased tetrazolium redox dye reduction through a major downregulation of citrate cycle genes and respiration transport chain subunits. These results suggest switching of respiratory metabolism at optimal growth temperature (23°C), to fermentative metabolism at suboptimal temperature (0°C). At this low temperature, *Rhodotorula* JG1b overexpressed ethanol and xylitol fermentation pathways, resulting in ethanol production, at the lowest know temperature described so far in any prokaryotic and fungal microorganisms, potentially to acquire energy and delay freezing. In addition, at low temperature *Rhodotorula* JG1b produced a significantly higher proportion of small non-coding RNAs, specifically miRNAs, and overexpressed the Dicer protein, suggesting RNAi as a novel mechanism of cold adaptation in polar yeast. Further characterization of the role of ethanol production and identification of mRNA targets in silencing are needed to gain better insight into cold adaptation of the extremophilic yeast *Rhodotorula* JG1b.

3.6 Acknowledgements

We acknowledge the precious input from Dr. Jennifer Ronholm and Dr. Jacqueline Goordial for their critical feedback and for the setting up of the project, and Dr. Barry R. Bochner, from Biolog Inc. for his precious advice with the Biolog Phenotypic MicroArray tests analysis.

3.7 Supplementary Material

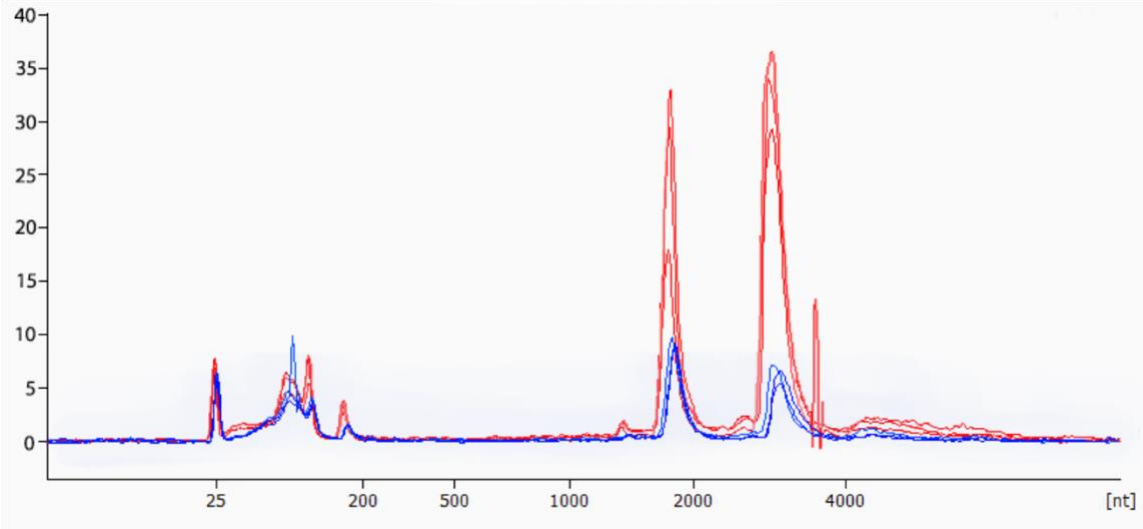

Figure S3.1. 2100 Bioanalyzer system electrogram for the *Rhodotorula* JG1b Total RNA at 0°C and 23°C

Superposition of the Total RNA Bioanalyzer system electrogram extracted from the three 23°C *Rhodotorula* JG1b cultures (*red*), and the three 0°C *Rhodotorula* JG1b cultures (*blue*).

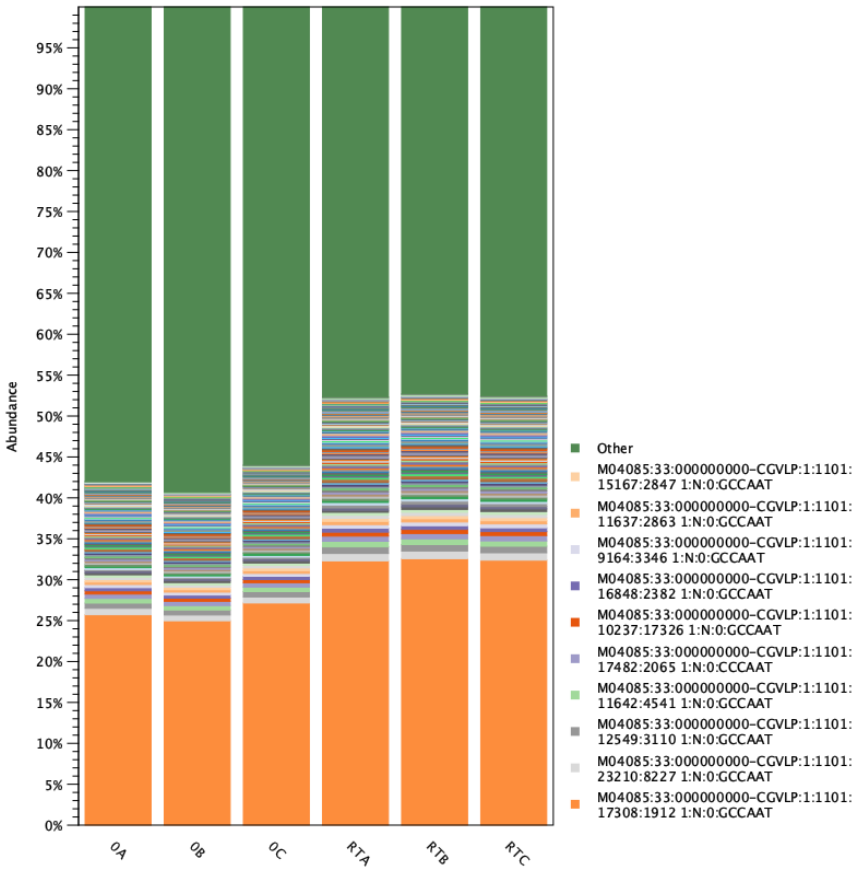

Figure S3.2. Diversity of small non-coding RNAs in *Rhodotorula* JG1b at 0°C and 23°C

Abundance and diversity of the small non-coding RNAs (>200nt) of three 0°C (*0A, 0B, 0C*), and the three 23°C (*RTA, RTB, RTC*) *Rhodotorula* JG1b cultures.

Table S.3.1. OD_{590} values for the Biolog Phenotypic MicroArray at 0°C

OD_{590} values average and normalized both the T0 and the negative control for each "positive" nutrient sources of the PM1 MicroPlate™, PM2A MicroPlate™, and PM3B MicroPlate™ incubated *Rhodotorula* JG1b for 91 days at 0°C.

		Time (days)											
		0	1	2	6	9	14	21	28	42	56	70	91
Carbon sources	Glycerol	0	0	0	0.0006	0	0	0.0145	0.0148	0.0261	0.0479	0.0965	0.3912
	Succinic Acid	0	0	0	0.0009	0	0	0.0058	0.0238	0.0375	0.0511	0.0882	0.2444
	Tween 20	0	0.0024	0.0061	0.0607	0.0622	0.0923	0.0614	0.0734	0.1038	0.0975	0.1039	0.4679
	Tween 40	0	0	0.0005	0.04	0.046	0.0827	0.0939	0.1051	0.1141	0.2036	0.3147	0.4907
	Tween 80	0	0.0012	0.0057	0.0347	0.0313	0.0633	0.044	0.0551	0.0939	0.0932	0.149	0.2328
	Fumaric Acid	0	0.0009	0	0.0014	0	0	0.0048	0.0105	0.0111	0.0331	0.1123	0.272
	D-Psicose	0	0	0	0.005	0.006	0	0.0056	0.0181	0.0402	0.0816	0.1499	0.238
	a-Keto-Glutaric Acid	0	0.0001	0	0.003	0	0	0.0048	0.0085	0.0304	0.0962	0.2113	0.4407
	D, L-a-Glycerol-Phospate	0	0	0	0.0058	0.0056	0.0157	0.036	0.036	0.051	0.089	0.1721	0.2627
	D-Fructose	0	0	0	0.0048	0.0025	0.0134	0.0566	0.1161	0.2477	0.3807	0.5756	0.8406
	Propionic Acid	0	0	0	0.0028	0	0.004	0.0191	0.0324	0.0565	0.1124	0.21	0.4431
	L-Proline	0	0	0	0.003	0.003	0.004	0.014	0.033	0.058	0.109	0.236	0.636
	D-Xylose	0	0.006	0.011	0.029	0.033	0.048	0.089	0.132	0.18	0.216	0.245	0.279
	a-Methyl-D-Glucoside	0	0	0	0.002	0	0	0.006	0.016	0.034	0.072	0.169	0.259
	D-Alanine	0	0	0	0.0046	0.0003	0.0004	0.001	0.0084	0.0397	0.0575	0.0983	0.2549
	a-D-Glucose	0	0	0	0.0058	0.0073	0.0271	0.1403	0.303	0.5369	0.649	0.7532	0.7926
	Adonitol	0	0	0	0.0006	0	0	0	0.0222	0.0462	0.1011	0.2368	0.4938
	D-Trealose	0	0	0	0.0078	0.0006	0.0025	0.0149	0.0333	0.0656	0.1125	0.2092	0.4005
	Maltotriose	0	0.0009	0	0.0076	0.006	0.0217	0.0615	0.0926	0.1389	0.2027	0.2988	0.3868
	Glyoxylic Acid	0	0	0	0	0	0	0	0	0.0124	0.0797	0.1589	0.2456
	D-Mannose	0	0.0013	0.0009	0.0058	0.0028	0.0107	0.0455	0.0915	0.1578	0.1998	0.2899	0.4043
	Sucrose	0	0	0	0.0044	0	0.0005	0.022	0.0462	0.0898	0.1909	0.3446	0.5398
	D-Raffinose	0	0	0	0	0.0024	0.0075	0.0304	0.0232	0.046	0.0899	0.1769	0.3412
	D-Lactic Acid Methyl Ester	0	0	0	0	0	0	0.0281	0.0336	0.0627	0.1263	0.2571	0.3663
	Chondroitin Sulfate C	0	0	0	0	0	0	0.0107	0.0152	0.0367	0.061	0.0972	0.2652
	Melibionic Acid	0	0.0014	0.0029	0.0084	0.0081	0.0134	0.0354	0.0395	0.0712	0.1428	0.2328	0.3253
	ß-Cyclodextrin	0	0.0134	0.0212	0.0215	0.0234	0.0302	0.0534	0.0625	0.0994	0.1688	0.276	0.3599
	γ-Cyclodextrin	0	0	0.001	0.0018	0.0012	0.0037	0.0206	0.0246	0.0483	0.0901	0.1611	0.3004
	Dextrin	0	0.0004	0	0.0079	0.0199	0.0374	0.0715	0.0799	0.1003	0.1192	0.1774	0.1999
	D-Arabitol	0	0	0.0024	0.0061	0.0094	0.0187	0.0501	0.0612	0.0963	0.1611	0.278	0.4761
	Quinic Acid	0	0	0	0	0	0	0.0408	0.0379	0.0641	0.2056	0.4837	0.8307
	Gelatin	0	0.1214	0.1767	0.2148	0.2463	0.3062	0.3809	0.4084	0.4649	0.525	0.6403	0.7333
	L-Arabitol	0	0	0	0.0018	0.0002	0.0087	0.0487	0.0539	0.0417	0.0935	0.2213	0.7452
	4-Hydroxy Benzoic Acid	0	0	0	0	0	0	0.029	0.0234	0.0487	0.0949	0.2416	0.4234
	Laminarin	0	0	0	0.0055	0.0275	0.0563	0.0806	0.0877	0.1167	0.1768	0.2571	0.2172
	Pectin	0	0.0362	0.0652	0.0708	0.0697	0.0764	0.1019	0.1134	0.1475	0.1995	0.3064	0.4689
Nitrogen sources	L-Proline	0	0.0002	0.0034	0	0	0	0.0114	0.0159	0.0279	0.0568	0.0808	0.2814
	L-Pyroglutamic Acid	0	0	0.0013	0.0051	0.0024	0.0008	0.0117	0.0061	0.0262	0.0337	0.0447	0.276

Table S.3.2. *Rhodotorula* JG1b strain information and transcriptomic result summary

	***Rhodotorula* JG1b (Goordial *et al* 2016b)**
Phylum	Basidiomycota
Location isolated	Permafrost, University Valley, Antarctica
Size of genome (Mbp)	19.3934
GC%	60.6
Total number of proteins	6,681
mRNA transcriptomic results	(this manuscript)
Total number of genes expressed*	5913
Total differentially expressed genes (≥ 1.5 FC)	1,772
Increased at 0°C compared to 23°C	994
Decrease at 0°C compared to 23°C	778
With KEGG annotation	924
% KEGG annotation	52%

*With an abundance ≥ 1

Table S.3.3. *Rhodotorula* JG1b differentially expressed homologous proteins summary

KO Number	KO Name	No. of homologs/analogs equally expressed	No. of homologs/analogs overexpressed at 23°C	No. of homologs/analogs overexpressed at 0°C	Function
K00101	lldD	0	2	1	L-lactate dehydrogenase (cytochrome)
K00128	ALDH	2	1	1	aldehyde dehydrogenase (NAD+)
K00698	CHS1	3	2	1	chitin synthase
K01183	-	2	1	1	chitinase
K01379	CTSD	2	1	2	cathepsin D (aspartic endo-protease)
K01273	DPEP	0	1	1	* membrane dipeptidase
K01530	-	0	1	1	* phospholipid-translocating ATPase
K03457	TC.NCS1	1	1	1	* nucleobase:cation symporter-1, NCS1family
K06689	UBE2C	1	1	1	ubiquitin-conjugating enzyme E2 D
K10756	RFC3_5	0	1	1	replication factor C subunit 3/5
K11253	H3	2	3	1	histone H3
K13348	MPV17	0	1	2	*protein Mpv17
K14686	SLC31A1	0	1	1	*SLC31A1, CTR1; solute carrier family 31 (copper transporter), member 1
K15109	SLC25A20_29	**3**	**1**	**1**	* solute carrier family 25 (mitochondrial carnitine/acylcarnitine transporter), member 20/29
K16261	YAT	**2**	**2**	**3**	* yeast amino acid transporter
K18065	CDC25	0	1	1	Cdc25 family phosphatase
K19355	MAN	1	1	1	mannan endo-1,4-beta-mannosidase
K21989	TMEM63	1	1	1	* calcium permeable stress-gated cation channel
Total		20	23	22	

* Genes involved with cellular membranes

Table S.3.4. Summary of small RNA and miRNA proportion in *Rhodotorula* JG1b cultures grown at 0°C and 23°C

The proportions were determined based on the 2100 Bioanalyzer system results.

	% small RNA / Total RNA	% miRNA / small RNA
A 0°C	52.6	1.16
B 0°C	55.4	1.91
C 0°C	52.3	0.74
Average 0°C	53.4	1.27
A RT	31.4	0.11
B RT	26.2	0.08
C RT	25.6	0.09
Average RT	27.7	0.09
p-value	0.0003	0.03

Table S.3 5. Figure 3.4 and 3.6 list of the abbreviations

Abbreviation	Name	Abbreviation	Name
GALM	aldose-1-epimerase	fum	fumarate hydratase
HK	hexokinase	MDH	malate dehydrogenase
G6P1I	glucose-6-phosphate 1-epimerase	ace	isocitrate lyase
GPI	glucose-6-phosphate isomerase	pck	malate synthase
PFK	6-phosphofructokinase	G6PD	glucose-6-phosphate 1-dehydrogenase
FBP	fructose-1, 6-biphoshatase	PGLS, pgl	6-phosphogluconolactonase
FBA	fructose-bisphosphate aldolase	gnl	gluconolactonase
GAPDH	glyceraldehyde 3-phosphate dehydrogenase	gntK	gluconokinase
PGK	phosphoglycerate kinase	PGD	6-phosphogluconate dehydrogenase
PGAM	2,3-bisphosphoglycerate-dependent phosphoglycerate mutase	rpi	ribose 5-phosphate isomerase
ENO	enolase	rpe	ribulose-phosphate 3-epimerase
PK	pyruvate kinase	rbsK	ribokinase
TPI	triosephosphate isomerase	PRPS	ribose-phosphate pyrophosphokinase
DAK	triose/dihydroxyacetone kinase	tkt	transketolase
GCY1	glycerol 2-dehydrogenase	tal	transaldolase
PDC	pyruvate decarboxylase	xfp	xylulose-5-phosphate/fructose-6-phosphate phosphoketolase
Adh	alcohol dehydrogenase	xyl	xylulokinase
ALDH	aldehyde dehydrogenase	xdh	D-xylulose reductase
Acs	acetyl-CoA synthetase	SORD	L-iditol 2-dehydrogenase
PC	pyruvate carboxylase	SPT	serine palmitoyltranferase
ACLY	ATP citrate lyase	KDSR	3-keto-deihydrosphingosine reductase
CS	citrate synthase	LAG	ceramide synthase
ACO	aconitate hydratase	DEGS	sphingolipid 4-desaturase/C4-monooxygenase
IDH	isocitrate dehydrogenase	SMPD	sphingomyelin phosphodiesterase
OGDH	2-oxoglutarate dehydrogenase	UGCG	ceramide glucosyltransferase
DLST	dihydrolipoamide succinyltransferase	SUR	sphinganine C4-monooxygenase
DLD	dihydrolipoamide dehydrogenase	LCB3	dihydrosphingosine 1-phosphate phosphatase
LSC	succinyl-CoA synthetase	SPHK	sphingosine kinase
SDH	succinate dehydrogenase	SGPL1	sphinganine-1-phosphate aldolase

Chapter 4. Discussion and Conclusions

Earth's cryosphere is represented by some of the most extreme conditions for microbial growth and metabolic activity. These environments are characterized by unique ecosystems similar to the one that could harbor life on Mars, Europa and Enceladus (Goordial *et al* 2013), therefore, the study of cryobiology is important to better understand astrobiology. Though the search for life on these planetary bodies is one of the major components of astrobiology (Hays 2015), no life detection missions have been performed in space since the 1970s (Davila *et al* 2010). The need for a robust and sensitive life detection instrument is more relevant than ever, since current scientific instruments related to astrobiology-targeted space missions are focused on the detection of biosignatures from past life, and are mainly large, heavy and require high levels of energy. The need for more specific astrobiological instruments is also highlighted by the current difficulties in defining biomarkers. Microorganisms are able to thrive in analog extreme habitats (Margesin and Miteva 2011); however, multiple challenges remain regarding the assessment of *in situ* activity and the understanding of cold adaptation.

In Chapter 2, the development of a novel automatized life-detection instrument, the µMAMA, was demonstrated, and the potential of metabolism-indicator redox dyes for utilization in an astrobiology context was assessed. The AlamarBlue® buffered in IF-0a, and the Biolog IF-C dye/buffer combinations were identified as the most sensitive to microbial metabolic activity while offering a broad physiochemical range of usage. Using these combinations, microbial activity was detected with the µMAMA from astrobiological analog sites from the Canadian high Arctic, which were characterized by a low microbial diversity. In addition, the µMAMA was able to detect sulfate-oxidizing and Fe(II)-oxidizing chemolithoautotrophic metabolism. This is important as chemotrophic organisms are the likeliest life form to developed or be present on Mars (Michalski

et al 2018; Sekine *et al* 2015). In this study, the redox dyes capability to detect metabolic activity of heterotrophic microorganisms was tested by using heterotrophic polar psychrophilic and psychrotolerant pure cultures and by characterizing the heterotrophic communities of our samples. In that matter, the need of a further testing of the chosen redox dye in regard to their capabilities with non-heterotrophic metabolisms is strongly suggested. The next steps of this research would include to perform a sensitivity assay using aerobic chemolithoautotrophs, such as the sulfate-oxidizing *Thiomicrospira* bacteria (Perreault *et al* 2008), and anaerobic chemolithoautotrophs, such as the Fe(II)-oxidizing bacterial culture KS (Hohmann *et al* 2009). These microorganisms and metabolisms are relevant as they are similar to the potential life forms that could be found beyond Earth (Priscu and Hand 2012; Xiong *et al.* 2015) and especially on Mars. Moreover, due to the limitations of the µMAMA design, minimal movement of fluid occurred across some wells in the µMAMA cards. This demonstrated the need of a new prototype where all wells can be independently inoculated with the environmental samples, thus avoiding well to well cross-contamination. Furthermore, for the future µMAMA iteration, we recommend fully drying the redox dye and buffer in the wells prior to *in situ* inoculations. This would considerably decrease the labor of sample preparation and improve the µMAMA platform by bringing it closer to a full automation. A full automation is required to establish µMAMA as a strong candidate for incorporation into future life detection missions on Mars, Europa, or Enceladus.

In Chapter 3, *Rhodotorula* JG1b was discovered to use numerous strategies to overcome cold growth challenges by comparing its growth at 23°C and at 0°C. At 0ºC, *Rhodotorula* increased its membrane fluidity, carotenoid production, and compatible solutes, while it decreased its protein synthesis, and induced a switch in its primary metabolism from respiration to ethanol fermentation. These adaptations are generally in accordance with other studies on cold adaptation mechanisms

previously reported in bacteria and yeast (Barria *et al* 2013; Gunde-Cimerman *et al* 2014; Raymond-Bouchard and Whyte 2017; Raymond-Bouchard *et al* 2018a; Tribelli and López 2018). Through the combination of transcriptomic analyses and phenotypic profiling, we further characterized the cold-induced switch in metabolism and identified novel cold-adaptation strategies in *Rhodotorula* JG1b. *Rhodotorula* appears to drastically change from a respiratory metabolism to a fermentative metabolism as primary source of energy, and produces ethanol when grown at 0°C compared to 23°C. This is the coldest ethanol production by a microorganism recorded to this date, without the help of biocatalyst, and the first time that ethanol production is linked to prokaryotic and fungal adaptation to cold. In addition of being a novel cold adaptation, the discovery of ethanol production in cold conditions may have implications in biotechnology. For example, alcoholic beverages have been shown to improve in quality while fermented at low temperatures (Kanellaki *et al.* 2014). To better characterize the importance of fermentation metabolism during *Rhodotorula* cold growth, additional studies are required. For instance, characterizing the ethanol production rate of *Rhodotorula* JG1b through HPLC, after an incubation in a specific ethanol production media (Rao *et al* 2008) or through GC/MS (Kourkoutas *et al* 2003) would be required. *Rhodotorula* uses the post-transcriptional regulation of gene expression through mRNA silencing by miRNAs. This is the first time RNA interference has been linked to cold adaptation in any microorganism. Further work would be required to clearly identify the function and role of the significantly overexpressed miRNAs through future molecular analyses. To confirm the difference in expression of these miRNA in cells growing under low temperatures, stem-loop RT-qPCR, and northern blot analysis would be required (Wang *et al* 2014; Zhang *et al* 2014). While miRNAs are known to play a role in cold adaptation in plants (Miura and Furumoto 2013), this is the first report of a similar mechanism occurring in fungi. Another important next

step would be to perform a proteomic survey of *Rhodotorula* JG1b growing at 0°C. This would allow us to better understand the proteins and pathways active under cold temperatures, and to correlate the protein translation to the findings of our transcriptomic study. In addition, the 0°C proteome of *Rhodotorula* JG1b could lead to the discovery of cold-adapted proteins and enzymes, which may have implications in biotechnology, especially for food industries and bioremediation processes (Gerday *et al.* 2000).

Together, chapters 2 and 3 showed the importance of studying polar environments and cold adaptation of their active microbial communities to have a better understanding of how life can thrive and survive under extreme conditions. The first objective of the thesis was to develop and field-test the µMANA platform with indicator redox dyes. This was achieved as we designed and tested µMAMA and the metabolism-indicator redox dyes with pure cultures, abiotic media, and environmental samples. This new instrument is able to detect microbial metabolic activity in extreme environments and shows potential for future astrobiology missions focused on extant microbial life detection. The second objective was to identify and characterize the metabolic mechanism changes of *Rhodotorula* JG1b in response to cold. This was achieved by performing transcriptomic and phenotypic analyses that provided insights on novel microbial adaptations to low temperature. These analyses led to the identification of ethanol production and RNAi regulation as novel mechanisms in microbial cold adaptation.

References

Aguilar PS, Hernandez-Arriaga AM, Cybulski LE, Erazo AC, de Mendoza D (2001). Molecular basis of thermosensing: a two-component signal transduction thermometer in Bacillus subtilis. *The EMBO journal* **20:** 1681-1691.

Aguilera J, Randez-Gil F, Prieto JA (2007). Cold response in Saccharomyces cerevisiae: new functions for old mechanisms. *FEMS microbiology reviews* **31:** 327-341.

Albanesi D, Mansilla MC, de Mendoza D (2004). The membrane fluidity sensor DesK of Bacillus subtilis controls the signal decay of its cognate response regulator. *Journal of bacteriology* **186:** 2655-2663.

Aliyu H, De Maayer P, Cowan D (2016). The genome of the Antarctic polyextremophile Nesterenkonia sp. AN1 reveals adaptive strategies for survival under multiple stress conditions. *FEMS microbiology ecology* **92**.

Altshuler I, Goordial J, Whyte LG (2017). Microbial life in permafrost. *Psychrophiles: from biodiversity to biotechnology*. Springer. pp 153-179.

Altshuler I, Ronholm J, Layton A, Onstott TC, W. Greer C, Whyte LG (2019). Denitrifiers, nitrogen-fixing bacteria and N2O soil gas flux in high Arctic ice-wedge polygon cryosols. *FEMS microbiology ecology* **95:** fiz049.

Ambros V (2003). MicroRNA pathways in flies and worms: growth, death, fat, stress, and timing. *Cell* **113:** 673-676.

Arvidson R, Squyres S, Bell J, Catalano J, Clark B, Crumpler L *et al* (2014). Ancient aqueous environments at Endeavour crater, Mars. *Science* **343:** 1248097.

Ayala-del-Río HL, Chain PS, Grzymski JJ, Ponder MA, Ivanova N, Bergholz PW *et al* (2010). The genome sequence of Psychrobacter arcticus 273-4, a psychroactive Siberian permafrost bacterium, reveals mechanisms for adaptation to low-temperature growth. *Appl Environ Microbiol* **76:** 2304-2312.

Bada JL (2001). State-of-the-art instruments for detecting extraterrestrial life. *Proceedings of the National Academy of Sciences* **98:** 797-800.

Bakermans C, Skidmore ML, Douglas S, McKay CP (2014). Molecular characterization of bacteria from permafrost of the Taylor Valley, Antarctica. *FEMS microbiology ecology* **89:** 331-346.

Bakermans C (2017). Determining the limits of microbial life at subzero temperatures. *Psychrophiles: From Biodiversity to Biotechnology*. Springer. pp 21-38.

Bakoyianis V, Kanellaki M, Kaliafas A, Koutinas A (1992). Low-temperature wine making by immobilized cells on mineral kissiris. *Journal of agricultural and food chemistry* **40:** 1293-1296.

Barrera LO, Ren B (2006). The transcriptional regulatory code of eukaryotic cells–insights from genome-wide analysis of chromatin organization and transcription factor binding. *Current opinion in cell biology* **18:** 291-298.

Barria C, Malecki M, Arraiano C (2013). Bacterial adaptation to cold. *Microbiology* **159:** 2437-2443.

Becerra M, Lombardia L, Gonzalez-Siso M, Rodriguez-Belmonte E, Hauser N, Cerdán M (2003). Genome-wide analysis of the yeast transcriptome upon heat and cold shock. *International Journal of Genomics* **4:** 366-375.

Bergholz PW, Bakermans C, Tiedje JM (2009). Psychrobacter arcticus 273-4 uses resource efficiency and molecular motion adaptations for subzero temperature growth. *Journal of bacteriology* **191:** 2340-2352.

Bertrand EM, McCrow JP, Moustafa A, Zheng H, McQuaid JB, Delmont TO *et al* (2015). Phytoplankton–bacterial interactions mediate micronutrient colimitation at the coastal Antarctic sea ice edge. *Proceedings of the National Academy of Sciences* **112:** 9938-9943.

Bhuiyan M, Tucker D, Watson K (2014). Gas chromatography–mass spectrometry analysis of fatty acid profiles of Antarctic and non-Antarctic yeasts. *Antonie Van Leeuwenhoek* **106:** 381-389.

Bochner BR, Gadzinski P, Panomitros E (2001). Phenotype microarrays for high-throughput phenotypic testing and assay of gene function. *Genome research* **11:** 1246-1255.

Bochner BR (2008). Global phenotypic characterization of bacteria. *FEMS microbiology reviews* **33:** 191-205.

Bore EK, Apostel C, Halicki S, Kuzyakov Y, Dippold MA (2017). Microbial metabolism in soil at subzero temperatures: adaptation mechanisms revealed by position-specific 13C labeling. *Frontiers in microbiology* **8:** 946.

Bowman JP, Rea SM, McCammon SA, McMeekin TA (2000). Diversity and community structure within anoxic sediment from marine salinity meromictic lakes and a coastal meromictic marine basin, Vestfold Hills, Eastern Antarctica. *Environmental Microbiology* **2:** 227-237.

Brakstad OG, Nonstad I, Faksness L-G, Brandvik PJ (2008). Responses of microbial communities in Arctic sea ice after contamination by crude petroleum oil. *Microbial ecology* **55:** 540-552.

Breaker RR (2010). RNA switches out in the cold. *Molecular cell* **37:** 1-2.

Buelow HN, Winter AS, Van Horn DJ, Barrett JE, Gooseff MN, Schwartz E *et al* (2016). Microbial community responses to increased water and organic matter in the arid soils of the McMurdo Dry Valleys, Antarctica. *Frontiers in microbiology* **7:** 1040.

Bulat S, Alekhina IA, Lipenkov VY, Lukin V, Marie D, Petit J-R (2009). Cell concentrations of microorganisms in glacial and lake ice of the Vostok ice core, East Antarctica. *Microbiology* **78:** 808.

Bura R, Vajzovic A, Doty SL (2012). Novel endophytic yeast Rhodotorula mucilaginosa strain PTD3 I: production of xylitol and ethanol. *Journal of industrial microbiology & biotechnology* **39:** 1003-1011.

Buzzini P, Branda E, Goretti M, Turchetti B (2012). Psychrophilic yeasts from worldwide glacial habitats: diversity, adaptation strategies and biotechnological potential. *FEMS microbiology ecology* **82:** 217-241.

Buzzini P, Margesin R (2014a). Cold-adapted yeasts: a lesson from the cold and a challenge for the XXI century. *Cold-adapted yeasts*. Springer. pp 3-22.

Buzzini P, Margesin R (2014b). Cold-adapted yeasts. *Miscellaneous Cold-Active Yeast Enzymes of Industrial Importance New York: Springer*.

Buzzini P, Turk M, Perini L, Turchetti B, Gunde-Cimerman N (2017). Yeasts in polar and subpolar habitats. *Yeasts in natural ecosystems: Diversity*. Springer. pp 331-365.

Cameron KA, Stibal M, Zarsky JD, Gözdereliler E, Schostag M, Jacobsen CS (2016). Supraglacial bacterial community structures vary across the Greenland ice sheet. *FEMS microbiology ecology* **92:** fiv164.

Cao-Hoang L, Dumont F, Marechal P-A, Gervais P (2010). Inactivation of Escherichia coli and Lactobacillus plantarum in relation to membrane permeabilization due to rapid chilling followed by cold storage. *Archives of microbiology* **192:** 299-305.

Carr MH, Belton MJ, Chapman CR, Davies ME, Geissler P, Greenberg R *et al* (1998). Evidence for a subsurface ocean on Europa. *Nature* **391:** 363.

Carvalhais LC, Dennis PG, Tyson GW, Schenk PM (2012). Application of metatranscriptomics to soil environments. *Journal of microbiological methods* **91:** 246-251.

Castro-Wallace SL, Chiu CY, John KK, Stahl SE, Rubins KH, McIntyre AB *et al* (2017). Nanopore DNA sequencing and genome assembly on the International Space Station. *Scientific reports* **7:** 18022.

Catling D, Claire M, Zahnle K, Quinn R, Clark B, Hecht M *et al* (2010). Atmospheric origins of perchlorate on Mars and in the Atacama. *Journal of Geophysical Research: Planets* **115**.

Cavicchioli R, Siddiqui KS, Andrews D, Sowers KR (2002). Low-temperature extremophiles and their applications. *Current opinion in biotechnology* **13:** 253-261.

Chan-Yam K, Goordial J, Greer C, Davila A, McKay CP, Whyte LG (2019). Microbial Activity and Habitability of an Antarctic Dry Valley Water Track. *Astrobiology* **19:** 757-770.

Chen C, Dickman MB (2005). Proline suppresses apoptosis in the fungal pathogen Colletotrichum trifolii. *Proceedings of the National Academy of Sciences* **102:** 3459-3464.

Chevrier V, Poulet F, Bibring J-P (2007). Early geochemical environment of Mars as determined from thermodynamics of phyllosilicates. *Nature* **448:** 60.

Chin M, Ricco A, Quinn R, Lee A, Boone T, Chinn T, Radosevich L, Wang J, Harrison J: SPLIce: A Microfluidic Sample Processor to Enable the Search for Life on Icy Worlds. *42nd COSPAR Scientific Assembly*. 2018

Cho DH, Chae HJ, Kim EY (2001). Synthesis and characterization of a novel extracellular polysaccharide by Rhodotorula glutinis. *Applied biochemistry and biotechnology* **95:** 183-193.

Chu-Ky S, Tourdot-Marechal R, Marechal P-A, Guzzo J (2005). Combined cold, acid, ethanol shocks in Oenococcus oeni: effects on membrane fluidity and cell viability. *Biochimica et Biophysica Acta (BBA)-Biomembranes* **1717:** 118-124.

Chyba CF, Phillips CB (2001). Possible ecosystems and the search for life on Europa. *Proceedings of the National Academy of Sciences* **98:** 801-804.

Coates JD, Achenbach LA (2004). Microbial perchlorate reduction: rocket-fuelled metabolism. *Nature Reviews Microbiology* **2:** 569-580.

Colley K, Varki A, Kinoshita T (2017). Chapter 4: cellular organization of glycosylation. Essentials in Glycobiology, 3rd Edn., eds Varki A., Cummings RD, Esko JD ….

Contreras G, Barahona S, Sepúlveda D, Baeza M, Cifuentes V, Alcaíno J (2015). Identification and analysis of metabolite production with biotechnological potential in Xanthophyllomyces dendrorhous isolates. *World Journal of Microbiology and Biotechnology* **31:** 517-526.

Cramer P (2002). Multisubunit RNA polymerases. *Current opinion in structural biology* **12:** 89-97.

da Silva TL, Feijão D, Roseiro JC, Reis A (2011). Monitoring Rhodotorula glutinis CCMI 145 physiological response and oil production growing on xylose and glucose using multi-parameter flow cytometry. *Bioresource technology* **102:** 2998-3006.

Davies PL, Baardsnes J, Kuiper MJ, Walker VK (2002). Structure and function of antifreeze proteins. *Philosophical Transactions of the Royal Society of London Series B: Biological Sciences* **357:** 927-935.

Davila AF, Skidmore M, Fairén AG, Cockell C, Schulze-Makuch D (2010). New priorities in the robotic exploration of Mars: the case for in situ search for extant life. *Astrobiology* **10:** 705-710.

De Maayer P, Anderson D, Cary C, Cowan DA (2014). Some like it cold: understanding the survival strategies of psychrophiles. *EMBO reports* **15:** 508-517.

Douglas MS, Smol JP (2000). Eutrophication and recovery in the high arctic: Meretta Lake (Cornwallis Island, Nunavut, Canada) revisited. *Hydrobiologia* **431:** 193-204.

Doyle S, Dieser M, Broemsen E, Christner B (2012). General characteristics of cold-adapted microorganisms. *Polar Microbiology: Life in a Deep Freeze*. American Society of Microbiology. pp 103-125.

Dozmorov MG, Giles CB, Koelsch KA, Wren JD: Systematic classification of non-coding RNAs by epigenomic similarity. *BMC bioinformatics*. 2013

Duncan SM, Farrell RL, Thwaites JM, Held BW, Arenz BE, Jurgens JA *et al* (2006). Endoglucanase-producing fungi isolated from Cape Evans historic expedition hut on Ross Island, Antarctica. *Environmental Microbiology* **8:** 1212-1219.

Duval B, Shetty K, Thomas WH (1999). Phenolic compounds and antioxidant properties in the snow alga Chlamydomonas nivalis after exposure to UV light. *Journal of Applied Phycology* **11:** 559.

Elberling B, Brandt KK (2003). Uncoupling of microbial CO2 production and release in frozen soil and its implications for field studies of arctic C cycling. *Soil Biology and Biochemistry* **35:** 263-272.

Eliasson A, Boles E, Johansson B, Österberg M, Thevelein J, Spencer-Martins I *et al* (2000). Xylulose fermentation by mutant and wild-type strains of Zygosaccharomyces and Saccharomyces cerevisiae. *Applied microbiology and biotechnology* **53:** 376-382.

Environment Canada CC (2014). Normals 1981-2010 Station Data [WWW]. *Environment Canada Fredericton, New Brunswick, Kanada* **13**.

Ernakovich JG, Wallenstein MD (2015). Permafrost microbial community traits and functional diversity indicate low activity at in situ thaw temperatures. *Soil Biology and Biochemistry* **87:** 78-89.

Fahnestock JT, Jones MH, Welker JM (1999). Wintertime CO2 efflux from arctic soils: implications for annual carbon budgets. *Global Biogeochemical Cycles* **13:** 775-779.

Fell JW, Boekhout T, Fonseca A, Scorzetti G, Statzell-Tallman A (2000). Biodiversity and systematics of basidiomycetous yeasts as determined by large-subunit rDNA D1/D2 domain sequence analysis. *International journal of systematic and evolutionary microbiology* **50:** 1351-1371.

Fenice M, Selbmann L, Zucconi L, Onofri S (1997). Production of extracellular enzymes by Antarctic fungal strains. *Polar Biology* **17:** 275-280.

Fong N, Burgess M, Barrow K, Glenn D (2001). Carotenoid accumulation in the psychrotrophic bacterium Arthrobacter agilis in response to thermal and salt stress. *Applied microbiology and biotechnology* **56:** 750-756.

Fonseca P, Moreno R, Rojo F (2011). Growth of Pseudomonas putida at low temperature: global transcriptomic and proteomic analyses. *Environmental microbiology reports* **3:** 329-339.

Frengova G, Simova E, Beshkova D (1997). Caroteno-protein and exopolysaccharide production by co-cultures of Rhodotorula glutinis and Lactobacillus helveticus. *Journal of Industrial Microbiology and Biotechnology* **18:** 272-277.

Gadkari PS, McGuinness LR, Männistö MK, Kerkhof LJ, Häggblom MM (2020). Arctic tundra soil bacterial communities active at subzero temperatures detected by stable isotope probing. *FEMS microbiology ecology* **96:** fiz192.

Garcia-Lopez E, Cid C (2017). Glaciers and ice sheets as analog environments of potentially habitable icy worlds. *Frontiers in microbiology* **8:** 1407.

Garland JL, Mills AL (1991). Classification and characterization of heterotrophic microbial communities on the basis of patterns of community-level sole-carbon-source utilization. *Appl Environ Microbiol* **57:** 2351-2359.

Garneau M-È, Michel C, Meisterhans G, Fortin N, King TL, Greer CW *et al* (2016). Hydrocarbon biodegradation by Arctic sea-ice and sub-ice microbial communities during microcosm experiments, Northwest Passage (Nunavut, Canada). *FEMS Microbiology Ecology* **92:** fiw130.

Gerday C, Aittaleb M, Bentahir M, Chessa J-P, Claverie P, Collins T *et al* (2000). Cold-adapted enzymes: from fundamentals to biotechnology. *Trends in biotechnology* **18:** 103-107.

Gianoli E, Inostroza P, Zúñiga-Feest A, Reyes-Díaz M, Cavieres LA, Bravo LA *et al* (2004). Ecotypic differentiation in morphology and cold resistance in populations of Colobanthus quitensis (Caryophyllaceae) from the Andes of central Chile and the maritime Antarctic. *Arctic, Antarctic, and Alpine Research* **36:** 484-489.

Gilichinsky D, Rivkina E, Shcherbakova V, Laurinavichuis K, Tiedje J (2003). Supercooled water brines within permafrost—an unknown ecological niche for microorganisms: a model for astrobiology. *Astrobiology* **3:** 331-341.

Gilichinsky D, Wilson G, Friedmann E, McKay C, Sletten R, Rivkina E *et al* (2007). Microbial populations in Antarctic permafrost: biodiversity, state, age, and implication for astrobiology. *Astrobiology* **7:** 275-311.

Gilichinsky D, Vishnivetskaya T, Petrova M, Spirina E, Mamykin V, Rivkina E (2008). Bacteria in permafrost. *Psychrophiles: from biodiversity to biotechnology*. Springer. pp 83-102.

Gómez F, Walter N, Amils R, Rull F, Klingelhöfer A, Kviderova J *et al* (2011). Multidisciplinary integrated field campaign to an acidic Martian Earth analogue with astrobiological interest: Rio Tinto. *International Journal of Astrobiology* **10:** 291-305.

Goordial J, Lamarche-Gagnon G, Lay C-Y, Whyte L (2013). Left out in the cold: life in cryoenvironments. *Polyextremophiles*. Springer. pp 335-363.

Goordial J, Davila A, Lacelle D, Pollard W, Marinova MM, Greer CW *et al* (2016a). Nearing the cold-arid limits of microbial life in permafrost of an upper dry valley, Antarctica. *The ISME journal* **10:** 1613.

Goordial J, Raymond-Bouchard I, Riley R, Ronholm J, Shapiro N, Woyke T *et al* (2016b). Improved high-quality draft genome sequence of the eurypsychrophile Rhodotorula sp. JG1b, isolated from permafrost in the hyperarid upper-elevation mcmurdo dry valleys, Antarctica. *Genome Announc* **4:** e00069-00016.

Goordial J, Altshuler I, Hindson K, Chan-Yam K, Marcolefas E, Whyte LG (2017). In situ field sequencing and life detection in remote (79° 26′ N) Canadian high Arctic permafrost ice wedge microbial communities. *Frontiers in microbiology* **8:** 2594.

Greetham D (2014). Phenotype microarray technology and its application in industrial biotechnology. *Biotechnology letters* **36:** 1153-1160.

Grotzinger JP, Sumner DY, Kah L, Stack K, Gupta S, Edgar L *et al* (2014). A habitable fluvio-lacustrine environment at Yellowknife Bay, Gale Crater, Mars. *Science* **343:** 1242777.

Grzesiak J, Górniak D, Świątecki A, Aleksandrzak-Piekarczyk T, Szatraj K, Zdanowski MK (2015a). Microbial community development on the surface of Hans and Werenskiold Glaciers (Svalbard, Arctic): a comparison. *Extremophiles* **19:** 885-897.

Grzesiak J, Zdanowski MK, Górniak D, Świątecki A, Aleksandrzak-Piekarczyk T, Szatraj K *et al* (2015b). Microbial community changes along the ecology glacier ablation zone (King George Island, Antarctica). *Polar Biology* **38:** 2069-2083.

Gu W, An G, Johnson E (1997). Ethanol increases carotenoid production in Phaffia rhodozyma. *Journal of Industrial Microbiology and Biotechnology* **19:** 114-117.

Gunde-Cimerman N, Zalar P, de Hoog S, Plemenitaš A (2000). Hypersaline waters in salterns–natural ecological niches for halophilic black yeasts. *FEMS microbiology Ecology* **32:** 235-240.

Gunde-Cimerman N, Plemenitaš A, Buzzini P (2014). Changes in lipids composition and fluidity of yeast plasma membrane as response to cold. *Cold-adapted yeasts*. Springer. pp 225-242.

Hamid R, Rotshteyn Y, Rabadi L, Parikh R, Bullock P (2004). Comparison of alamar blue and MTT assays for high through-put screening. *Toxicology in vitro* **18:** 703-710.

Hamilton TL, Peters JW, Skidmore ML, Boyd ES (2013). Molecular evidence for an active endogenous microbiome beneath glacial ice. *The ISME journal* **7:** 1402-1412.

Hansen AA, Herbert RA, Mikkelsen K, Jensen LL, Kristoffersen T, Tiedje JM *et al* (2007). Viability, diversity and composition of the bacterial community in a high Arctic permafrost soil from Spitsbergen, Northern Norway. *Environmental microbiology* **9:** 2870-2884.

Hassan N, Rafiq M, Hayat M, Shah AA, Hasan F (2016). Psychrophilic and psychrotrophic fungi: a comprehensive review. *Reviews in Environmental Science and Bio/Technology* **15:** 147-172.

Hays L (2015). NASA Astrobiology Strategy 2015. *National Aeronautics and Space Administration https://nai nasa gov/media/medialibrary/2016/04*.

Hazen TC, Jiménez L, de Victoria GL, Fliermans CB (1991). Comparison of bacteria from deep subsurface sediment and adjacent groundwater. *Microbial Ecology* **22:** 293-304.

Hecht M, Kounaves S, Quinn R, West S, Young S, Ming D *et al* (2009). Detection of perchlorate and the soluble chemistry of martian soil at the Phoenix lander site. *Science* **325:** 64-67.

Heino P, Palva ET (2003). Signal transduction in plant cold acclimation. *Plant Responses to Abiotic Stress*. Springer. pp 151-186.

Hemmingsson O, Zhang Y, Still M, Naredi P (2009). ASNA1, an ATPase targeting tail-anchored proteins, regulates melanoma cell growth and sensitivity to cisplatin and arsenite. *Cancer chemotherapy and pharmacology* **63:** 491-499.

Hodson A, Anesio AM, Tranter M, Fountain A, Osborn M, Priscu J *et al* (2008). Glacial ecosystems. *Ecological monographs* **78:** 41-67.

Hohmann C, Winkler E, Morin G, Kappler A (2009). Anaerobic Fe (II)-oxidizing bacteria show As resistance and immobilize As during Fe (III) mineral precipitation. *Environmental Science & Technology* **44:** 94-101.

Homma T, Iwahashi H, Komatsu Y (2003). Yeast gene expression during growth at low temperature. *Cryobiology* **46:** 230-237.

Hoover RB, Gilichinsky D (2001). Significance to astrobiology of micro-organisms in permafrost and ice. *Permafrost response on economic development, environmental security and natural resources*. Springer. pp 553-579.

Hotaling S, Hood E, Hamilton TL (2017). Microbial ecology of mountain glacier ecosystems: biodiversity, ecological connections and implications of a warming climate. *Environmental microbiology* **19:** 2935-2948.

Huang G-T, Ma S-L, Bai L-P, Zhang L, Ma H, Jia P *et al* (2012). Signal transduction during cold, salt, and drought stresses in plants. *Molecular biology reports* **39:** 969-987.

Hultman J, Waldrop MP, Mackelprang R, David MM, McFarland J, Blazewicz SJ *et al* (2015). Multi-omics of permafrost, active layer and thermokarst bog soil microbiomes. *Nature* **521:** 208-212.

Insam H, Amor K, Renner M, Crepaz C (1996). Changes in functional abilities of the microbial community during composting of manure. *Microbial Ecology* **31:** 77-87.

Insam H, Goberna M (2004). Use of Biolog® for the Community Level Physiological Profiling (CLPP) of environmental samples. *Molecular Microbial Ecology Manual* **4.01:** 853-860

Itcus C, Pascu MD, Lavin P, Perşoiu A, Iancu L, Purcarea C (2018). Bacterial and archaeal community structures in perennial cave ice. *Scientific reports* **8:** 1-14.

Iţcuş C, Pascu M-D, Brad T, Perşoiu A, Purcarea C (2016). Diversity of cultured bacteria from the perennial ice block of Scarisoara Ice Cave, Romania. *International Journal of Speleology* **45:** 9.

Jiang N, Yang Y, Janbon G, Pan J, Zhu X (2012). Identification and functional demonstration of miRNAs in the fungus Cryptococcus neoformans. *PloS one* **7:** e52734.

Jiang W, Hou Y, Inouye M (1997). CspA, the major cold-shock protein of Escherichia coli, is an RNA chaperone. *Journal of Biological Chemistry* **272:** 196-202.

Johansson B, Hahn-Hägerdal B (2002). The non-oxidative pentose phosphate pathway controls the fermentation rate of xylulose but not of xylose in Saccharomyces cerevisiae TMB3001. *FEMS yeast research* **2:** 277-282.

Jones PG, Inouye M (1996). RbfA, a 30S ribosomal binding factor, is a cold-shock protein whose absence triggers the cold-shock response. *Molecular microbiology* **21:** 1207-1218.

Junge K, Imhoff F, Staley T, Deming J (2002). Phylogenetic diversity of numerically important Arctic sea-ice bacteria cultured at subzero temperature. *Microbial Ecology***:** 315-328.

Kanehisa M, Sato Y, Morishima K (2016). BlastKOALA and GhostKOALA: KEGG tools for functional characterization of genome and metagenome sequences. *Journal of molecular biology* **428:** 726-731.

Kanellaki M, Koutinas A (1999). Low temperature fermentation of wine and beer by cold-adapted and immobilized yeast cells. *Biotechnological Applications of Cold-Adapted Organisms*. Springer. pp 117-145.

Kanellaki M, Bekatorou A, Koutinas AA (2014). Low-temperature production of wine, beer, and distillates using cold-adapted yeasts. *Cold-adapted Yeasts*. Springer. pp 417-439.

Kawahara H, Omori N, Obata H (2008). Cryoprotective activity of mannoprotein from the cell membrane of Pichia anomala. *CryoLetters* **29:** 437-445.

Kawahara H (2017). Cryoprotectants and ice-binding proteins. *Psychrophiles: from biodiversity to biotechnology*. Springer. pp 237-257.

Kawamoto J, Kurihara T, Esaki N (2017). Proteomic insights of psychrophiles. *Psychrophiles: from biodiversity to biotechnology*. Springer. pp 423-435.

Kawamoto S, Nozaki C, Tanaka A, Fukui S (1978). Fatty acid β-oxidation system in microbodies of n-alkane-grown Candida tropicalis. *European journal of biochemistry* **83:** 609-613.

Kirby BM, Easton S, Tuffin IM, Cowan DA (2012). Bacterial diversity in polar habitats. *Polar Microbiology: Life in a Deep Freeze*. American Society of Microbiology. pp 3-31.

Kite ES, Rubin AM (2016). Sustained eruptions on Enceladus explained by turbulent dissipation in tiger stripes. *Proceedings of the National Academy of Sciences* **113:** 3972-3975.

Koga K, Yoshizumi H (1979). Differential scanning calorimetry (DSC) studies on the freezing processes of water-ethanol mixtures and distilled spirits. *Journal of Food Science* **44:** 1386-1389.

Koh HY, Park H, Lee JH, Han SJ, Sohn YC, Lee SG (2017). Proteomic and transcriptomic investigations on cold-responsive properties of the psychrophilic A ntarctic bacterium P sychrobacter sp. PAMC 21119 at subzero temperatures. *Environmental microbiology* **19:** 628-644.

Konopka A, Oliver L, Turco Jr R (1998). The use of carbon substrate utilization patterns in environmental and ecological microbiology. *Microbial Ecology* **35:** 103-115.

Kourkoutas Y, Komaitis M, Koutinas A, Kaliafas A, Kanellaki M, Marchant R *et al* (2003). Wine production using yeast immobilized on quince biocatalyst at temperatures between 30 and 0 C. *Food Chemistry* **82:** 353-360.

Krüger J, Rehmsmeier M (2006). RNAhybrid: microRNA target prediction easy, fast and flexible. *Nucleic acids research* **34:** W451-W454.

Lamarche-Gagnon G, Comery R, Greer CW, Whyte LG (2015). Evidence of in situ microbial activity and sulphidogenesis in perennially sub-0 C and hypersaline sediments of a high Arctic permafrost spring. *Extremophiles* **19:** 1-15.

Larsen KS, Jonasson S, Michelsen A (2002). Repeated freeze–thaw cycles and their effects on biological processes in two arctic ecosystem types. *Applied Soil Ecology* **21:** 187-195.

Lau SK, Chow W-N, Wong AY, Yeung JM, Bao J, Zhang N *et al* (2013). Identification of microRNA-like RNAs in mycelial and yeast phases of the thermal dimorphic fungus Penicillium marneffei. *PLoS neglected tropical diseases* **7:** e2398.

Lay C-Y, Mykytczuk NC, Niederberger TD, Martineau C, Greer CW, Whyte LG (2012). Microbial diversity and activity in hypersaline high Arctic spring channels. *Extremophiles* **16:** 177-191.

Lay C-Y, Mykytczuk NC, Lamarche-Gagnon G, Greer CW, Whyte LG (2013). Defining the functional potential and active community members of a sediment microbial community in a high-arctic hypersaline subzero spring. *Appl Environ Microbiol* **79:** 3637-3648.

Lee JK, Park KS, Park S, Park H, Song YH, Kang S-H *et al* (2010). An extracellular ice-binding glycoprotein from an Arctic psychrophilic yeast. *Cryobiology* **60:** 222-228.

Levin GV, Straat PA (1976). Labeled release—an experiment in radiorespirometry. *Origins of Life* **7:** 293-311.

Levin GV: The Viking labeled release experiment and life on Mars. *Instruments, Methods, and Missions for the Investigation of Extraterrestrial Microorganisms*. 1997

Lewis BS, Hanel RP, Rademacher AT, Benton JE, Bhattacharya S, Ricco AJ *et al* (2014). BioSentinel: Monitoring DNA damage repair beyond low earth orbit on a 6U nanosatellite.

Li W-H, Yang J, Gu X (2005). Expression divergence between duplicate genes. *TRENDS in Genetics* **21:** 602-607.

Libkind D, Arts M, Van Broock M (2008). Fatty acid composition of cold-adapted carotenogenic basidiomycetous yeasts. *Revista Argentina de microbiologia* **40:** 193-197.

Liu GY, Nizet V (2009). Color me bad: microbial pigments as virulence factors. *Trends in microbiology* **17:** 406-413.

Loffeld B, Keweloh H (1996). cis/trans isomerization of unsaturated fatty acids as possible control mechanism of membrane fluidity inPseudomonas putida P8. *Lipids* **31:** 811-815.

López-Malo M, García-Ríos E, Chiva R, Guillamon JM (2014). Functional analysis of lipid metabolism genes in wine yeasts during alcoholic fermentation at low temperature. *Microbial Cell* **1:** 365.

Love MI, Huber W, Anders S (2014). Moderated estimation of fold change and dispersion for RNA-seq data with DESeq2. *Genome biology* **15:** 550.

Lynch M, Marinov GK (2015). The bioenergetic costs of a gene. *Proceedings of the National Academy of Sciences* **112:** 15690-15695.

Mackenzie R, Barros JA, Martínez MA (2011). Characterization of aerobic heterotrophic bacteria in cold and nutrient-poor freshwater ecosystems. *World Journal of Microbiology and Biotechnology* **27:** 2499-2504.

Magnuson E, Mykytczuk NC, Pellerin A, Goordial J, Twine SM, Wing B *et al* (2020). Thiomicrorhabdus streamers and sulfur cycling in perennial hypersaline cold springs in the Canadian high Arctic. *Environmental Microbiology*.

Maldonado F, Packard T, Gómez M (2012). Understanding tetrazolium reduction and the importance of substrates in measuring respiratory electron transport activity. *Journal of Experimental Marine Biology and Ecology* **434:** 110-118.

Mao C, Wadleigh M, Jenkins GM, Hannun YA, Obeid LM (1997). Identification and characterization of Saccharomyces cerevisiae dihydrosphingosine-1-phosphate phosphatase. *Journal of Biological Chemistry* **272:** 28690-28694.

Marchant DR, Head III JW (2007). Antarctic dry valleys: Microclimate zonation, variable geomorphic processes, and implications for assessing climate change on Mars. *Icarus* **192:** 187-222.

Margesin R, Fonteyne P-A, Schinner F, Sampaio JP (2007). Rhodotorula psychrophila sp. nov., Rhodotorula psychrophenolica sp. nov. and Rhodotorula glacialis sp. nov., novel psychrophilic basidiomycetous yeast species isolated from alpine environments. *International journal of systematic and evolutionary microbiology* **57:** 2179-2184.

Margesin R, Miteva V (2011). Diversity and ecology of psychrophilic microorganisms. *Research in microbiology* **162:** 346-361.

Marion GM, Fritsen CH, Eicken H, Payne MC (2003). The search for life on Europa: limiting environmental factors, potential habitats, and Earth analogues. *Astrobiology* **3:** 785-811.

Marteinsson VT, Runarsson A, Stefánsson A, Thorsteinsson T, Johannesson T, Magnusson SH *et al* (2013). Microbial communities in the subglacial waters of the Vatnajökull ice cap, Iceland. *The ISME journal* **7:** 427-437.

Mata-Gómez LC, Montañez JC, Méndez-Zavala A, Aguilar CN (2014). Biotechnological production of carotenoids by yeasts: an overview. *Microbial cell factories* **13:** 12.

Matin A, Wang J-H, Keyhan M, Singh R, Benoit M, Parra MP *et al* (2017). Payload hardware and experimental protocol development to enable future testing of the effect of space microgravity on the resistance to gentamicin of uropathogenic Escherichia coli and its σs-deficient mutant. *Life sciences in space research* **15:** 1-10.

McCollom TM (2006). The habitability of Mars: past and present. *Solar System Update*. Springer. pp 159-175.

McCord TB, Orlando TM, Teeter G, Hansen GB, Sieger MT, Petrik NG *et al* (2001). Thermal and radiation stability of the hydrated salt minerals epsomite, mirabilite, and natron under Europa environmental conditions. *Journal of Geophysical Research: Planets* **106:** 3311-3319.

McSween HY, Taylor GJ, Wyatt MB (2009). Elemental composition of the Martian crust. *Science* **324:** 736-739.

Meng Z, Simmons-Willis TA, Limbach PA (2004). The use of mass spectrometry in genomics. *Biomolecular engineering* **21:** 1-13.

Michaelson G, Ping C (2003). Soil organic carbon and CO2 respiration at subzero temperature in soils of Arctic Alaska. *Journal of Geophysical Research: Atmospheres* **108:** ALT 5-1-ALT 5-10.

Michalski JR, Onstott TC, Mojzsis SJ, Mustard J, Chan QH, Niles PB *et al* (2018). The Martian subsurface as a potential window into the origin of life. *Nature Geoscience* **11:** 21.

Mikami K, Kanesaki Y, Suzuki I, Murata N (2002). The histidine kinase Hik33 perceives osmotic stress and cold stress in Synechocystis sp. PCC 6803. *Molecular microbiology* **46:** 905-915.

Miteva V, Sowers T, Brenchley J (2007). Production of N 2 O by ammonia oxidizing bacteria at subfreezing temperatures as a model for assessing the N 2 O anomalies in the Vostok ice core. *Geomicrobiology Journal* **24:** 451-459.

Miteva V (2008). Bacteria in snow and glacier ice. *Psychrophiles: from biodiversity to biotechnology*. Springer. pp 31-50.

Miura K, Furumoto T (2013). Cold signaling and cold response in plants. *International journal of molecular sciences* **14:** 5312-5337.

Mock T, Hoch N (2005). Long-term temperature acclimation of photosynthesis in steady-state cultures of the polar diatom Fragilariopsis cylindrus. *Photosynthesis research* **85:** 307-317.

Mohamad N, Mustapa Kamal S, Mokhtar M (2015). Xylitol biological production: a review of recent studies. *Food reviews international* **31:** 74-89.

Moliné M, Libkind D, del Carmen Diéguez M, van Broock M (2009). Photoprotective role of carotenoids in yeasts: response to UV-B of pigmented and naturally-occurring albino strains. *Journal of Photochemistry and Photobiology B: Biology* **95:** 156-161.

Moliné M, Flores MR, Libkind D, del Carmen Diéguez M, Farías ME, van Broock M (2010). Photoprotection by carotenoid pigments in the yeast Rhodotorula mucilaginosa: the role of torularhodin. *Photochemical & Photobiological Sciences* **9:** 1145-1151.

Morita RY (1975). Psychrophilic bacteria. *Bacteriological reviews* **39:** 144.

Munshi S, Twining RC, Dahl R (2014). Alamar blue reagent interacts with cell-culture media giving different fluorescence over time: Potential for false positives. *Journal of pharmacological and toxicological methods* **70:** 195-198.

Murray AE, Kenig F, Fritsen CH, McKay CP, Cawley KM, Edwards R *et al* (2012). Microbial life at− 13 C in the brine of an ice-sealed Antarctic lake. *Proceedings of the National Academy of Sciences* **109:** 20626-20631.

Mykytczuk N, Lawrence J, Omelon CR, Southam G, Whyte L (2016). Microscopic characterization of the bacterial cell envelope of Planococcus halocryophilus Or1 during subzero growth at− 15 C. *Polar Biology* **39:** 701-712.

Mykytczuk NC, Foote SJ, Omelon CR, Southam G, Greer CW, Whyte LG (2013). Bacterial growth at− 15 C; molecular insights from the permafrost bacterium Planococcus halocryophilus Or1. *The ISME journal* **7:** 1211.

Naganuma T, Hua PN, Okamoto T, Ban S, Imura S, Kanda H (2005). Depth distribution of euryhaline halophilic bacteria in Suribati Ike, a meromictic lake in East Antarctica. *Polar Biology* **28:** 964-970.

Nichols WW, Evans MJ, Slack MP, Walmsley HL (1989). The penetration of antibiotics into aggregates of mucoid and non-mucoid Pseudomonas aeruginosa. *Microbiology* **135:** 1291-1303.

Nicholson WL, Ricco AJ, Agasid E, Beasley C, Diaz-Aguado M, Ehrenfreund P *et al* (2011). The O/OREOS mission: first science data from the Space Environment Survivability of Living Organisms (SESLO) payload. *Astrobiology* **11:** 951-958.

Niederberger TD, Perreault NN, Tille S, Lollar BS, Lacrampe-Couloume G, Andersen D *et al* (2010). Microbial characterization of a subzero, hypersaline methane seep in the Canadian High Arctic. *The ISME journal* **4:** 1326-1339.

Ojha L, Wilhelm MB, Murchie SL, McEwen AS, Wray JJ, Hanley J *et al* (2015). Spectral evidence for hydrated salts in recurring slope lineae on Mars. *Nature Geoscience* **8:** 829.

Orosei R, Lauro SE, Pettinelli E, Cicchetti A, Coradini M, Cosciotti B *et al* (2018). Radar evidence of subglacial liquid water on Mars. *Science* **361:** 490-493.

Örvar BL, Sangwan V, Omann F, Dhindsa RS (2000). Early steps in cold sensing by plant cells: the role of actin cytoskeleton and membrane fluidity. *The Plant Journal* **23:** 785-794.

Patro R, Duggal G, Love MI, Irizarry RA, Kingsford C (2017). Salmon provides fast and bias-aware quantification of transcript expression. *Nature methods* **14:** 417.

Pavlova K, Panchev I, Hristozova T (2005). Physico-chemical characterization of exomannan from Rhodotorula acheniorum MC. *World Journal of Microbiology and Biotechnology* **21:** 279-283.

Pearson GA, Lago-Leston A, Cánovas F, Cox CJ, Verret F, Lasternas S *et al* (2015). Metatranscriptomes reveal functional variation in diatom communities from the Antarctic Peninsula. *The ISME journal* **9:** 2275-2289.

Perini L, Gostinčar C, Anesio AM, Williamson C, Tranter M, Gunde-Cimerman N (2019). Darkening of the Greenland Ice Sheet: fungal abundance and diversity are associated with algal bloom. *Frontiers in Microbiology* **10:** 557.

Perreault NN, Greer CW, Andersen DT, Tille S, Lacrampe-Couloume G, Lollar BS *et al* (2008). Heterotrophic and autotrophic microbial populations in cold perennial springs of the high arctic. *Appl Environ Microbiol* **74:** 6898-6907.

Pessi IS, de Oliveira Elias S, Simões FL, Simões JC, Macedo AJ (2009). Functional diversity of microbial communities in soils in the vicinity of Wanda Glacier, Antarctic Peninsula. *Microbes and environments***:** 1111240335-1111240335.

Phadtare S (2012). E scherichia coli cold-shock gene profiles in response to over-expression/deletion of C sd A, RN ase R and PNP ase and relevance to low-temperature RNA metabolism. *Genes to Cells* **17:** 850-874.

Pollard W, Haltigin T, Whyte L, Niederberger T, Andersen D, Omelon C *et al* (2009). Overview of analogue science activities at the McGill Arctic research station, axel heiberg island, canadian high arctic. *Planetary and Space Science* **57:** 646-659.

Priscu JC, Hand KP (2012). Microbial habitability of icy worlds. *Microbe* **7:** 167-172.

Rampersad SN (2012). Multiple applications of Alamar Blue as an indicator of metabolic function and cellular health in cell viability bioassays. *Sensors* **12:** 12347-12360.

Rao R, Bhadra B, Shivaji S (2008). Isolation and characterization of ethanol-producing yeasts from fruits and tree barks. *Letters in applied microbiology* **47:** 19-24.

Raymond-Bouchard I, Whyte LG (2017). From transcriptomes to metatranscriptomes: cold adaptation and active metabolisms of psychrophiles from cold environments. *Psychrophiles: from biodiversity to biotechnology*. Springer. pp 437-457.

Raymond-Bouchard I, Goordial J, Zolotarov Y, Ronholm J, Stromvik M, Bakermans C *et al* (2018a). Conserved genomic and amino acid traits of cold adaptation in subzero-growing Arctic permafrost bacteria. *FEMS microbiology ecology* **94:** fiy023.

Raymond-Bouchard I, Tremblay J, Altshuler I, Greer CW, Whyte LG (2018b). Comparative transcriptomics of cold growth and adaptive features of a eury-and steno-psychrophile. *Frontiers in microbiology* **9:** 1565.

Raymond-Bouchard I, Chourey K, Altshuler I, Iyer R, Hettich RL, Whyte LG (2017). Mechanisms of subzero growth in the cryophile Planococcus halocryophilus determined through proteomic analysis. *Environmental microbiology* **19:** 4460-4479.

Rehmsmeier M, Steffen P, Höchsmann M, Giegerich R (2004). Fast and effective prediction of microRNA/target duplexes. *RNA* **10:** 1507-1517.

Rico A, Preston GM (2008). Pseudomonas syringae pv. tomato DC3000 uses constitutive and apoplast-induced nutrient assimilation pathways to catabolize nutrients that are abundant in the tomato apoplast. *Molecular Plant-Microbe Interactions* **21:** 269-282.

Rini JM, Esko JD (2017). Glycosyltransferases and glycan-processing enzymes. *Essentials of Glycobiology [Internet]. 3rd edition*. Cold Spring Harbor Laboratory Press.

Rodrigues DF, Ivanova N, He Z, Huebner M, Zhou J, Tiedje JM (2008). Architecture of thermal adaptation in an Exiguobacterium sibiricum strain isolated from 3 million year old permafrost: a genome and transcriptome approach. *BMC genomics* **9:** 547.

Rodrigues DF, Tiedje JM (2008). Coping with our cold planet. *Appl Environ Microbiol* **74:** 1677-1686.

Rogers SO, Shtarkman YM, Koçer ZA, Edgar R, Veerapaneni R, D'Elia T (2013). Ecology of subglacial Lake Vostok (Antarctica), based on metagenomic/metatranscriptomic analyses of accretion ice. *Biology* **2:** 629-650.

Rosa LH, Vaz AB, Caligiorne RB, Campolina S, Rosa CA (2009). Endophytic fungi associated with the Antarctic grass Deschampsia antarctica Desv.(Poaceae). *Polar Biology* **32:** 161-167.

Rossi M, Buzzini P, Cordisco L, Amaretti A, Sala M, Raimondi S *et al* (2009). Growth, lipid accumulation, and fatty acid composition in obligate psychrophilic, facultative psychrophilic, and mesophilic yeasts. *FEMS microbiology ecology* **69:** 363-372.

Rutishauser A, Blankenship DD, Sharp M, Skidmore ML, Greenbaum JS, Grima C *et al* (2018). Discovery of a hypersaline subglacial lake complex beneath Devon Ice Cap, Canadian Arctic. *Science advances* **4:** eaar4353.

Sabra W, Bommareddy RR, Maheshwari G, Papanikolaou S, Zeng A-P (2017). Substrates and oxygen dependent citric acid production by Yarrowia lipolytica: insights through transcriptome and fluxome analyses. *Microbial cell factories* **16:** 78.

: Effect of temperature on growth of psychrophilic and psychrotrophic members of Rhodotorula aurantiaca. *Twenty-First Symposium on Biotechnology for Fuels and Chemicals*.

Sahara T, Goda T, Ohgiya S (2002). Comprehensive expression analysis of time-dependent genetic responses in yeast cells to low temperature. *Journal of Biological Chemistry* **277:** 50015-50021.

Sánchez-García L, Fernández-Martínez MA, Moreno-Paz M, Carrizo D, García-Villadangos M, Manchado JM *et al* (2020). Simulating Mars Drilling Mission for Searching for Life: Ground-Truthing Lipids and Other Complex Microbial Biomarkers in the Iron-Sulfur Rich Río Tinto Analog. *Astrobiology*.

Santa Maria SR, Marina DB, Massaro Tieze S, Liddell LC, Bhattacharya S (2020). BioSentinel: Long-Term Saccharomyces cerevisiae Preservation for a Deep Space Biosensor Mission. *Astrobiology*.

Sarkar D, Bhowmik PC, Kwon Y-I, Shetty K (2009). Clonal response to cold tolerance in creeping bentgrass and role of proline-associated pentose phosphate pathway. *Bioresource technology* **100:** 5332-5339.

Schade B, Jansen G, Whiteway M, Entian KD, Thomas DY (2004). Cold adaptation in budding yeast. *Molecular biology of the cell* **15:** 5492-5502.

Schmidt B, Blankenship DD, Patterson G, Schenk P (2011). Active formation of ‘chaos terrain’over shallow subsurface water on Europa. *Nature* **479:** 502-505.

Schmidt S, Wilson K, Monson R, Lipson D (2009). Exponential growth of “snow molds” at sub-zero temperatures: an explanation for high beneath-snow respiration rates and Q 10 values. *Biogeochemistry* **95:** 13-21.

Schmidt-Nielsen S (1902). Ueber einige psychrophile Mikroorganismen und ihr Vorkommen. *Zentr Bakteriol Parasitenkd Infektionsk Hyg Abt* **9:** 145-147.

Schneider CA, Rasband WS, Eliceiri KW (2012). NIH Image to ImageJ: 25 years of image analysis. *Nature methods* **9:** 671.

Sekine Y, Shibuya T, Postberg F, Hsu H-W, Suzuki K, Masaki Y *et al* (2015). High-temperature water–rock interactions and hydrothermal environments in the chondrite-like core of Enceladus. *Nature communications* **6:** 1-8.

Selbmann L, Onofri S, Fenice M, Federici F, Petruccioli M (2002). Production and structural characterization of the exopolysaccharide of the Antarctic fungus Phoma herbarum CCFEE 5080. *Research in Microbiology* **153:** 585-592.

Shetty K, Wahlqvist M (2004). A model for the role of the proline-linked pentose-phosphate pathway in phenolic phytochemical bio-synthesis and mechanism of action for human health and environmental applications. *Asia Pacific Journal of Clinical Nutrition* **13**.

Shiloh MU, Ruan J, Nathan C (1997). Evaluation of bacterial survival and phagocyte function with a fluorescence-based microplate assay. *Infection and Immunity* **65:** 3193-3198.

Shivaji S, Prasad G (2009). Antarctic yeasts: biodiversity and potential applications. *Yeast biotechnology: Diversity and applications*. Springer. pp 3-18.

Skelley AM, Scherer JR, Aubrey AD, Grover WH, Ivester RH, Ehrenfreund P *et al* (2005). Development and evaluation of a microdevice for amino acid biomarker detection and analysis on Mars. *Proceedings of the National Academy of Sciences* **102:** 1041-1046.

Song W, Kim M, Tripathi BM, Kim H, Adams JM (2016). Predictable communities of soil bacteria in relation to nutrient concentration and successional stage in a laboratory culture experiment. *Environmental microbiology* **18:** 1740-1753.

Starmer WT, Lachance M-A (2011). Yeast ecology. *The yeasts*. Elsevier. pp 65-83.

Steven B, Briggs G, McKay CP, Pollard WH, Greer CW, Whyte LG (2007). Characterization of the microbial diversity in a permafrost sample from the Canadian high Arctic using culture-dependent and culture-independent methods. *FEMS microbiology ecology* **59:** 513-523.

Storey KB, Storey JM (2001). Signal transduction and gene expression in the regulation of natural freezing survival. *Cell and Molecular Response to Stress*. Elsevier. pp 1-19.

Strassburg K, Walther D, Takahashi H, Kanaya S, Kopka J (2010). Dynamic transcriptional and metabolic responses in yeast adapting to temperature stress. *Omics: a journal of integrative biology* **14:** 249-259.

Sunkar R, Li Y-F, Jagadeeswaran G (2012). Functions of microRNAs in plant stress responses. *Trends in plant science* **17:** 196-203.

Tai SL, Daran-Lapujade P, Walsh MC, Pronk JT, Daran J-M (2007). Acclimation of Saccharomyces cerevisiae to low temperature: a chemostat-based transcriptome analysis. *Molecular Biology of the Cell* **18:** 5100-5112.

Tamppari L, Anderson R, Archer P, Douglas S, Kounaves S, McKay C *et al* (2012). Effects of extreme cold and aridity on soils and habitability: McMurdo Dry Valleys as an analogue for the Mars Phoenix landing site. *Antarctic Science* **24:** 211-228.

Tang W, Wang Y, Zhang J, Cai Y, He Z (2019). Biosynthetic Pathway of Carotenoids in Rhodotorula and Strategies for Enhanced Their Production. *Journal of microbiology and biotechnology* **29:** 507-517.

Taylor B, Hoare D (1971). Thiobacillus denitrificans as an obligate chemolithotroph. II. Cell suspension and enzymic studies. *Archiv fur Mikrobiologie* **80:** 262-276.

Team RC (2013). R: A language and environment for statistical computing.

Telling J, Anesio AM, Tranter M, Irvine-Fynn T, Hodson A, Butler C *et al* (2011). Nitrogen fixation on Arctic glaciers, Svalbard. *Journal of Geophysical Research: Biogeosciences* **116**.

Terao Y, Nakamori S, Takagi H (2003). Gene dosage effect of L-proline biosynthetic enzymes on L-proline accumulation and freeze tolerance in Saccharomyces cerevisiae. *Appl Environ Microbiol* **69:** 6527-6532.

Thomas-Hall S, Watson K (2002). Cryptococcus nyarrowii sp. nov., a basidiomycetous yeast from Antarctica. *International journal of systematic and evolutionary microbiology* **52:** 1033-1038.

Tojo M, Newsham KK (2012). Snow moulds in polar environments. *Fungal Ecology* **5:** 395-402.

Tribelli PM, López NI (2018). Reporting key features in cold-adapted bacteria. *Life* **8:** 8.

Tsuji M, Yokota Y, Kudoh S, Hoshino T (2014). Improvement of direct ethanol fermentation from woody biomasses by the Antarctic basidiomycetous yeast, Mrakia blollopis, under a low temperature condition. *Cryobiology* **68:** 303-305.

Tsuji M (2016). Cold-stress responses in the Antarctic basidiomycetous yeast Mrakia blollopis. *Royal Society open science* **3:** 160106.

Tuorto SJ, Darias P, McGuinness LR, Panikov N, Zhang T, Häggblom MM *et al* (2014). Bacterial genome replication at subzero temperatures in permafrost. *The ISME journal* **8:** 139-149.

Turchetti B, Hall SRT, Connell LB, Branda E, Buzzini P, Theelen B *et al* (2011). Psychrophilic yeasts from Antarctica and European glaciers: description of Glaciozyma gen. nov., Glaciozyma martinii sp. nov. and Glaciozyma watsonii sp. nov. *Extremophiles* **15:** 573.

Turk M, Plemenitaš A, Gunde-Cimerman N (2011). Extremophilic yeasts: plasma-membrane fluidity as determinant of stress tolerance. *Fungal biology* **115:** 950-958.

Van den Brink J, Canelas AB, Van Gulik WM, Pronk JT, Heijnen JJ, De Winde JH *et al* (2008). Dynamics of glycolytic regulation during adaptation of Saccharomyces cerevisiae to fermentative metabolism. *Appl Environ Microbiol* **74:** 5710-5723.

Van Heerden J, Korf C, Ehlers MM, Cloete TE (2002). Biolog for the determination of diversity in microbial communities. *Water Sa* **28:** 29-36.

Varki A, Gagneux P (2017). Biological functions of glycans. *Essentials of Glycobiology [Internet]. 3rd edition*. Cold Spring Harbor Laboratory Press.

Vartoukian SR, Palmer RM, Wade WG (2010). Strategies for culture of 'unculturable'bacteria. *FEMS microbiology letters* **309:** 1-7.

Vaz AB, Rosa LH, Vieira ML, Garcia Vd, Brandão LR, Teixeira LC *et al* (2011). The diversity, extracellular enzymatic activities and photoprotective compounds of yeasts isolated in Antarctica. *Brazilian Journal of Microbiology* **42:** 937-947.

Villarreal P, Carrasco M, Barahona S, Alcaíno J, Cifuentes V, Baeza M (2016). Tolerance to ultraviolet radiation of psychrotolerant yeasts and analysis of their carotenoid, mycosporine, and ergosterol content. *Current microbiology* **72:** 94-101.

Vishnivetskaya TA, Petrova MA, Urbance J, Ponder M, Moyer CL, Gilichinsky DA *et al* (2006). Bacterial community in ancient Siberian permafrost as characterized by culture and culture-independent methods. *Astrobiology* **6:** 400-414.

Viti C, Decorosi F, Marchi E, Galardini M, Giovannetti L (2015). High-throughput phenomics. *Bacterial Pangenomics*. Springer. pp 99-123.

Wagner A (2002). Asymmetric functional divergence of duplicate genes in yeast. *Molecular biology and evolution* **19:** 1760-1768.

Waite JH, Combi MR, Ip W-H, Cravens TE, McNutt RL, Kasprzak W *et al* (2006). Cassini ion and neutral mass spectrometer: Enceladus plume composition and structure. *science* **311:** 1419-1422.

Waite JH, Glein CR, Perryman RS, Teolis BD, Magee BA, Miller G *et al* (2017). Cassini finds molecular hydrogen in the Enceladus plume: evidence for hydrothermal processes. *Science* **356:** 155-159.

Wang B, Sun Y-f, Song N, Wei J-p, Wang X-j, Feng H *et al* (2014). MicroRNAs involving in cold, wounding and salt stresses in Triticum aestivum L. *Plant physiology and biochemistry* **80:** 90-96.

Westall F, Loizeau D, Foucher F, Bost N, Betrand M, Vago J *et al* (2013). Habitability on Mars from a microbial point of view. *Astrobiology* **13:** 887-897.

Westall F, Foucher F, Bost N, Bertrand M, Loizeau D, Vago JL *et al* (2015). Biosignatures on Mars: what, where, and how? Implications for the search for martian life. *Astrobiology* **15:** 998-1029.

Wilhelm RC, Radtke KJ, Mykytczuk NC, Greer CW, Whyte LG (2012). Life at the wedge: the activity and diversity of Arctic ice wedge microbial communities. *Astrobiology* **12:** 347-360.

Williams MW, Helmig D, Blanken P (2009). White on green: under-snow microbial processes and trace gas fluxes through snow, Niwot Ridge, Colorado Front Range. *Biogeochemistry* **95:** 1-12.

Williams PJ, Smith MW (1989). *The frozen earth: fundamentals of geocryology*. Cambridge University Press.

Woodman S, Trousdale C, Conover J, Kim K (2018). Yeast membrane lipid imbalance leads to trafficking defects toward the Golgi. *Cell biology international* **42:** 890-902.

Xiong MY, Shelobolina ES, Roden EE (2015). Potential for microbial oxidation of ferrous iron in basaltic glass. *Astrobiology* **15:** 331-340.

Yakovlev IA, Fossdal CG, Johnsen Ø (2010). MicroRNAs, the epigenetic memory and climatic adaptation in Norway spruce. *New Phytologist* **187:** 1154-1169.

Zhang D-C, Brouchkov A, Griva G, Schinner F, Margesin R (2013a). Isolation and characterization of bacteria from ancient Siberian permafrost sediment. *Biology* **2:** 85-106.

Zhang S, Wang Y, Li K, Zou Y, Chen L, Li X (2014). Identification of cold-responsive miRNAs and their target genes in nitrogen-fixing nodules of soybean. *International journal of molecular sciences* **15:** 13596-13614.

Zhang X, Zhao L, Xu Jr S, Liu Y, Liu H, Cheng G (2013b). Soil moisture effect on bacterial and fungal community in B eilu R iver (T ibetan P lateau) permafrost soils with different vegetation types. *Journal of applied microbiology* **114:** 1054-1065.

Zhou Q, Wang Z, Zhang J, Meng H, Huang B (2012). Genome-wide identification and profiling of microRNA-like RNAs from Metarhizium anisopliae during development. *Fungal biology* **116:** 1156-1162.